UNIVERSIDADE FEDERAL DE PELOTAS
PROGRAMA DE PÓS-GRADUAÇÃO EM BIOQUÍMICA E BIOPROSPECÇÃO

Tese

Concentração de pigmentos, desempenho fotossintético e perfil de ácidos graxos em macroalgas da região de Magalhães, Chile

Marco Aurélio Ziemann dos Santos

Pelotas, 2019

MARCO AURÉLIO ZIEMANN DOS SANTOS

Concentração de pigmentos, desempenho fotossintético e perfil de ácidos graxos em macroalgas da região de Magalhães, Chile

Tese apresentada ao programa de Pós-Graduação em Bioquímica e Bioprospecção da Universidade Federal de Pelotas, como requisito à obtenção do título de Doutor em Ciências (Área do conhecimento: Bioquímica e Bioprospecção)

Orientador: Prof. Dr. Claudio Martin Pereira de Pereira

Co-Orientador: Prof$_a$. Dr$_a$. Carla Rosane Barboza Mendonça

Pelotas, 2019

A Comissão Examinadora, abaixo assinada, aprova a Tese de Doutorado

Concentração de pigmentos, desempenho fotossintético e perfil de ácidos graxos em macroalgas da região de Magalhães, Chile

elaborada por

Marco Aurélio Ziemann dos Santos

Como requisito à obtenção do título de **Doutor em Ciências (Área do conhecimento: Bioquímica e Bioprospecção)**

Banca Examinadora

Prof. Dr. Claudio Martin Pereira de Pereira (UFPel/CCQFA) - ORIENTADOR

Fernanda Nedel

Profa. Dra. Fernanda Nedel (UCPel)

Prof. Dr. Rui Carlos Zambiazi (UFPel - CCQFA/QUÍMICA DE ALIMENTOS)

Prof. Dr. Rafael Guerra Lund (UFPel – FACULDADE DE ODONTOLOGIA)

Pelotas, 2019

Catalogação na fonte
Gabriela Machado Lopes CRB: 10/1842

S586c Santos, Marco Aurélio Ziemann dos

Concentração de pigmentos, desempenho fotossintético e perfil de ácidos graxos em macroalgas da região de Magalhães, Chile/ Marco Aurélio Ziemann dos Santos; Claudio Martin Pereira de Pereira, orientador — Pelotas, 2019

156 f. : il.

Tese (Doutorado) — Programa de Pós-Graduação em Bioquímica e Bioprospecção. Universidade Federal de Pelotas, 2019.

1. Poliinsaturados. 2. Rhodophyta. 3. Ochrophyta. 4. Pigmentos. 5. Performace Fotossintética. I. Pereira, Claudio Martin Pereira de, orient. II.Título.

CDD : 574.192

Universidade Federal de Pelotas

“O GRANDE INIMIGO DO CONHECIMENTO NÃO É A IGNORÂNCIA, É A ILUSÃO DE TER CONHECIMENTO...”

STEPHEN HAWKING

Agradecimentos

Primeiramente a Deus por permitir estar vivenciando este momento mantendo minha mente e alma tranquila em todos os momentos e me dando forças para superar as dificuldades que passamos em nossas vidas.

Aos meus pais Rosa e Enis (*in memorian*) e meu irmão Sérgio pelo incentivo, conversas e conselhos, quando os dias se tornam pesados e difíceis, amo vocês.

Um agradecimento especial a minha amada esposa Patricia que SEMPRE está ao meu lado, me apoiando, incentivando, me mantendo firme em todos os momentos, seja na doença, nos momentos de péssimo humor ou nos momentos bons que passamos juntos. Que esteve ao meu lado nas coletas e preparativos das amostras para este trabalho. Obrigado por ser minha esposa, companheira, mulher e principalmente minha amiga. TE AMO.

Aos meus filhos Lorran e Richele por me mostrarem que filhos dão trabalho, mas que também nos dão muitas e muitas alegrias, felicidades e no fazem ver que a vida tem mais sentido quando temos alguém para transmitirmos nosso conhecimento e amor.

Aos meus netos Arthur, Stella e Nick que mesmo estando longe nos encantam e nos enchem de felicidades. Um dia estarão com certeza trilhando este caminho do conhecimento.

Ao Prof. Dr. Claudio pela orientação em inúmeros trabalhos que realizamos juntos, pela oportunidade de poder trabalhar ao seu lado e abrir espaço para novas pesquisas, novos trabalhos, novas vivências. Obrigado pela confiança em mim e pelas conversas entre um cafés, almoços e churrascos que permitiu mantermos um laço grande de amizade.

A Prof$_{a.}$Dra. Carla Rosane Barboza Mendonça pela coorientação e amizade ao longo destes anos dentro e fora da UFPel.

Aos colegas do laboratório que me auxiliaram no desenvolvimento deste trabalho e que me acompanharam durante o Doutorado auxiliando em todas as análises, disponibilizando seu tempo, inclusive mantendo os trabalhos em desenvolvimento no laboratório enquanto estive fora do Brasil.

A minha grande amiga e colega de trabalho Marina que me escuta nos momentos difíceis, que me aconselha, que muitas e muitas vezes me substituiu em vários horários para poder realizar a parte experimental deste trabalho.

Aos professores Dr. Andres Mansilla e a Dra. Prof$_a$. Maria Soledad que me receberam de braços abertos quando estive realizando minhas pesquisas no Chile. Um carinho especial por estes profissionais e a toda a equipe que me auxiliou no Laboratório de Macroalgas Sub-Antárticas (LEMAS). Silvia, Fábio, Jaime, Ralf, Sebastián, Alejandra, Armando, Karla, Joahana, Claudio Gonzales, Paula, Juan Pablo, Karin....

Aos coordenadores e todos os professores do Programa de Pós-Graduação em Bioquímica e Bioprospecção, pelo aprendizado, companheirismo, dedicação, crescimento profissional e pessoal.

Por fim, a todos aqueles que aqui não foram citados, mas de alguma forma fizeram parte da minha vida e me auxiliaram neste momento tão importante.

Muito obrigado!!!

Resumo

SANTOS, Marco Aurélio Ziemann dos. **Concentração de pigmentos, desempenho fotossintético e perfil de ácidos graxos em macroalgas da região de Magalhães, Chile**. 2019. 162f. Tese (Doutorado) – Programa de Pós-Graduação em Bioquímica e Bioprospecção. Universidade Federal de Pelotas, Pelotas.

A região sub-Antártica é uma área biogeográfica compreendendo a massa de terra mais meridional do continente americano conhecida por suas condições ambientais extremas que incluem, por exemplo, baixas temperaturas, fotoperíodo limitado no inverno e alta exposição à luz ultravioleta no verão. Aspectos fisiológicos, incluindo o desempenho fotossintético e informações químicas, como a concentração de pigmentos e o perfil lipídico associado às fases de desenvolvimento de macroalgas marinhas, têm sido pouco estudados. Nesse sentido, o objetivo deste estudo foi investigar a diferença da concentração de pigmentos, ácidos graxos e desempenho fotossintético nas fases vegetativa e reprodutiva de macroalgas *Durvillae antarctica* (Chamisso) Hariot, *Lessonia flavicans* Bory, *Macrocystis pyrifera* (Linnaeus) C. Agardh, *Gigartina skottsbergii* Setchell & N.L.Gardner, *Iridaea cordata* (Turner) Bory de Saint-Vincent and *Mazzaella laminarioides* (Bory) Fredericq da região de Magalhães (Chile). As macroalgas foram analisadas por Fluorometria de Pulso Modulada sob oito condições de irradiação (11 a 490 µmol fotons m^{-2} s^{-1}), sendo a pigmentação avaliada por Espectrofotometria UV / VIS (400 a 700 nm). O perfil de ácidos graxos (FA) seguiu o método extrativo de Bligh & Dyer (1959) e a análise foi realizada por Cromatografia Gasosa por Ionização em Chamas. A eficiência fotosintética (*α*) apresentou varaições significativa para *L. flavicans* (0.31 ± 0.01 to 0.38 ± 0.01 µmol e^- m^{-2} s^{-1}.µmol fotons m^{-2} s^{-1}) e *M. pyrifera* (0.26 ± 0.02 to 0.31 ± 0.03 µmol e^- m^{-2} s^{-1}.µmol fotons m^{-2} s^{-1}) para as fases reprodutiva e vegetative respectivamente. Nas algas vermelhas *I. cordata* (tetraesporofiticas) e *M. laminarioides* (carposporofitica) a variação foi entre 0.09 a 0.18 µmol e^- m^{-2} s^{-1} . µmol fotons m^{-2} s^{-1}. A taxa de transferência máxima relativa de elétrons (rETRmax) variou significativamente para algas pardas em *L. flavicans* (8,10 ± 0,84 a 12,40 ± 1,57 µmol e^-s^{-1}) e *M. pyrifera* (6,49 ± 1,30 a 12,89 ± 1,53 µmol e^- s^{-1}) em fases distintas de desenvolvimento. A análise da saturação da irradiância (E_k) mostrou diferenças significativas para *D. antártica*, variando de 166,18 ± 14,33 (vegetativa) a 132,98 ±

18,43 µmol foton m^{-2} s^{-1} (reprodutiva). As maiores concentrações de pigmentos em algas pardas foram encontradas em *M. pyrifera* reprodutiva com 35,36 ± 0,21 de clorofila *a*, 7,04 ± 0,93 de clorofila c e 15,75 ± 1,42 µg g^{-1} de fucoxantina. Finalmente, em algas pardas as maiores concentrações de ácidos graxos totais foram 35,24 ± 2,38% (saturados) e 22,02 ± 1,95% (monoinsaturados) em *M. pyrifera* e 63,53 ± 3,36% (poliinsaturados) em *D. antarctica*. Os resultados mostraram em algas vermelhas que os lipídios totais variaram entre 1,25 a 2,72%, enquanto as classes de ácidos graxos encontradas foram de 23,34 a 59,93%, 11,20 a 18,47% e 21,60 a 65,47% para acidos graxos saturados, monoinsaturados e poliinsaturados, respectivamente. Os dados mostram que as diferenças nos parâmetros fotossintéticos, concentração de pigmentos e perfil de ácidos graxos espécies estão relacionadas ao habitat e estagio de desenvolvimento das algas.

Palavra chave: Poliinsaturados – Rhodophyta – Ochrophyta - Pigmentos – Performace Fotossintética.

Abstract

SANTOS, Marco Aurélio Ziemann dos. **Pigment concentration, photosynthetic performance and fatty acid profile of the Magalhães region, Chile.** 2019. 162f. Thesis (Doctoral) – Postgraduate Program in Biochemistry and Bioprospecting. Federal University of Pelotas, Pelotas.

The sub-Antarctic region is a biogeographic area comprising the southernmost landmass of the American continent known for its extreme environmental conditions that include, for instance, low temperatures, limited photoperiod in the winter and high exposure to ultraviolet light in summer. Physiological aspects including photosynthetic performance and chemical information such as the concentration of pigments and the lipid profile associated to the phases of development of marine macroalgae have been remotely studied. In this sense, the aim of this study was to investigate the difference of the concentration of pigments, fatty acids and photosynthetic performance in vegetative and reproductive phases of macroalgae *Durvillae antarctica* (Chamisso) Hariot, *Lessonia flavicans* Bory, *Macrocystis pyrifera* (Linnaeus) C. Agardh, *Gigartina skottsbergii* Setchell & N.L. Gardner, *Iridaea cordata* (Turner) Bory de Saint-Vincent and *Mazzaella laminarioides* (Bory) Fredericq of the Magellan region (Chile). Macroalgae were analyzed by Pulse Amplitude Modulated Fluorometry under eight irradiation conditions (11 to 490 µmol photons m^{-2} s^{-1}) and pigmentation was assessed by UV/VIS Spectrophotometry (400 to 700 nm). Fatty acids (FA) extraction followed the Bligh & Dyer method (1959) and analysis was performed by Gas Chromatography Coupled to Flame Ionization Detection. Photosynthetic efficiency (α) had significant differences for *L. flavicans* (0.31 ± 0.01 to 0.38 ± 0.01 µmol e^- m^{-2} s^{-1}. µmol photons m^{-2} s^{-1}) and *M. pyrifera* (0.26 ± 0.02 to 0.31 ± 0.03 µmol e^- m^{-2} s^{-1}. µmol photons m^{-2} s^{-1}) for reproductive and vegetative phases, respectively. In red algae I. *cordata* (tetrasporophytic) and *M. laminarioides* (carposporophytic) values varied from 0.09 a 0.18 µmol e^- m^{-2} s^{-1} . µmol photons m^{-2} s^{-1}. The relative maximum electron transfer rate (rETR max) differed significantly for brown algae in *L. flavicans* (8.10 ± 0.84 to 12.40 ± 1.57 µmol e^- m^{-2} s^{-1}) and *M. pyrifera* (6.49 ± 1.30 to 12.89 ± 1.53 µmol e^- m^{-2} s^{-1}1) in distinct development phases. Saturation irradiance (E_k) analysis showed significant differences for *D. antarctica*

(reproductive phase) varying from 166.18 ± 14.33 (vegetative) to 132.98 ± 18.43 µmol photon m^{-2} s^{-1}.The highest concentrations of pigments in brown algae were found in *M. pyrifera* (reproductive phase) with 35.36 ± 0.21 of Chl *a*, 7.04 ± 0.93 of Chl *c* and 15.75 ± 1.42 µg g^{-1} of fucoxanthin. Finally in brown algae the highest concentrations of total FAs were 35.24 ± 2.38 % (saturated) and 22.02 ± 1.95 % (monounsaturated) in *M. pyrifera* and 63.53 ± 3.36 % (polyunsaturated) in *D. antarctica*. Results showed in red algae that total lipids varied between 1.25 to 2.72 % while FA classes were distributed from 23.34 to 59.93 %, 11.20 to 18.47 % and 21.60 to 65.47 % for saturated, monounsaturated and polyunsaturated FAs, respectively. The data how that differences in photosynthetic parameters, pigment concentration and fatty acid profile species are related with as habitat and development phase of the algae.

Keywords: Polyunsaturated – Rhodophyta – Ochrophyta – Pigments - photosynthetic performance

Lista de Figuras

Capitulo 1 Introdução Geral

Lista de tabelas

Lista de abreviaturas

AFC	Aloficocianina
Alfa	Eficiência Fotossintetizante
Beta	Fotoinibição
EPA	Ácido Eicosapentaenóico
ETR	Taxa de Transporte de Elétrons
ETR_{max}	Fotossíntese máxima
FAME	Fatty Acids Methyl Esters
FC	Ficocianina
FE	Ficoeritrina
F_m	Fluorescência Máxima de uma Planta Aclimatada ao Escuro
F_m'	Fluorescência Máxima de uma Planta Aclimatada à Luz
F_0	Fluorescência Basal de uma Planta Aclimatada ao Escuro
F'_0	Fluorescência Basal de uma Planta Aclimatada à Luz
E_K	Irradiância de Saturação
CG/DIC	Cromatografia gasosa com detector por ionização em chama
NPQ	Dissipação Não-Fotoquímica
PAM	Pulso de Amplitude Modulada
PS	Pulso de Luz Saturante
PSI	Fotossistema I
PSII	Fotossistema II
RQE	Rendimento Quântico Efetivo
n-3	Ômega 3
n-6	Ômega 6

Índice

Capitulo 2 - Pigment concentration, photosynthetic performance and fatty acid profile of Sub-Antarctic brown macroalgae in different phases of development from the Magellan Region, Chile.

Capitulo 3 - Fatty acids of subantarctic red algae at different development stages.

Capitulo 4 - Photosynthetic performance and pigment concentration of three Rhodophyta species in different development phases of the Magellan Region.

1. Introdução Geral

1.1 Algas

1.1.1 Fatores Abióticos

A radiação solar ou também conhecida como irradiância solar pode ser definida como o fluxo de energia radiante emitido pelo Sol que atinge a terra em forma de radiação eletromagnética. Esta energia solar anteriormente explorada somente por organismos fotossintetizantes para suas necessidades metabólicas, hoje se encontra como uma das grandes alternativas de energia renovável para suprir a grande demanda energética causada pelo aumento populacional e redução de recursos não renováveis (Kannan e Vakeesan, 2016).

A energia que atinge a estratosfera, maior camada com incidência de ozônio (O_3) segue três caminhos distintos, isto é, pode sofrer espalhamento, causado por partículas de aerossóis e por nuvens contendo cristais de gelo, pode sofrer também reflexão e por último pode ser absorvida. O total de energia que chega a terra em média na superfície é de 71 %, provenientes do espalhamento (23 %) e de absorção (48 %), sendo que 29 % retorna ao espaço como reflexão (NASA, 2009).

A radiação eletromagnética que chega a superfície da Terra basicamente é a forma de energia produzida por oscilações elétricas e magnéticas ou por movimento de partículas eletricamente carregadas propagadas no vácuo (Howell, Menguc e Siegel, 2015). Estas ondas apresentam características especificas como amplitude, comprimento de onda e frequência (Cifra, Fields e Farhadi, 2011). Essa ampla faixa de comprimentos de onda é conhecida como espectro eletromagnético, a qual definimos como a faixa de frequências da radiação eletromagnética com seus respectivos comprimentos de ondas (Fig. 1).

O espectro eletromagnético é dividido em sete regiões, desde raios gama (y) até ondas de rádio, e representam faixas de radiação em ordem decrescente de comprimento de onda, aumento de energia e frequência. Nesta região do espectro existe uma pequena faixa considerada a única detectável ao olho humano e assimilável pelos organismos fotossintetizantes, chamada de luz visível (UV). Esta região é formada por cores, onde cada uma apresenta um comprimento de onda diferente que vai de 380 (violeta) até 700 nm (vermelho) (Singhal et al., 1999).

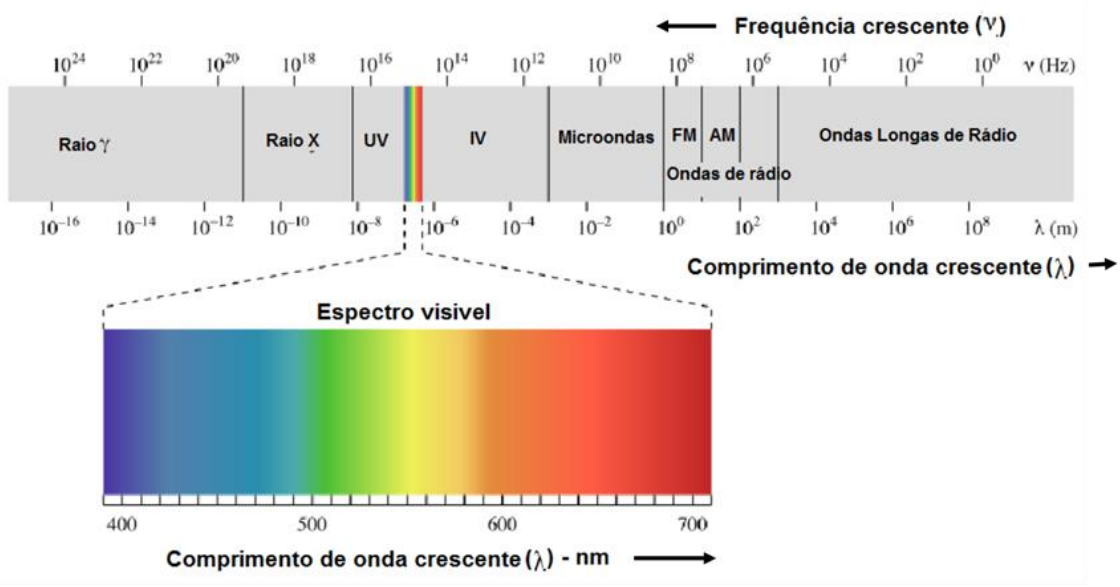

Figura 1 – Espectro eletromagnético com as faixas de frequências da radiação eletromagnética e seus respectivos comprimentos de ondas (Adaptado de Santana e Santos, 2017).

Os organismos fotossintetizantes que transformam esta energia radiante em energia química, tais como as algas, apresentam comportamento diferenciado na captação de energia entre as espécies, exemplo disso temos as diatomáceas (algas pardas) que apresentam a fucoxantina como um pigmento acessório capaz de absorver a luz na região do azul - verde ao amarelo – verde (Fu et al., 2017). Algumas algas verdes como as espécies *Scenedesmus quadricauda* em estudos de irradiância utilizando luz vermelha e azul, exibiram melhor desenvolvimento entre os comprimentos de onda de 450 – 490 nm (azul), mostrando que o acúmulo de biomassa e a concentração pigmentos e clorofila *a* (Chl *a*) está relacionada a composição espectral que o organismo está exposto (Leonardi et al., 2018). Em algas Rhodophytas como *Gigartina skottsbergii,* que habita regiões intertidais (>10 m) a absorção de luz pelas ficobiliproteínas ocorre principalmente no comprimento de onda azul (450 – 490 nm), zona de melhor eficiência fotossintética e que estimula principalmente o acúmulo de ficoeritrinas (FE) (Yokoya et al., 2007; Marambio et al., 2017).

Inúmeros trabalhos relatam que não somente a composição espectral exerce mudanças fisiológicas nas algas, mas fatores como intensidade e poder energético de radiação por tempo de exposição, habitat e a sazonalidade que atuam sobre estes organismos podendo também causar variações estruturais e metabólicas de maior

veemência. Espécie de algas pardas intertidais *Ascophyllum nodosum*, *Fucus vesiculosus* e *Fucus distichus* subsp. *edentatus* (Pyl.) analisadas perto de Mont-Joli (Québec, Canada) por Fluorômetro de Amplitude Modulada para fotossíntese em condições de campo, mostraram que o estresse destes organismos é ocasionado pelo tempo de emersão associados a outros fatores abióticos como aumento da temperatura e velocidade do vento. Algas encontradas nas regiões intertidais baixas, próximos as rochas, apresentam uma condição, menor de estresse e desenvolvem a fotossíntese de forma mais eficiente (Lamote, Johnson e Lemoine, 2012).

A sazonalidade tem se apresentado também como um dos principais fatores que atuam diretamente no metabolismo das algas, principalmente em regiões polares como a Antártica que apresentam os verões com grandes períodos de luminosidade e invernos com quase nenhuma radiação luminosa. Regiões sub-Antárticas apresentam algumas similaridades ao clima Antártico, onde locais da Patagônia Chilena podem ter até 17 h de luminosidade no verão (dezembro) e menos de 7 horas no inverno (junho) (Armada del Chile, 2018). Estes locais têm apresentado grande incidências de intensidade de raios ultravioletas da classe A e B (UVA e UVB), principalmente decorrentes da redução acentuada da camada de ozônio.

O termo buraco na camada de ozônio não representa uma zona totalmente isenta de ozônio e sim um afinamento nesta camada, onde 220 unidades Dobson (UD) é considerado unidade básica padrão de referência para monitorar a qualidade da camada de ozônio na Terra, segundo a NASA.

No ano de 1979 quando se começou os estudos sobre a camada de ozônio ocorria uma concentração de 194 UD, posteriormente na década de 80 e 90 o decréscimo nesta camada foi rápido e acentuado, sendo que em setembro de 1994 ocorreu a maior profundidade nesta camada apresentando uma concentração de 74 UD, porém dados atuais mostram que no século XXI as concentrações se mantiveram estáveis. A figura 2 representa dados da atualidade sobre o buraco de ozônio nos hemisférios norte e sul, onde as colorações entre vermelho e laranja representam as maiores concentrações de ozônio e as colorações entre azul e violeta, apresentam as menores concentrações deste gás na atmosfera terrestre (NASA, 2019).

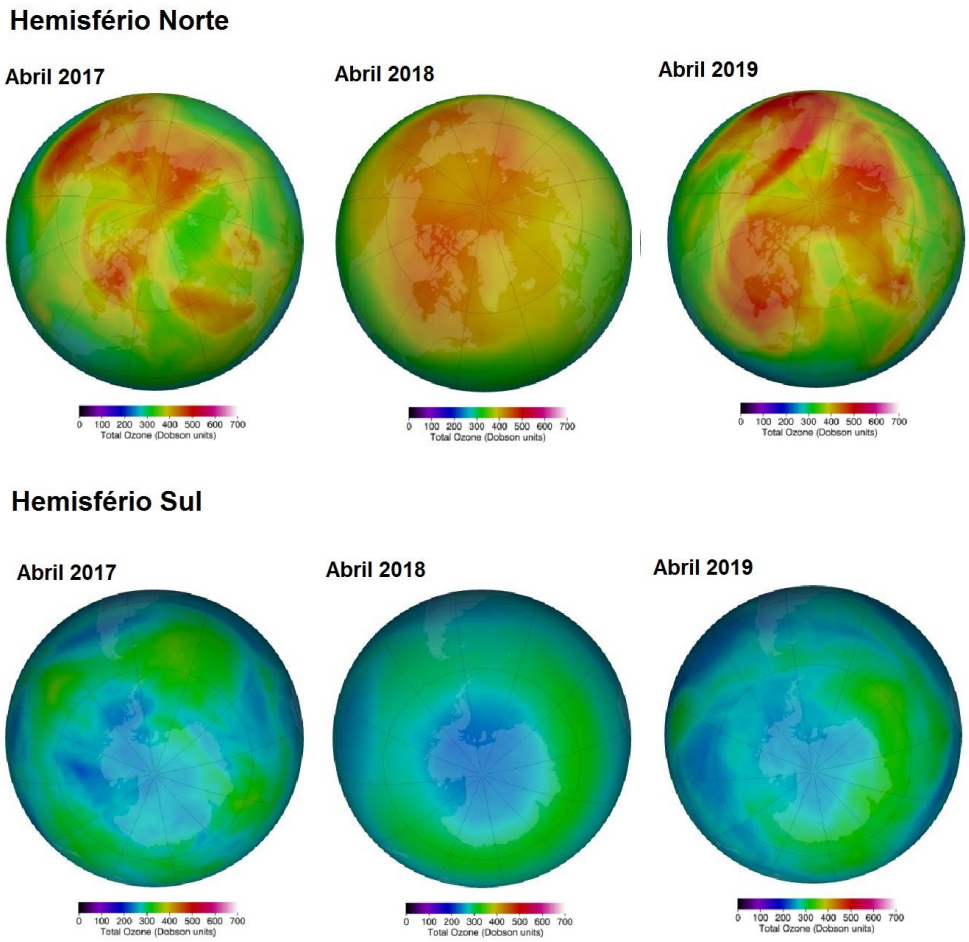

Figura 2 – Representação da redução da camada de ozônio nos Hemisférios Norte e Sul da Terra. Coloração amarela e laranja demonstram maior concentração de ozônio na estratosfera e cores azuis e violetas demonstram redução na camada de ozônio (NASA, 2019).

Alguns trabalhos demostram que a intensidade alta de raios UV, que chegam a Terra ocasionadas pela depleção da camada de ozônio e que incidem sobre todos os organismos vivos, entre eles as algas, bactérias fotossintetizantes e fitoplâncton são extremamente prejudiciais, principalmente os raios UVB, que atuam negativamente no metabolismo, podendo provocar degradação de pigmentos, modificações no metabolismo do nitrogênio (Zubia, Freile-Pelegrín e Robledo, 2014) e até mesmo danos irreparáveis ao DNA (Rastogi et al., 2010).

Os raios UV quando incidem nos oceanos tendem a penetrar com intensidades diferentes nas camadas de água e esta penetração está relacionada principalmente ao tipo de radiação que será absorvida pelos pigmentos de cada espécie de alga (Sarmiento e Gruber, 2006). O espectro de luz na faixa de 600 a 700 nm (vermelho)

quando penetra nos oceanos, acaba desaparecendo rapidamente a poucos metros, sendo que somente as radiações verde e azul tendem a chegar na zona de compensação, onde poucos organismos fotossintetizantes habitam.

A zona de compensação nos oceanos, que se encontra entre a zona eufótica (~100 m) e zona afótica (> 200 m), pode ser definida como a profundidade que a radiação espectral (400 – 700 nm) alcança e a radiação fotossintética (PAR) é 1 % da zona de superfície (~100% %). Essa penetração de raios UVB (280 – 315 nm) e UVA (315 – 400 nm) nos oceanos é medida através do coeficiente de atenuação (K_d) que representa a distribuição angular da luz incidente e coeficientes de absorção e retrodifusão da água.

Alguns efeitos deletérios da intensidade dos raios UV que atuam sobre as algas em regiões intertidais ou sublitorais altas são principalmente o estresse oxidativo e o branqueamento que provoca principalmente a decomposição da clorofila *a*, podendo causar consequente a senescência e morte celular (Cheloni e Slaveykova, 2018). A diminuição da concentração de clorofila *a* e pigmentos fotossintetizantes resultam no decréscimo de biomassa, provocando a redução no crescimento destes organismos. Porém, algumas algas vermelhas e cianobactérias desenvolveram mecanismos adaptativos de prevenção e reparo contra os danos causados pelos raios UVB.

Estes organismos utilizam pigmentos como as ficoeritrinas (FE) na função de agente modulador da captação de energia, isto é, a ficobiliproteína (PBP) tem a capacidade de redirecionar o excesso de energia na forma de autofluorescência, evitando sua chegada ao fotossistema II (PSII). Este mecanismo de audefesa evita danos ao sistema fotossintético onde o acumulo de PBP em determinados órgãos dos organismos fotossintetizantes tem a função de fotoproteção (Xue et al., 2015).

As radiações que incidem sobre todo o ser vivo são formadas por unidades simples de partículas sem massa e que viajam num padrão de onda na velocidade da luz, os fótons. Cada unidade carrega uma quantidade de energia que define o tipo de radiação, isto é, ondas de rádio contém fótons de baixa energia, enquanto raios ultravioletas, raios X e gama contém fótons de alta energia (Cifra, Fields e Farhadi, 2011). Os fótons serão as partículas de energia que participarão diretamente no processo mais importante executado pelos organismos fotossintetizantes, a fotossíntese.

1.1.2 Fotossíntese

A fotossíntese pode ser considerada o único processo biológico realizado por organismos fotossintetizantes com capacidade de captar luz e transformar em energia química necessária para inúmeras reações metabólicas. Os processos fotossintéticos em organismos eucariotos ocorrem em estruturas especializadas denominadas de cloroplastos que são os plastídios mais comuns. Internamente, estas estruturas possuem membranas achatadas que formam um conjunto de sacos intercomunicáveis denominadas de tilacóides (Larkum, Douglas e Raven, 2003).

Os tilacóides são as estruturas responsáveis por conter em sua superfície os pigmentos acessórios e principalmente a clorofila, sendo considerado o local onde começas o processo fotossintético. Estas estruturas como as demais organelas existentes nos cloroplastos provêm de um processo endossimbiótico que evoluiu junto com as algas e plantas superiores tornando esta estrutura diferenciada entre alguns organismos.

Nas algas verdes, pardas e demais plantas os tilacóides se apresentam de forma empilhada juntamente com os complexos coletores de luz contendo na sua membrana principalmente clorofila *a*, *b*, *c* de acordo com a espécie. No filo Rhodophyta, cianobactérias e Glaucophytas (algas de água doce) os tilacóides não se apresentam empilhados e contém complexos coletores de luz diferenciados, os ficobilissomas que contem clorofila *a* e ficobiliproteinas. A divisão Glaucophytas apresenta plastos modificados, com uma fina e residual membrana de pepidioglicanos os quais são denominados, cianelas (Larkum, 2016).

Nas algas em geral ocorre além das clorofilas normais um outro tipo de clorofila *a* especial responsável pela captação e absorção de energia em comprimentos de onda diferenciados para a realização das reações fotoquímicas no fotossistema II (PSII). O local onde esta clorofila *a* se encontra é denominado centro de reção do PSII, em Rhodophytas e cianobactérias se encontram abaixo dos ficobilissomas. Todos os pigmentos inclusive as clorofilas têm a capacidade de absorção de energia, porém somente a clorofila *a* especial tem a capacidade de realizar as reações no centro de reação com liberação de elétrons para a cadeia transportadora de elétrons entre os fotossitemas. O conjunto formado pelo centro de reação, clorofila *a* e pigmentos acessórios formam uma estrutura especializada em captar a energia solar com maior eficiência, o qual denominamos de complexo antena (Gantt, Grabowski e Cunningham, 2003).

Em todos os organismos fotossintetizantes o complexo antena se localiza na região superior de complexos fotoquímicos conhecidos como fotossistemas. Atualmente são conhecidos dois fotossistemas o qual chamamos fotossistema I ou PSI (P700) com uma ótima absorção em 700 nm e o fotossistema II ou PSII (P680) que absorve em 680 nm. Os dois fotossitemas trabalham interligados através do transporte de elétrons, para a realização das reações de armazenamento de energia da fotossíntese (Heldt e Piechulla, 2011).

O processo de reações da fotossíntese começa no PSII, onde este centro de reação recebe um quanta (e) de energia que provoca a excitação dos elétrons. Esta energia ocasionada pela excitação é transferida pelos elétrons até o primeiro receptor primário a feofitina (Phe) que fica com carga negativa (Phe^-) e converte o PSII ao estado oxidado ($P680^+$). Os elétrons neste momento são transferidos para as plastoquinonas A (Q_A) e posteriormente para a quinona B (Q_B) que ao receber os elétrons e íon H^+ passam ao seu estado reduzido (Q_BH_2). A Q_BH_2 transfere íon H^+ para a o citocromo *b*$_6$*f* que posteriormente transfere elétrons para a plastocianina (PC) e os íons H^+ para os tilacóides. Os elétrons da PC são transferidos ao PSI para que ocorra a redução da P700 em P700* (forma excitada). No PSI ocorre a transferência de elétrons ao receptor final, o $NADP^+$ para formação do NADPH (Heldt e Piechulla, 2011) (Fig. 3).

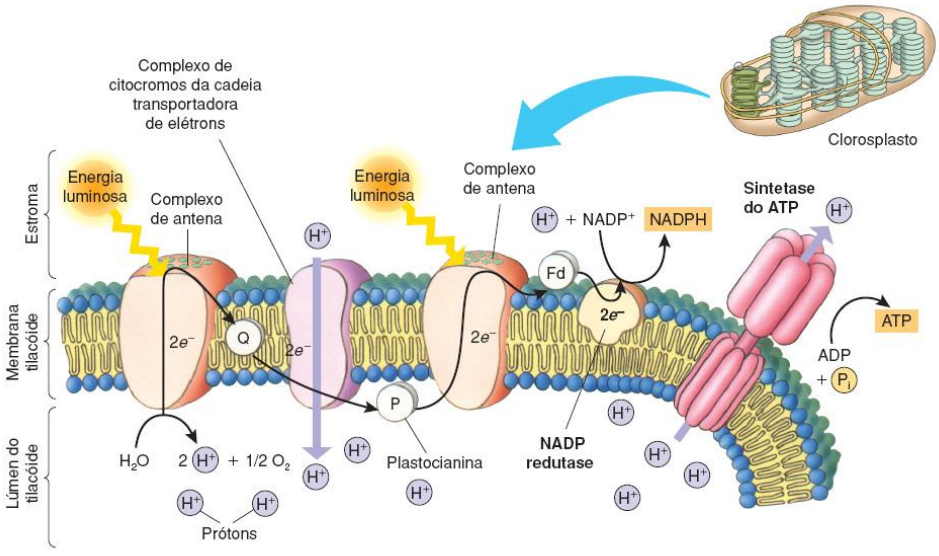

Figura 3 – Representação gráfica simplificada da membrana fotossintética com a captação de energia e fluxo de elétrons entre os dois fotossitemas PSI (P700) e o PSII (P680) através da cadeia transportadora de elétrons e seus respectivos centros de reações fotoquímicas; P - plastocianina; Q – plastoquinona; Fd – ferrodoxina solúvel;

NADP (nicotinamida adenina dinucleótido fosfato); ADP (adenosina difosfato); ATP (adenosina trifosfato); Pi (fosfato inorgânico) (Silva, 2016).

A radiação solar que beneficia os organismos fotossintetizantes com energia luminosa para que seja transformada em energia química, pela fotossíntese, e com isso ocorra os processos metabólicos, pode ser ao mesmo tempo prejudicial. O excesso de energia luminosa causa condições adversas de estresse a estes organismos, provocando o que chamamos de fotoinibição, ou basicamente a inibição da fotossíntese por excesso de luz (Raven, 2011).

A dinâmica do processo fotossintético esta relacionado a escala de tempo, onde uma fotoresposta rápida ocorre em minutos, uma fotoinibição pode ocorrer em horas e uma fotoadaptação leva dias para que ocorra. Segundo Han et al., (2000) a fotoinibição ocorre principalmente na cadeia transportadora de elétrons e atua diretamente no PSII e a fotoadaptação esta relacionada a mudança na composição fisiológica e bioquímica do processo de captação de luz. Estes dois processos estão ligados pontualmente e exercem efeitos diretos na produção fotossintética.

O processo de fotoinibição pode ocorrer de forma dinâmica e descreve todas as reações que diminuem a eficiência da fotossíntese quando expostas a um determinado nível de radiação sendo reversível em um curto período de tempo ou pode ocorrer na forma crônica onde o processo de recuperação é lento e pode levar um longo período de tempo para que ocorra a reversão após exposição prolongada a fluxos excessivos de fótons. Este processo afeta o rendimento quântico potencial máximo do PSII (F_v/F_m) e expressa uma condição de estresse do organismo fotossintetizante (Werner, Correia e Beyschlag, 2002).

A fotoinibição ocorre principalmente quando a taxa de inativação e fotodano excedem a taxa de reparo do PS II, isto é, a taxa de reparo de PS II depende criticamente da síntese de novos compostos como a proteína D_1, religação de pigmentos e cofatores, bem como a reativação do fluxo de elétrons no fotossistema (Niyogi, 2009). Alguns trabalhos reportam que a taxa de fotodano aumenta linearmente com a densidade do fluxo de fótons, sugerindo que após a saturação do centro de reação, cada fóton absorvido danifica mais o fotossistema (Park et al., 1995).

Proteínas como a D_1 e D_2 que fazem parte dos centros de reação do PSII sofrem oxidações geradas por espécies reativas de oxigênio (ROS) (Nanba e Satoh,1987), porém não são totalmente degradadas, somente danificadas, e com isso são novamente sintetizadas e substituídas por novas proteínas A presença

principalmente da proteína D_1 é crucial no centro de reação, pois atua como componente estrutural e multifuncional mediando o transporte de elétrons e a evolução da taxa de oxigênio (Oncel, Kose e Faraloni, 2015). A redução de plastoquinona e oxidação da água no PSII causam um acúmulo de radicais oxidantes, incluindo ROS que aumenta com a intensidade de luz provocando a fotoinibição e reduz a capacidade fotossintética de qualquer organismo fotossintetizante (Edelman e Mattoo, 2008).

1.2 Algas

A expressão alga representa organismos provenientes de um grupo polifilético em sua maioria eucariontes, porém com representantes também procariotos, tais como as cianobactérias. Segundo a Ficologia, área especializada da Botânica que estuda as algas, estes organismos são talófitas, que podem se apresentar de formas unicelulares ou multicelulares, vivendo em aguas doces ou salgadas, são em sua grande maioria fotossintetizantes, contendo principalmente em seus pigmentos a clorofila *a* (Lee, 2008).

O ciclo reprodutivo, a anatomia e principalmente os inúmeros pigmentos como os carotenoides e ficobiliproteinas (pigmentos proteicos) que absorvem a energia solar no espectro de luz visível (UV – 400 a 700 nm) em diferentes comprimentos de onda, sempre foram as principais características utilizadas na separação entre os Filos Chlorophytas, Ochrophytas e Rodophytas (Pratama et al., 2015). Porém hoje o estudo de grupos químicos do metabolismo primário e secundário de algas vem sendo utilizado também para diferenciar estes grupos (Ocaranza-Barrera et al., 2018).

Vários estudos demonstram, porém, que as flutuações no ambiente como variação de salinidade, pH, temperatura, nutrientes e principalmente a irradiância solar, são fatores que muitas vezes modificam o metabolismo das algas e principalmente a concentração de pigmentos para uma melhor absorção e consequente metabolização. Alguns pigmentos são caractristicos de cada espécie e excercem funções diferenciadas nas algas, sendo o principal pigmento encontrado em todos os organismos fotossintetizantes é a clorofila *a*. Estudos mostram que existem outros tipos de clorofila como a clorofila *b* (Chl *b*), *c* (Chl *c*), *d* (Chl *d*) em cianobactérias, a clorofila *f* (Chl *f*) descoberta em 2010 em estromatólitos e ainda algumas variante da clorofila *c*, tais como a clorofila c_1 (algas castanhas, diatomáceas e dinoflagelados), c_2 (dinoflagelados e criptomonados) (Jeffrey, 1976) e c_3 em

cocolitoforídeos (algas unicelulares do fitoplâncton) (Fookes e Jeffrey,1989) (Fig. 4 **a** e **b**).

a

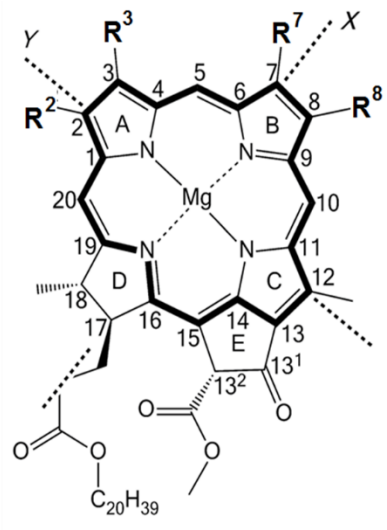

Chl	R^2	R^3	R^7	R^8
Chl *a*	CH_3	$CH=CH_2$	CH_3	CH_2 - CH_3
Chl *b*	CH_3	$CH=CH_2$	CHO	CH_2 - CH_3
Chl *d*	CH_3	CHO	CH_3	CH_2 - CH_3
Chl *f*	CHO	$CH=CH_2$	CH_3	CH_2 - CH_3

b

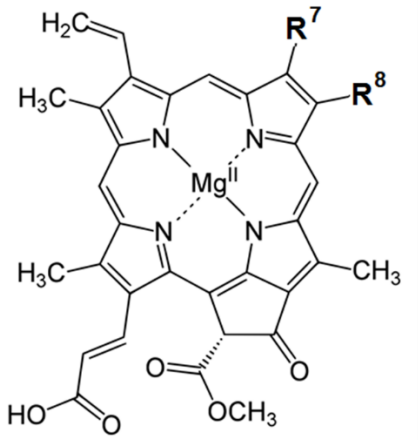

Chl	R^7	R^8
Chl c_1	CH_3	CH_2 - CH_3
Chl c_2	CH_3	$CH=CH_2$
Chl c_3	$COOCH_3$	$CH=CH_2$

Figura 4 – **(a)** Estrutura química da Chl *a*, Chl *b*, Chl *d* e Chl *f* com as ligações duplas conjugadas destacado os planos X e Y (eixos) pelo sistema de numeração da IUPAC. **(b)** Estrutura química da Chl c_1, Chl c_2 e Chl c_3 com as ligações duplas e sistema de numeração da IUPAC (Adaptado de Sawicki, Willows e Chen, 2019).

Os fatores abióticos, bióticos, sazonalidade entre outros, podem influenciar diretamente uma espécie, fazendo com que indivíduos se utilizem de estratégicas fisiológicas, bioquímicas e modificações anatômicas em respostas ao estresse ambiental como forma de adaptação aos mais diversos ambientes, tornando muitas

vezes um indivíduo com características peculiares a uma determinada região (Mendéz, 2017).

As algas apresentam grande tolerância a variações sazonais, de pH, O_2 e CO_2 (Barsanti et al., 2007) podendo ser encontradas em locais úmidos, em lagos, mares e oceanos, habitando zonas intertidal, bentônicas (López-Cristoffanini et al., 2015), supralitoral, sublitoral, zonas de pulverização (Satyam eThiruchitrambalam, 2018) ou simplesmente na suspensão na coluna de água formando o fitoplâncton (Brothers, Vadeboncoeur e Sibley, 2016).

Na sua nutrição, algumas algas se utilizam de sistemas de captação de energia solar, chamadas de fototróficas. Neste sistema a luz solar é captada servindo como fonte de energia e o CO_2 como fonte de carbono para produção de ATP. Muitas destas algas quando estão em regiões com pouca luminosidade podem se utilizar de sistemas osmotrófico ou fagotrófico como complemento em suas necessidades nutricionais (Sahoo e Baweja, 2015).

Algumas espécies de algas apresentam limitações na síntese de substâncias como a glicose a partir da energia solar, necessitando de outros alimentos para suprir suas necessidades, são organismos heterotróficos obrigatórios (Barsanti et al., 2007). Outras algas, porém, adaptaram seu sistema nutricional paralelamente a sua evolução, mantendo os dois sistemas de nutrição, fototrofismo e heterotrofismo no mesmo organismo, são as chamadas mixotróficas. Muitas se utilizam de aminoácidos e ácidos graxos encontrados nos locais onde vivem para manter sua taxa de crescimento e proteção em ambientes diversificados (Cardozo et al., 2011).

No mesmo sentido que o sistema nutricional das algas se adaptou às diferentes situações bióticas e abióticas, o sistema reprodutor também evoluiu, apresentando-se de modo variado e permitindo que a reprodução no meio algal seja rápida. Neste sentido muitas espécies apresentam como meio reprodutivo a forma vegetativa por divisão celular e a forma sexuada com produção de esporos, zoósporos, se forem flageladas, e aplanósporos se não possuírem flagelo (Sahoo e Baweja, 2015).

1.2.1 Caracterização dos Filos Ochrophyta e Rhodophytas

Filo Ochrophyta

O Filo Ochrophyta onde está inserida a classe Phaeophyceae ou algas pardas, apresentam algumas particularidades importantes que caracterizam este filo, tais como, a presença de manitol e laminarina como substância de reserva, pigmento fotossintetizante principal como a clorofila *a* e pigmentos acessórios como a clorofilas c_1, c_2 , β caroteno, violaxantina, zeaxantina e principalmente fucoxantina, a qual se apresenta em maior quantidade entre os pigmentos acessórios e dá a coloração amarronzada as algas pardas (Lee, 2008).

Pode se apresentar desde formas filamentosas ramificadas, que se dividem entre filamentos de fixação do talo até filamentos especializados para fotossíntese, bem como, talos pseudoparenquimáticos que forma estrturas aglomeradas amorfas e parenquimáticos com divisões celulares multiplanares formando estruturas em forma de talos ou laminares, podendo gerar indivíduos de vários metros (ex:. *Macrocystis pyrifera*, 60 m), não ocorrendo espécies unicelulares e nem coloniais. Apresenta em sua parede celular uma fração sólida constituída de pequenas fibrilas de celulose e alginato e uma parte membranosa composta de alginato e fucoidanas (Harper et al., 2012).

A presença de algas pardas, hoje com aproximadamente 300 gêneros e mais de 2000 espécies ocorre principalmente em aguas marinhas desde regiões tropicais a zonas frias como Antártica e regiões sub-Antárticas, sendo que somente quatro gêneros são de aguas doces, sendo eles: Pleurocladia, Heribaudiella, Bodanella e poucas espécies do gênero Ectocarpus (Appeltans et al., 2012).

As algas pardas apresentam células reprodutivas móveis contendo dois flagelos, um plumoso e um simples, que facilitam sua locomoção no momento da fecundação. O ciclo de vida da classe Phaeophycea apresenta alternância de gerações isomórficas ou heteromórficas principalmente nas subclasses Isogeneratae e Heterogeneratae, porém na suclasse Cyclosporeae não corre alternância de gerações de vida livre. A reprodução ocorre de forma gamética, espórica ou vegetativa, sendo que os gametas podem apresentar isogamia, anisogamia ou oogamia (Harper et al., 2012).

As espécies em estudo, *M. pyrifera* e *Lessonia flavicans* que pertencem a ordem Laminariales apresentam reprodução sexuada por isogamia (Heterogeneratae) onde os órgãos uniloculares, os zooesporângios, se desenvolvem sobre a porção laminar sempre reunidos em soros. O gametófito se apresenta filamentoso e ramificado de tamanho microscópico e o anterozoide são formados em órgãos pluriloculares. As oosferas são formadas isoladamente com fecundação externa (AlgaeBase: http://www.algaebase.org).

A espécie *Durvillaea antarctica* da ordem Fucales, não apresenta alternância de gerações, sendo os gametas formados na parte interna de órgãos unilocurales do esporófito. A reprodução em Cyclosporeae sempre é sexuada e oogâmica. Todos os órgãos reprodutores são formados na parte interna de estruturas chamadas conceptáculos, se apresentam isolados ou em ramos, quando férteis são denominados receptáculos. Os conceptáculos se encontram sempre nas extremidades dos ramos, onde cada oogônio contém 8 oosferas (AlgaeBase: http://www.algaebase.org).

Filo Rhodophyta

O Filo Rhodophyta apresenta como uma das características principais a presença de um polissacarídeo como substância de reserva encontrado somente em algas vermelhas, chamado de amido das florídeas. Apresenta clorofila *a* como principal pigmento fotossintetizante e pigmentos acessórios encontrados nos ficobissomos, como *β*-caroteno, zeaxantina, anteraxantina, luteína, além de pigmentos proteicos encontrados sobre os tilacóides, como as ficobilinas, entre elas, as ficoeritrina, ficocianina, aloficocianina que em muitas algas vermelhas devido sua alta concentração inibem a coloração de outros pigmentos e dão a coloração avermelhada característica das rodófitas (Sharif et al., 2017).

A parede celular destas algas apresenta celulose, em forma de microfibrilas (interna) e outros dois polissacarídeos de grande interesse comercial o ágar e as carragenanas, que formam a parte mucilaginosa (externa). São algas que vão de uma organização unicelular, com poucos representantes, até a grande maioria que são multicelulares, podendo ter o talo filamentoso uni ou multisseriados, apresentando ou não ramicações, podendo ser foliáceo ou pseudoparenquimatoso (Cecere, Petrocelli e Verlaque, 2011).

Sua distribuição pode ocorrer desde zonas, temperadas equatoriais até regiões polares como a Antártica, o Ártico até regiões sub-Antárticas. O ciclo reprodutivo de rodófitas pode ser vegetativo, gamético ou espórico, onde a reprodução vegetativa ocorre por fragmentação do talo, na reprodução espórica ocorre através da formação de monósporos, bisporos, tetrásporos e polísporos, sendo todos sem mobilidade flagelar (aplanósporos). A reprodução gamética ocorre por oogamia onde o oogônio recebe o nome de carpogônio que apresenta uma estrutura prolongado chamado de tricogina com a função de captar os espermácios (Cecere, Petrocelli e Verlaque, 2011).

Este filo em especial pode apresentar alternância de gerações em modo difásico ou trifásico, dependendo das espécies. No modo difásico o gametófito haplóide (*n*) é diferente do esporófito (2*n*) morfologicamente, sendo chamado de geração heteromórfica. A fase gametofítica é foleacea e macroscópica e a fase esporofítica chamada de "*conchocelis"* se apresenta de forma microscópica e filamentosa. O gametófito haplóide (*n*) irá produzir os gametas masculinos chamados de espermácios e as os femininos de carpogônios, onde estão a oosfera (Lee, 2008).

Os espermácios são liberados e irão fecundar a oosfera produzindo um zigoto diplóide (2*n*), o qual irá sofrer mitoses formando os carpósporos que germinarão e formarão o esporófito diplóide (2*n*), estes produzirão os esporângios que por meiose irá dar origem a células haplóides (*n*) chamadas de conchósporos, os quais germinarão e produzirão os gametófitos (fase foliácea). O ciclo de vida com alternâncias de gerações trifásico foi uma evolução das algas, onde teria uma geração haplóide (*n*), uma geração diplóide (2*n*) e surgiu uma terceira geração, sendo denominada de diplobionte com geração trifásica. Nesta geração os gametófitos masculinos com haploidia (*n*) proveniente de um indivíduo, produzem os gametas masculinos chamados de espermácios, que serão liberados pelos gametângios masculinos e fecundarão a oosfera, a qual faz parte do ramo carpogonial do gametófito feminino, também com haploidia (*n*) (Barsanti et al., 2007).

Após a fecundação da oosfera pelos espermácios será formado o núcleo zigótico que irá se desenvolver e formar a terceira fase do ciclo de vida das algas rodófitas. O zigoto irá se dividir mitoticamente formando a terceira fase carposporofitica de haploidia 2*n* e irá formar o carposporângio (2*n*), o qual liberará carposporos que germinarão e formarão uma fase adulta diplóide (2*n*), denominada de tetraesporófito. Os ramos terminais dos tetraesporófitos irão conter os

tetraesporângios que formarão por sucessivas meioses os tetraesporos com haploidia (*n*) que germinarão e formarão novos gametófitos masculinos e femininos (Lee, 2008).

1.2.2 Biossíntese de ácidos graxos poliinsaturados em macroalgas

As algas marinhas apresentam um grande potencial nutricional e farmacológico, de acordo com seus constituintes, mas os ácidos graxos vêm sendo estudados não somente como uma fonte nutricional, mas na utilização como alimentos nutracêuticos e em pesquisas contra inúmeras doenças. Os ácidos graxos, bem como seus produtos oxidados (oxilipinas) e esteróis fazem parte da classe de lipídeos de grande interesse para o metabolismo das algas. Estes lipídeos podem ser divididos em dois grupos de acordo com suas funções celulares, os lipídeos neutros e os lipídeos polares (glicolipideos e fosfolipideos). Sua principal função tem sido descrita na literatura como fonte energética, porém participam na constituição de membranas dos tilacóides nos cloroplastos (glicolipideos) e como constituintes em outras membranas celulares nas algas (MacDougall et al., 2011).

Na classe de lipídeos que apresentam importância ao metabolismo algal temos os três principais glicolipideos sintetizados que são os monogalactosildiacilglicerol (MGDG), digalactosildiacilglicerol (DGDG) e sulfoquinovosildiacilglicerol (SQDG), que representam os maiores constituintes em tecidos fotossintetizantes (Yunoki et al., 2009). Os triacilgliceróis, que são lipídeos neutros são considerados as maiores fontes de reserva energética para as algas (Khotimchenko, 2000).

Os principais ácidos graxos nestes organismos são os ácidos graxos poliinsaturados (PUFAs), porém em algumas espécies os ácidos graxos saturados (SFA) e monoinsaturados (MUFAs) são encontrados em maior concentração, que segundo alguns autores esta intimamente relacionado as diferentes diferenças sazonais, habitat, localização geográfica (Khotimchenko, Vaskovsky e Titlyanova, 2002; Santos et al., 2017) e ao seu ciclo de vida (Khotimchenko, 2006).

A biossíntese de ácidos graxos da série ômega nos organismos ocorre a partir do ácido palmítico (C16:0), o qual sofre alongamento na cadeia por enzimas alongases formando o ácido esteárico (C18:0). A Δ9 dessaturase atua acrescentando uma insaturação formando o ácido oleico (C18:1*n*-9). Em vegetais ocorre a presença de duas enzimas importantes que atuam no processo de dessaturação a Δ12 e a Δ15 dessaturase (Fig. 5). Estas enzimas não estão presentes em animais, impossibilitando

a formação do ácido *α*-linolênico (C18:3*n*-3) e do linoleico (C18:2*n*-6) no organismo humano (Vance e Vance, 2008)

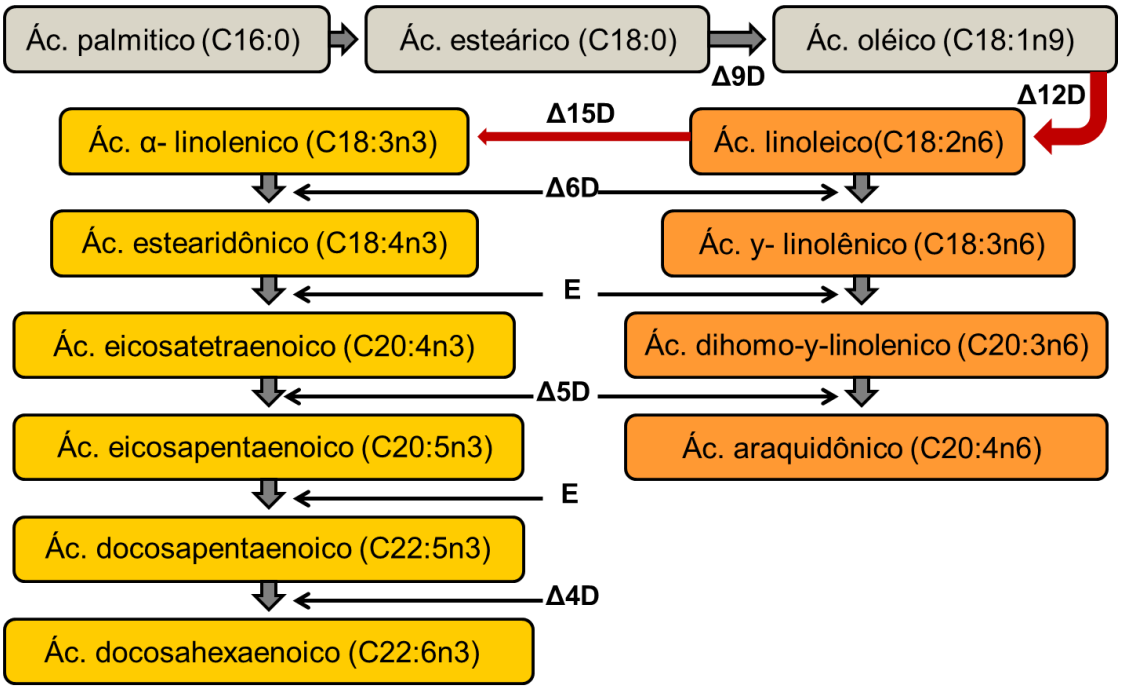

Figura 5 - Biossíntese de ácidos graxos poliinsaturados das famílias ômegas 3 e 6 em vegetais: Δ4D – enzima delta 4 dessaturase; Δ5D – enzima delta 5 dessaturase; Δ8D – enzima delta 8 dessaturase; Δ9D – enzima delta 9 dessaturase; Δ12D – enzima delta 12 dessaturase; Δ15D – enzima delta 15 dessaturase; E - enzimas elongase (Adaptado de Bishop et al., 2015).

Os ácidos essenciais *α*-linolênico (C18:3*n*-3) e linoleico (C18:2*n*-6) são formadores de ácidos graxos importantes das séries ômegas 3 e 6 como o eicosapentaenóico (C20:5*n*-3 - EPA) descrito como antiparasitário (Lira et al., 2016), anti-inflamatório (Fernando, Nah e Jeon, 2016), auxilia na prevenção da fibrose e disfunções cardíacas (Jakobsen et al., 2009; Chen, 2011) e em doenças graves como o câncer (Giros et al., 2009). O docosahexaenóico (C22:6*n*-3 - DHA), também formado pela síntese dos ácidos graxos essenciais, é particularmente importante no desenvolvimento neuronal de crianças prematuras e auxilia no melhor desenvolvimento de tecidos do cérebro e retina (San Giovanni e Chew, 2005).

Na série ômega-6 o ácido araquidônico (C20:4*n*-6) é precursor de moléculas sinalizadoras que atuam a curtas distâncias nas células, chamadas de tromboxanos, prostaglandinas, leucotrienos, hidroperóxidos e tem sua formação a partir da cascata do ácido araquidônico (Hammond e O'Donnell, 2012).

Estas moléculas sinalizadoras são produzidas em todo tecido humano e são responsáveis principalmente pelas respostas inflamatórias, contração do músculo liso do intestino e útero, alguns servem como vasodilatadores e outros como vasoconstritores, por isso estão ligados intimamente com a pressão sanguínea (Smith et al., 2009).

Hipóteses

1. A concentração de pigmentos e a performance fotossintética apresentam resultados diferenciados de acordo com a fase de desenvolvimento de Rhodophytas e Ochrophytas independentes das variações abiótica.

2. As algas pardas e vermelhas apresentam uma resposta diferenciada no perfil ácido graxo e lipídeos totais em decorrência de suas diferentes fases de desenvolvimento.

2. Objetivos

Objetivo Geral

Avaliar a performance fotossintética, concentração de pigmentos e perfil ácido graxo em três espécies de macroalgas pardas *Durvillae antarctica*, *Lessonia flavicans*, *Macrocystis pyrifera* e três macroalgas vermelhas *Gigartina skottsbergii*, *Iridaea cordata* e *Mazzaella laminarioides* em fases de desenvolvimento diferenciada da região sub-Antártica.

Objetivos Específicos

- Pesquisar e explorar a biodiversidade da região, seus recursos genéticos e bioquímicos de valor comercial;

- Coletar as algas em suas fases de desenvolvimento em curtos períodos de tempo (sazonalidade) e em locais próximos, evitando variação nos parâmetros a serem analisados em função de fatores abióticos;

- Avaliar os parâmetros de eficiência fotossintética nas algas *in vivo* após coleta utilizando um Fluorômetro Subaquático de Pulso Modulado (PAM) para verificar a fluorescência da clorofila *a;*

- Caracterizar por Cromatografia Gasosa por Ionização em Chama o perfil de ácidos graxos em cada fase distinta de desenvolvimento;

3 Materiais e Métodos

3.1 Coleta de Algas

Amostras de algas marinhas pardas e vermelhas foram coletadas entre os meses de dezembro de 2016 e março de 2017 na região do Estreito de Magalhães (Punta Arenas, Chile) (Fig. 3) sob maré baixa com auxílio de mergulho em profundidade (Fig. 4). As espécies analisadas do Filo Ochrophyta da ordem Fucales foram *D. antarctica* (53° 08S, 71° 30W), da ordem Laminariales foram *L. flavicans* (53° 36S, 70° 55W) e *M. pyrifera* (53° 36S, 70° 55 W) nas fases vegetativa e reprodutiva de desenvolvimento. As espécies do Filo Rodophyta pertencem a ordem Gigartinales e as espécies coletadas foram *Gigartina skottsbergii* (53° 36S, 70° 55W), *Iridaea cordata* e *Macrocystis laminarioides* (53° 43S, 70° 58W) nas fases gametofíticas, casposporofiticas e tetresporofiticas, como mostra os pontos de coleta nas Figuras 6 a 16.

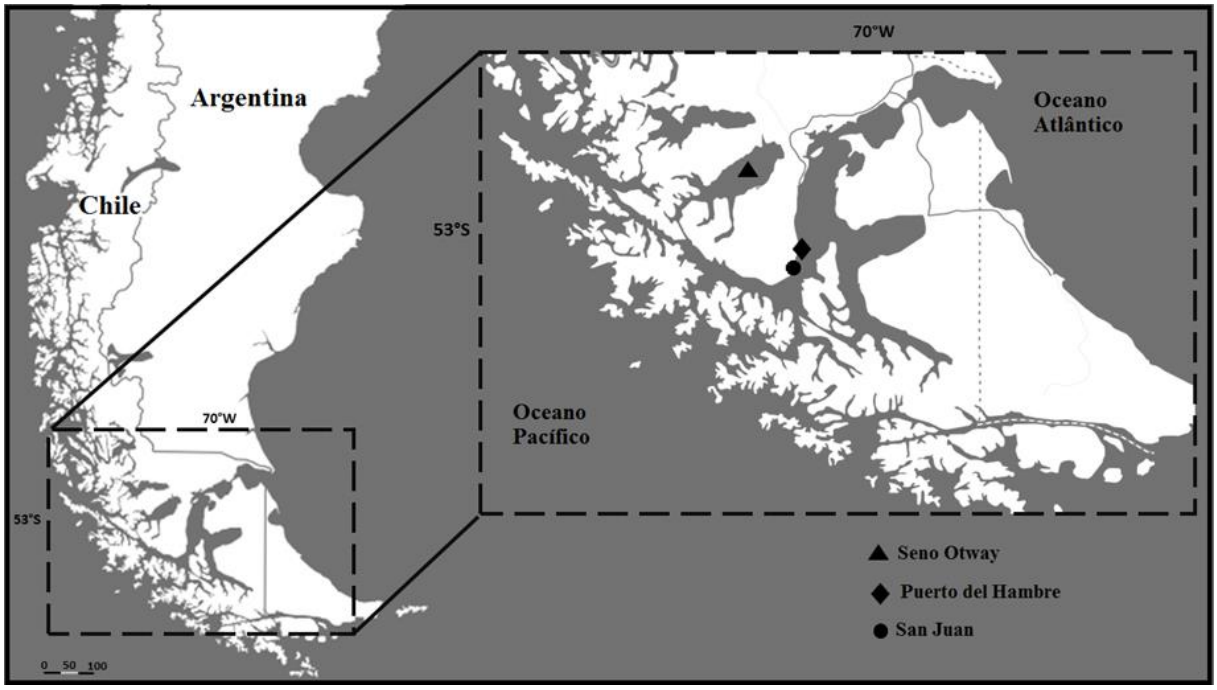

Figura 6 - Locais de amostragem no Estreito de Magalhães, região Subantártica do Chile: (a) Seno Otway (53° 08S, 71° 30W) coleta de *D. antarctica*; (b) Puerto del Hambre (53° 36S, 70° 55 W) coleta de *M. pyrifera*, *L. flavicans* e *G. skottsbergii*; (c) San Juan (53° 43S, 70° 58W) *I. cordata* e *M. laminarioides* nas fases vegetativa e reprodutiva.

Figura 7 – Coleta sob mergulho em profundidade na localidade de Puerto del Hambre (53° 36S, 70° 55W) das espécies *M. pyrifera*, *L. flavicans* e *G. skottsbergii* em fases vegetativas e reprodutivas.

Figura 8 –Aspecto geral da zona de coleta em Puerto del Hambre sob maré baixa (A) e (B); Substrato rochoso exposto sob maré baixa (C); Individuo de *M. pyrifera* na fase vegetativa (D).

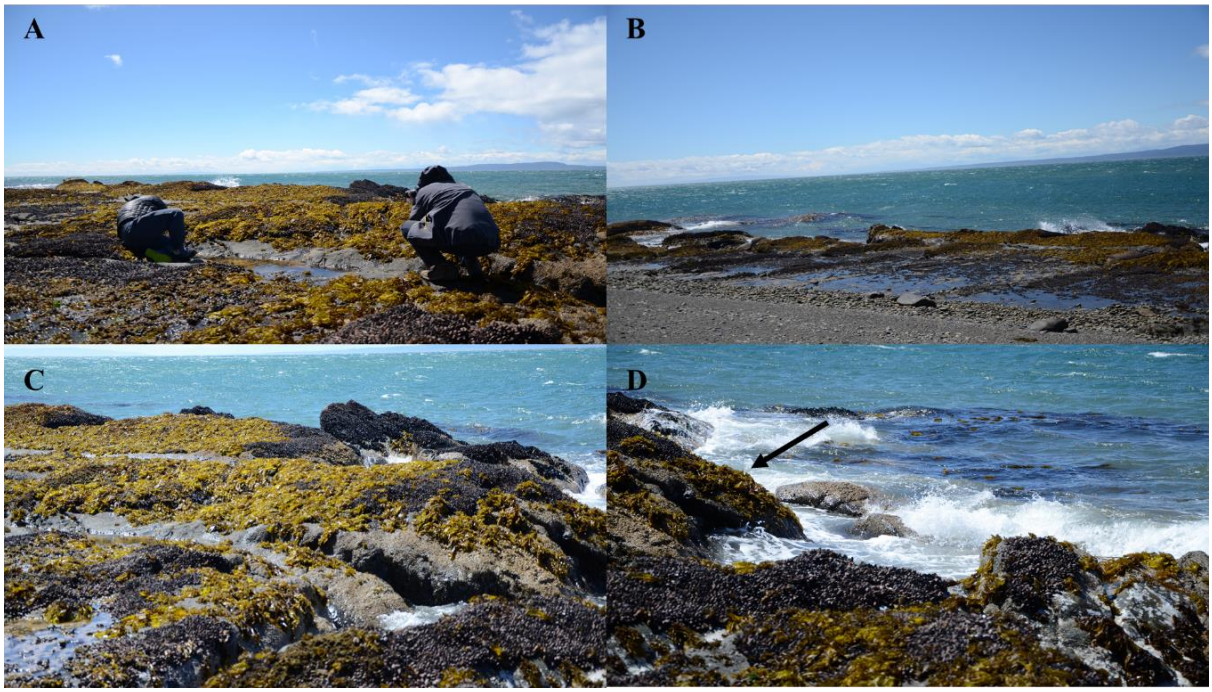

Figura 9 – Aspecto geral da zona de coleta em San Juan sob maré baixa (A) e (B); Substrato rochoso exposto sob maré baixa com algas da espécie *M. laminarioides* nas fases vegetativa e reprodutiva (C); Individuo de *I. cordata* nas fases vegetativas e reprodutivas (D).

Figura 10 – Aspecto geral da zona de coleta em Seno Otway sob maré alta (A); Aspecto geral da zona de coleta em Seno Otway sob maré baixa (B); Coleta de dados de temperatura, salinidade e pH sob maré baixa (C); Indivíduos de *D. antarctica* na fase vegetativa (D).

Figura 11 – Aspecto geral da alga *D. antarctica* do Filo Ochrophyta, ordem Fucales coletada em Seno Otway (Magalhães, Chile); Vegetativa (A); Reprodutiva (B).

Figura 12 – Aspecto geral da alga *L. flavicans* do Filo Ochrophyta, ordem Laminariales coletada em Puerto del Hambre (Magalhães, Chile); Vegetativa (A); Reprodutiva com soros em evidência (B).

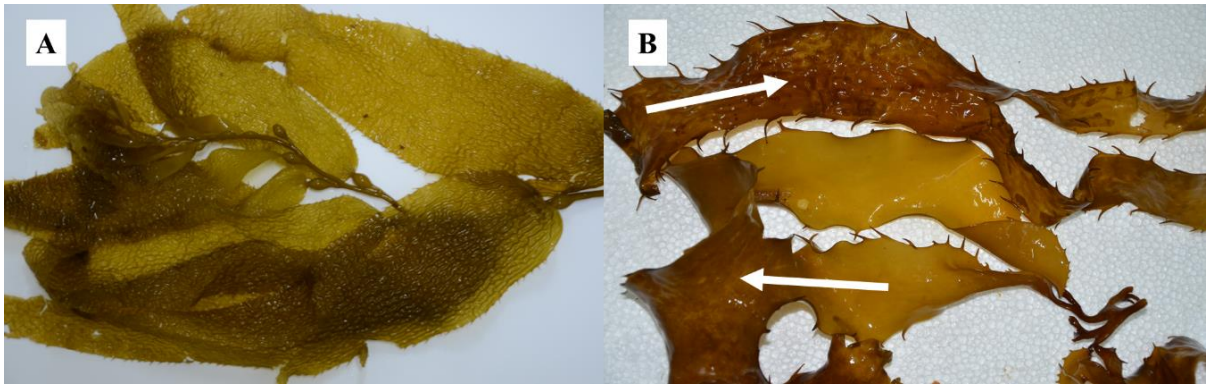

Figura 13 – Aspecto geral da alga *M. pyrifera* do Filo Ochrophyta, ordem Laminariales coletada em Puerto del Hambre (Magalhães, Chile); Vegetativa (A); Reprodutiva (B).

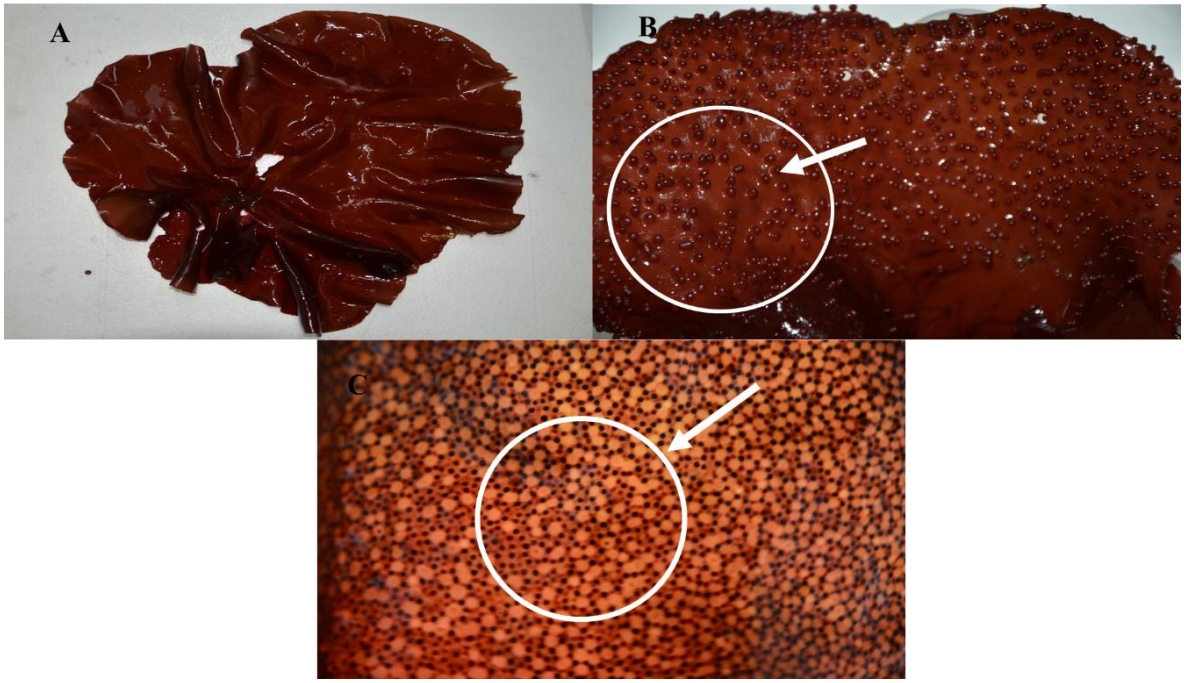

Figura 14 – Aspecto geral da alga *G. skottsbergii* do Filo Ochrophyta, ordem Gigartinales coletada em Puerto del Hambre (Magalhães, Chile); Fase gametofítica (A); Fase carposporofitica com detalhe dos carposporos (B); Fase tetraesporofitica com detalhes dos soros tetraesporangial (C).

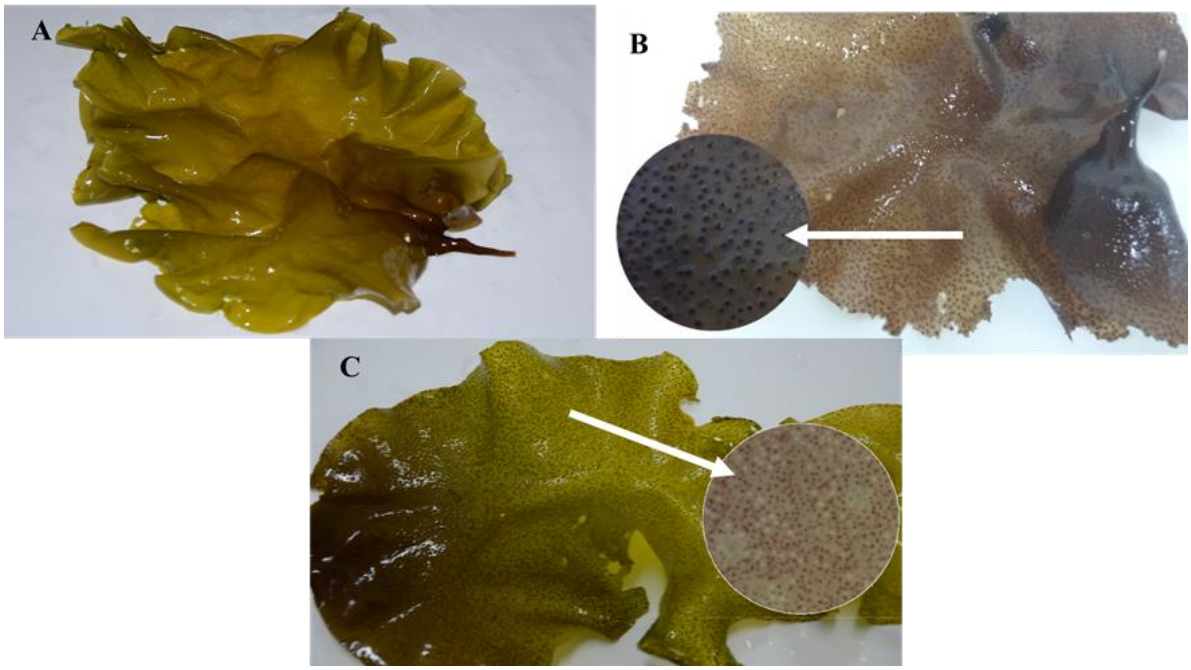

Figura 15 – Aspecto geral da alga *I. cordata* do Filo Ochrophyta, ordem Gigartinales coletada em Puerto del Hambre (Magalhães, Chile); Fase gametofítica (A); Fase carposporofitica com detalhe dos carposporos (B); Fase tetrasporofitica com detalhes dos soros tetraesporangial (C).

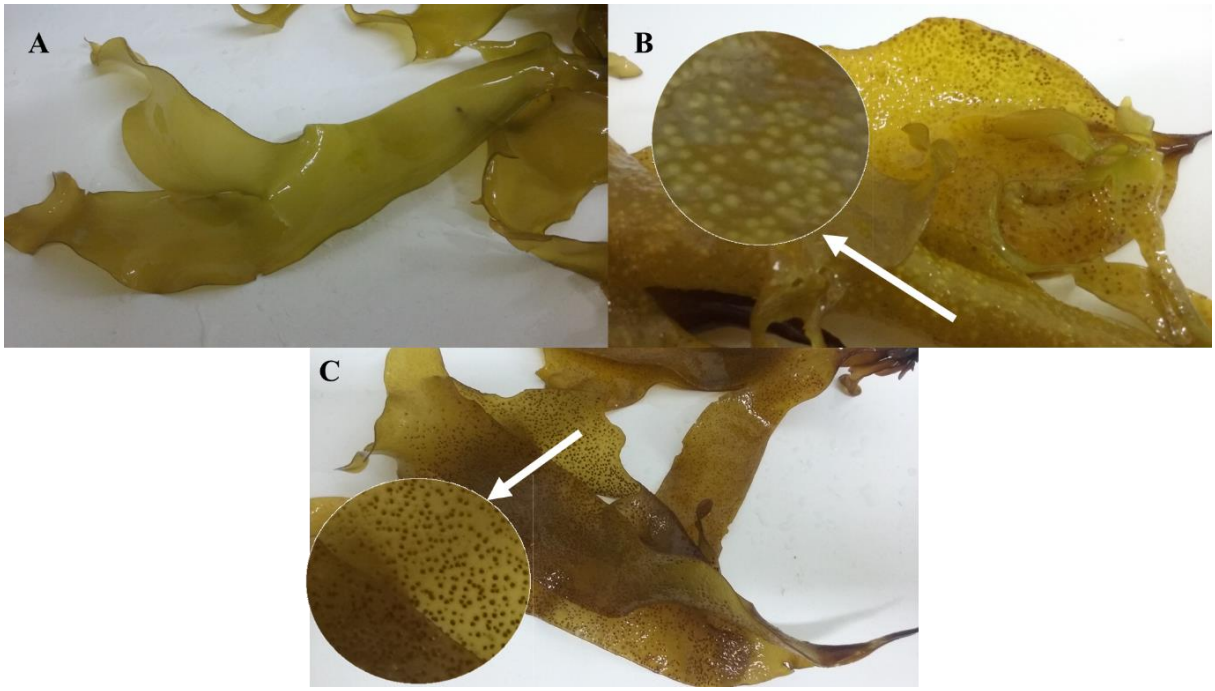

Figura 16 – Aspecto geral da alga *M. laminarioides* do Filo Ochrophyta, ordem Gigartinales coletada em Puerto del Hambre (Magalhães, Chile); Fase gametofítica (A); Fase carposporofitica com detalhe dos carposporos (B); Fase tetraesporofitica com detalhes dos soros tetraesporangial (C).

3.2 Caracterização das espécies em estudo

3.2.1 Classificação das algas no Filo Ochrophyta

***Durvillaea antarctica* (Chamisso) Hariot**

Tabela 1 – Classificação taxonômica da macroalga espécie *Durvillaea antarctica* (Chamisso) Hariot coletada na região de Magalhães, Chile (2016 – 2017)

Classificação	
Domínio	Eukaryota
Reino	Chromista
Filo	Ochrophyta
Classe	Phaeophyceae
Subclasse	Fucophycidae

Ordem	Fucales
Família	Durvillaeaceae
Gênero	Durvillaea
Espécie	*Durvillaea antarctica* (Chamisso) Hariot

Fonte: AlgaeBase: http://www.algaebase.org

Descrição geral da espécie *D. antarctica*

A espécie *D. antarctica* (Fig. 17) se caracteriza por apresentar indivíduos com estirpe cilíndrica, lisa e robusta, com certa flexibilidade e elasticidade evitando um rompimento da estrutura quando em movimento pelo fluxo de ondas no mar. Apresenta uma estrutura cônica e compacta que fixa a alga ao substrato, chamada disco basal ou rizóide. As frondas são de tamanhos grandes dividida em segmentos mais finos, apresentando uma consistência de couro (Fig. 18), contendo em seu interior uma estrutura em forma de "*favo de mel*" (Fig. 19) que contém ar e dá resistência ao embate contra as ondas e o substrato onde estão presas. Sua coloração vai de um verde castanho na forma vegetativa, sendo que na forma reprodutiva apresenta uma coloração amarronzada, sendo indivíduos que podem chegar até 10 m (Stevens et al. 2002 Collantes et al. 2002).

Figura 17 - Aspecto geral da alga *D. antarctica* em estágios reprodutivos e vegetativos sobre rochas na maré baixa em Seno Otway

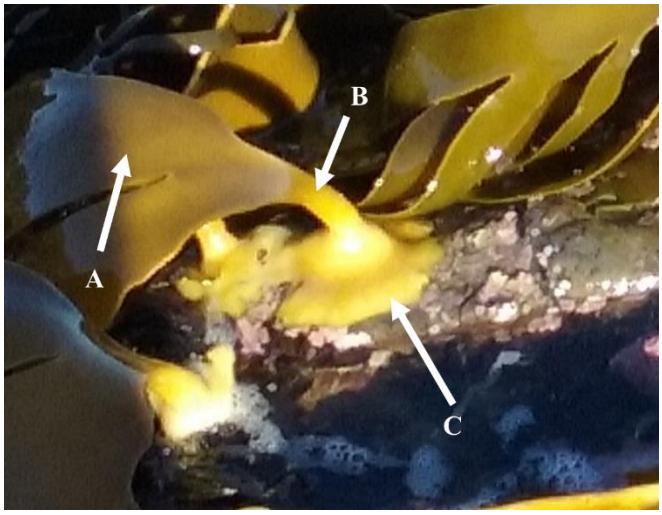

Figura 18 – Estruturas anatômicas da alga *D. antarctica* em Seno Otway: fronda (A), estirpe (B) e apressório (C).

Figura 19 - Seção transversal da fronda de *Durvillaea antarctica* mostrando a estrutura em forma de "*favo de mel*.

***Lessonia flavicans* Bory**

Tabela 2 – Classificação taxonômica da macroalga espécie *Durvillaea antarctica* (Chamisso) Hariot coletada na região de Magalhães, Chile (2016 – 2017)

Classificação	
Domínio	Eukaryota
Reino	Chromista
Filo	Ochrophyta
Classe	Phaeophyceae
Subclasse	Fucophycidae
Ordem	Laminariales

Família	Lessoniaceae
Gênero	Lessonia
Espécie	*Lessonia flavicans* Bory

Fonte: AlgaeBase: http://www.algaebase.org

Descrição geral da espécie *L. flavicans*

A espécie Lessonia flavicans (Fig. 20) está dentro da ordem Laminariales e membro da família Lessoniaceae, apresenta uma estirpe ramificada a partir da base superior com leve torção e apresentando somente uma lâmina por ramo. Apresenta lâminas simples com comprimentos de 0.5 – 2 m de comprimento e 1 -5 cm de largura com margens denticuladas, com superfície lisa ou corrugada. A lâmina contém divisões longitudinais com lâminas separadas resultando numa ramificação dicotômica sem nervura central (Guiry & Guiry 2011). Diferente de outras algas pardas como *M. pyrifera* não possui estruturas flutuantes sem habilidades de dispersão a longas distâncias.

A distribuição mais meridional de L. flavicans é o Canal de Beagle desde ao norte na costa chilena e ao sul em Puerto Deseado na costa argentina e a leste das Ilhas Falkland. As espécies de *L. flavicans* habitam a zona subtidal (0.5 a 2 m), porém em espécies nas Ilhas Falkland podem desenvolver enormes estirpes com vários metros de altura e com 8 m de altura a profundidades de 0.5 a 15 m. As Laminariales apresentam tecido parenquimatoso com várias camadas de células. A reprodução é anisogâmica e ciclo de vida heteromórfico, onde um esporófito macroscópico e microscópico, gametóficos dióico e esporófitos perenes. Sua maior fase de crescimento ocorre no verão (Tala et al. 2004, Nelson 2005) e maior período de reprodução no inverno com esporulação no perído da priimavera (Schwarz et al., 2006).

Comercialmente, L. flavicans e grande parte das Laminariales, tem coo produto mais importante os alginatos, comercializados em forma de sais hidrossolúveis, sendo o principal o ácido algínico. Agrande importância deste produto proveniente das algas pardas são suas propriedades hidrocolóides, isto é, capaz de se dissolver em água fria ou quente para formar soluções viscosas ou géis, muito utilizados nas indústrias alimentícias e farmacêuticas (Thakur et al., 2018).

Figura 20 - Aspecto geral da alga *L. flavicans* em estágio vegetativo

***Macrocystis pyrifera* (Linnaeus) C.Agardh**

Tabela 3 – Classificação taxonômica da macroalga espécie *Macrocystis pyrifera* (Linnaeus) C.Agardh coletada na região de Magalhães, Chile (2016 – 2017)

Classificação	
Domínio	Eukaryota
Reino	Chromista
Filo	Ochrophyta
Classe	Phaeophyceae
Subclasse	Fucophycidae
Ordem	Laminariales
Família	Laminariaceae
Gênero	Macrocystis
Espécie	*Macrocystis pyrifera* (Linnaeus) C.Agardh

Fonte: AlgaeBase: http://www.algaebase.org

Descrição geral da espécie *M. pyrifera*

A morfologia de *M. pyrifera* (Fig. 21) pode ser muito variada em alguns aspectos, como tamanho das frondas, tamanho do indivíduo, bem como lâminas mais largas, pneumatocistos menores, decorrência das condições ambientais que estão submetidas (Buschmann et al., 2006). Porém, as características gerais para a espécie

M. pyrifera são de estirpes extensas para transporte de nutrientes, uma grande estrutura na base para fixação ao leito do mar, chamada de apressório (Figura 22 A) e grandes ramificações com lâminas (frondas) e pneumatocistos que são estruturas arredondadas, chamadas também de vesículas, encontradas na base de cada lâmina foliar (Figura 22 B) que contém gases, entre eles o O_2 (17 – 35%), CO_2 (1%) e N_2 (65 - 83%) com a função principal de fornecer flutuabilidade as estruturas laminares da alga, mantendo-as na superfície, possibilitando uma maior absorção de energia solar para o processo fotossintético (Dromgoole, 1981).

Estas algas que podem ir de poucos metros até 60 m de comprimento (giant kelps) formam enormes florestas densas de algas por grandes extensões no mar, tanto no hemisfério norte como no hemisfério sul. A sua constituição química apresenta um composto de grande interesse comercial, os alginatos. A reprodução de *M. pyrifera* é diplobionte heteromórfico, sendo a fase macroscópica um esporófito diplóide (2*n*) e apresenta esporângios sobre suas lâminas basais (soros). Os zoósporos aplóides biflagelados são liberados (masculinos e femininos) germinam e formam os gametófitos masculinos (anterídeos → anterozoides - móvel) e femininos (oogonia → oosfera – imóvel), logo após ocorre a fecundação formando o zigoto (2*n*), que irá germinar e formar o gametófito (*n*) (Rodríguez et al., 2018). O processo reprodutivo desta alga ocorre o ano todo, tanto para espécies do hemisfério norte como no hemisfério sul, produzindo uma grande quantidade de propágulos suficiente para colonizar grandes área em pouco tempo (Buschmann et al., 2006)

Figura 21 - Aspecto geral da alga *M. pyrifera* em estágio vegetativo em solo para medição de dados sobre o indivíduo como parte de estudos do grupo de pesquisa LEMAS durante experimento em Puerto del Hambre.

Figura 22 - Aspecto geral de um apressório (A) e lâminas (frondas) com pneumatocistos (B) de um indivíduo de *M. pyrifera* em Puerto del Hambre.

3.2.2 Classificação das algas no Filo Rodophyta

***Gigartina skottsbergii* Setchell & N.L.Gardner**

Tabela 4 – Classificação taxonômica da macroalga espécie *Gigartina skottsbergii* Setchell & N.L.Gardner coletada na região de Magalhães, Chile (2016 – 2017)

Classificação	
Domínio	Eukaryota
Reino	Plantae
Filo	Rodophyta
Classe	Florideophyceae
Subclasse	Rhodymeniophycidae
Ordem	Gigartinales
Família	Gigartinaceae
Gênero	Gigartina
Espécie	*Gigartina skottsbergii* Setchell & N.L.Gardner

Fonte: AlgaeBase: http://www.algaebase.org

Descrição geral da espécie *G. skottsbergii*

A alga *G. skottsbergii* (Fig. 23) se apresenta em forma geralmente circular, com uma textura como couro, não apresenta ramificações e sua ligação ao substrato ocorre por uma pequena estirpe. As lâminas podem alcançar até 1 a 2 m de diâmetro

e são encontradas nas zonas infralitorâneas abaixo de 10 m de profundidade. A propagação é alcançada através da reprodução sexual tendo um ciclo de vida trifásico, com uma alternância de gerações isomórficas (Billard et al., 2015). Apresenta a cor avermelhada ocorre principalmente pela grande concentração de ficoeritrinas (ficobiliproteína) (Rao, Ganesan, Kurar, 2009). Na indústria o composto de maior interesse extraído do gênero Gigartinales são as carragenans, em especial da espécie *G. skottsbergii*, que é um polissacarídeo que compõe em média de 30 a 60 % do peso seco destas algas. Este peso pode variar de acordo coma as condições abióticas como luminosidade, pH, salinidade, temperatura e quantidade de O_2, incluindo uma variação no o tipo de carregenana que pode ser kappa (k), iota (ı) e lambda (λ). A alga *G. skottsbergii* é encontrada desde o sul da Argentina (Boraso e Zaixso, 2013), Ilhas Falkland (Wiencke, Clayton 2002) e nas regiões Antártica (Dubrasquet et al. 2018) e sub-Antárticas (Wiencke, Clayton 2002).

Figura 23 - Aspecto geral da alga *G. skottsbergii* em estágio vegetativo

***Iridaea cordata* (Turner) Bory de Saint-Vincent**

Tabela 5 – Classificação taxonômica da macroalga espécie *Iridaea cordata* Bory de Saint-Vincent coletada na região de Magalhães, Chile (2016 – 2017)

Classificação	
Domínio	Eukaryota
Reino	Plantae
Filo	Rodophyta
Classe	Florideophyceae
Subclasse	Rhodymeniophycidae
Ordem	Gigartinales
Família	Gigartinaceae
Gênero	Iriidaea
Espécie	*Iridaea cordata* (Turner) Bory

Fonte: AlgaeBase: http://www.algaebase.org

Descrição geral da espécie *I. cordata*

A espécie I. cordata (Fig. 24) tem sido encontrada desde o norte da Califórnia, norte do México, Japão (Hansen, 1977) e regiões polares como Antárticas e sub-Antárticas (Santos et al., 2017). Habitam especialmente na zona intertidal, na zona entre marés, em costões rochosos em temperaturas acima de 1 ºC com zonas de pouca variação na sanilidade, suporta desde baixa a altas intensidade de radiação solar (Martín et al., 2015). A estirpe é freqüentemente escuro de 1 a 4 cm de comprimento e lâminas esverdeado escuras até um tom pouco avernmelhada e lâminas que pode chegar a 35 cm (Boraso, 2013). Na sua composição básica apresenta carragenanas, comum as Gegartinales, apresentando a forma kappa em maior concentração. As carregenans extraídas de *I. cordata* são polissacarídeos sulfatados de grande importância na indústria alimentícia como espessantes e gelificantes (Cunha, Grenha, 2016) e apresentam atividade anti-câncer (Kim et al., 2016).

Figura 24 - Aspecto geral da alga *I. cordata* em estágio tetraesporofita

***Mazzaella laminarioides* (Bory) Fredericq**

Tabela 6 – Classificação taxonômica da macroalga espécie *Mazzaella laminarioides* (Bory) Fredericq coletada na região de Magalhães, Chile (2016 – 2017)

Classificação	
Domínio	Eukaryota
Reino	Plantae
Filo	Rodophyta
Classe	Florideophyceae
Subclasse	Rhodymeniophycidae
Ordem	Gigartinales
Família	Gigartinaceae
Gênero	Mazzaella
Espécie	*Mazzaella laminarioides* (Bory) Fredericq

Fonte: AlgaeBase: http://www.algaebase.org

Descrição geral da espécie *M. laminarioides*

A espécie *M. laminarioides* (Fig. 25) é encontrada ao longo da costa do Chile, onde habita a zona intertidal superior nas plataformas rochosas criando grandes extensões de biomassa algal. Sua coloração ocorre desde um verde amarelado até um verde escuro e depende da sazonalidade, principalmente com mudanças de coloração nas estações entre primavera e verão (Montecinos et al., 2012).

A alga *M. laminarioides* junto com *G. skottsbergii* são uma das mais exploradas do Chile sendo colhidas em torno de 25.000 mil t/ano e exportadas para países asiáticos para alimentação, extraçãoe de ágar e carragenanas. Possui alternância de gerações isomórficas como a maioria de Gigartinales, apresentando a forma gametófica na região do infralitoral alto e a forma tetraespofica na zona do infralitoral baixo, com dispersão curta de seus esporos. Posui uma estirpe sulcado, com muitas lâminas eretas e grossas que emergem de um disco basal, apresenta ramificações com frondas largas, com 10 a 15 cm de comprimento e 5 cm de largura, não apresentam dicotomia e são achatadas ou côncavo-convexo (Caceres, Otaíza, 2015).

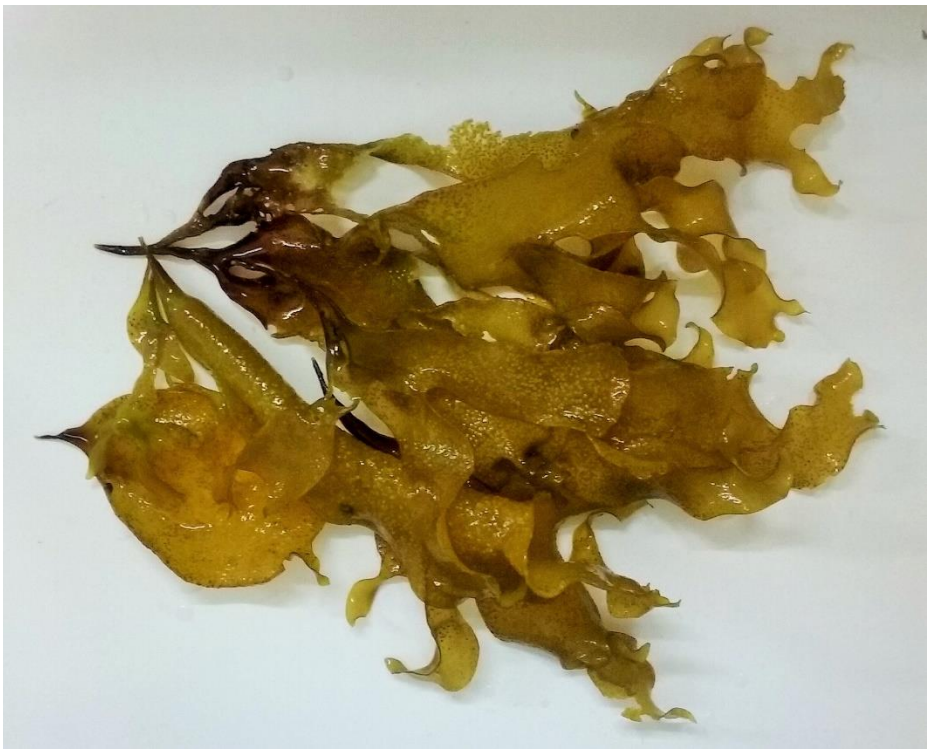

Figura 25 - Aspecto geral da alga *M. laminarioides* em estágio tetraesporofita

3.3 Preparação das Amostras Pós Coleta

Aproximadamente 6 indivíduos de cada fase de *D. antarctica* foram coletados manualmente na maré baixa na zona intertidal e na zona litorânea inferior. Aproximadamente 10 indivíduos de *M. pyrifera* nas fases vegetativa e reprodutiva foram coletados ao nível do mar e na zona infralitoral (cerca de 10 m de profundidade), respectivamente. Na zona infralitoral, foram coletados 10 indivíduos de cada fase de *L. flavicans*. As espécies *I. cordata* e *M. liminarioides* foram coletas em média de 20 individuos na zona infralitoral e 10 individuos na zona infralitoral da espécie *G. skottsbergii*, todas nas fases gametofíticas, cistocárpicas e tetraesporofiticas.

O material coletado foi acondicionado em caixa térmica com água do mar e enviado ao laboratório para ser acondicionado em câmara de cultura com aeração por 24 h de aclimatização a 5 ± 1 ° C, com radiação artificial de 40 µmol fótons m^{-2} s^{-1} PAR, fornecido por lâmpada fluorescente de luz diurna (Osram, Alemanha) e sob um fotoperíodo padrão de 12 h/12h. Após um período de aclimatação, as algas coletadas foram classificadas e realizada a análise através do Fluorômetro Modulado por Amplitude de Pulso (PAM).

As análises de pigmentos e atividade fotossintética, foram realizadas utilizando os tecidos médio e marginal das frondas. As informações gerais de coleta de algas, estágios de desenvolvimento, indivíduos armazenados para exsicação e posterior identificação morfológica sob numeração especificada foram realizadas no Herbário do Laboratório de Ecossistemas Marinhos Antárticos e Submarinos Antárticos (LEMAS- Chile), e estão indicados na Tabela 7.

Tabela 7 – Dados de coletas, fases de desenvolvimento, ponto de localização, zona marinha de coleta e número de exsicata de macroalgas pardas e vermelhas coletadas na região de Magalhães, Chile (2016 e 2017)

Espécie	Fase de Desenvolvimento	Data de coleta	Ponto de Coleta	Zona Marinha	Número Herbário
L. flavicans	Vegetativa	21.12.16	Puerto del Hambre	MLBO	522p
L. flavicans	Reprodutiva	15.01.17	Puerto del Hambre	MLBO	523p
M. pyrifera	Vegetativa	15.12.16	Puerto del Hambre	NMR	518p

M. pyrifera	Reprodutiva	15.12.16	Puerto del Hambre	INLT	520p
D.antarctica	Vegetativa	23.03.17	Seno Otway	MLLW	582p
D.antarctica	Reprodutiva	23.03.17	Seno Otway	MLLW	583p
I. cordata	Gametofitica	10.02.17	San Juan	MLMD	1307r
I. cordata	Tetrasporofitica	10.02.17	San Juan	MLMD	1308r
I. cordata	Carposporofitica	10.02.17	San Juan	MLMD	1306r
M. laminarioides	Gametofitica	04.01.17	San Juan	MLAL	1298r
M. laminarioides	Tetrasporofitica	04.01.17	San Juan	MLAL	1299r
M. laminarioides	Carposporofitica	04.01.17	San Juan	MLAL	1300r
G. skottsbergii	Gametofitica	15.02.17	Puerto del Hambre	INLT	1303r
G. skottsbergii	Tetrasporofitica	15.02.17	Puerto del Hambre	INLT	1301r
G. skottsbergii	Carposporofitica	15.02.17	Puerto del Hambre	INLT	1302r

Infralittoral – INLT; mesolitoral médio (MLMD); mesolitoral baixo (MLBO) mesolitoral alto (MLAL); nível do mar (NMR);

Antes do congelamento, o material foi lavado com água corrente e destilada para remover as sujidades. As espécies foram devidamente identificadas, pesadas e colocadas em sacos plásticos escuros e colocadas em freezer horizontal a -20 ° C. Após o congelamento a biomassa algal foi resfriada e seca em estufa de circulação de ar JOSF 700T a 35 ° C (± 1 ° C) por 24 a 30 h e posteriormente pulverizada em moinho de facas Lucadema modelo 226/2. A determinação do peso seco (PS) em algas foi realizada seguindo a Farmacopéia Brasileira (2010), que é baseada na perda de umidade e voláteis eliminados pela dessecação. Foram pesados aproximadamente 2 g do material em triplicado (n = 3) e posteriormente se efetuou a dessecação numa estufa DeLeo modelo A58EAF a 105 ° C durante 5 h até se obter um peso constante. O teor de umidade foi calculado pela diferença entre o peso inicial e final das amostras e expresso em porcentagem.

3.4 Performance Fotossintética

3.4.1 Fluorescência e Análise da Clorofila *a*

A energia absorvida pelas moléculas de Chl *a* que se encontram nos tilacóides, são dissipadas de quatro formas, como transferência de energia para outras

moléculas que auxiliam os processos metabólicos na produção de compostos importantes ao processo fisiológico dos vegetais. Podem ocorrer a conversão direta da energia de excitação em calor sem que ocorra a emissão de fótons, e ainda a dissipação de energia na forma fotoquímica, isto é, a utilização da energia absorvida pela planta para a realização de reações químicas no processo metabólico (Murchie, Lawson, 2013).

A quarta maneira de dissipação da energia é pela fluorescência, onde podemos definir como a capacidade que uma substância tem de emitir luz quando exposta a radiações do tipo ultravioleta (UV). Esta forma de dissipação de energia pela fluorescência ocorre em plantas quando a Chl *a* no seu estado excitado reenvia um fóton e retorna ao seu estado base, neste momento a fluorescência tem um comprimento de onda mais longo, isto é, contém menos energia do que o comprimento de onda absorvido, pois parte desta energia do estado excitada da Chl *a* é convertido em calor antes da emissão do fóton fluorescente (Murchie, Lawson, 2013).

A análise da fluorescência da Chl *a* apresenta resultados que relacionam os efeitos dos fatores ambientais (abióticos), tais como radiação solar, sazonialidade, habitat, entre outros fatores sobre o processo fisiológico dos organismos fotossintetizantes (Kuckenberg, Tartachnyk, Noga, 2009). Esta análise é realizada por um Fluorômetro com Pulso de Amplitude Modulada (PAM) (Fig. 26), o qual se baseia na emissão de uma luz actínia modulada e consequente detecção da fluorescência (Kuckenberg, Tartachnyk, Noga, 2008).

Estes dados adquiridos a partir do PAM irão fornecer informações sobre o desempenho do PSII e se apresenta como uma ferramenta amplamente utilizada em algas e plantas superiores como uma técnica não invasiva que permite avaliar o desempenho fotossintético "*in vivo*" estimando principalmente a atividade do fotossistema II (PSII) (Szymański et al., 2017).

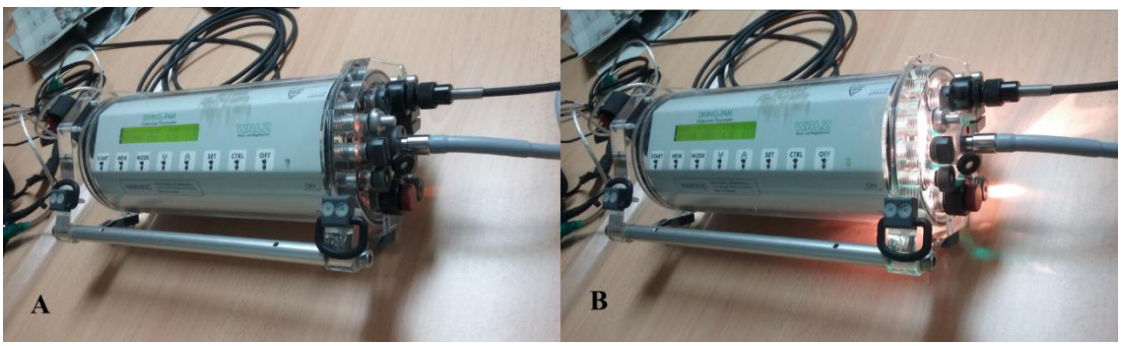

Figura 26 – Detalhe do Fluorômetro Subaquático com Pulso de Amplitude Modulada (PAM) (A) no modo desligado e (B) em análise com pulso de luz saturante.

A análise de uma amostra em PAM inicia após a adaptação ao escuro com a finalidade de ter os centros de reação do PSII abertos sem perdas de energia por calor (*quenching* não fotoquímicos -NPQ), neste momento se emite uma luz de intensidade baixa, incapaz de induzir o transporte de elétron no PSII. Esta luz de baixa intensidade não actínia induz uma fluorescência mínima a qual denominamos fluorescência basal ou mínima (F_0), logo após é emitida uma luz vermelha de baixa intensidade (< 0,5 µmol fótons m^{-2} s^{-1}), onde teremos o rendimento mínimo da fluorescência no estado aclimatado à luz (F'_0) sem redução da quinona A (Q_A) e com todos os centros de reação fechados. Neste momento, a energia que atinge os centros de reação tem a máxima chance de utilização como processo fotoquímico e uma mínima chance de dissipação como calor ou florescência.

A segunda luz a ser emitida sobre a amostra é um pulso luz saturante (<10.000 µmol fótons m^{-2} s^{-1}; 4s a 8s) para avaliar a atividade fotossintética, neste momento, todos os centros de reação do PSII estarão fechados, isto é, todas Q_A totalmente reduzidas e o processo fotoquímico é reduzido a quase zero e a fluorescência será máxima (F_m). Se a amostra não for adaptada ao escuro antes do pulso saturante, teremos NPQ e neste caso a fluorescência não será máxima, teremos então fluorescência máxima adaptada a luz (F'_m).

O terceiro pulso de luz saturante, em torno de 2.000 µmol fótons m^{-2} s^{-1}, é uma luz actínia e tem função de induzir a fotossíntese (Fig. 27). A medição da eficiência fotossintética é calculada a partir dos valores mínimos (F_0) e máximos (F_m) permitindo o cálculo do rendimento quântico máximo do PSII (F_v / F_m) (Eq. 1) para plantas adaptadas ao escuro, se tivermos plantas adaptadas a luz teremos o rendimento quântico efetivo ΦPSII (Eq. 2).

$$PSII = Fv / Fm = (Fm - F0) / Fm \quad \textbf{(1)}$$

$$\Phi PSII = \Delta F / F'm = (F'm - F'0) / F'm \quad \textbf{(2)}$$

O cálculo do ΦPSII irá fornecer as informações da quantidade de energia gasta no processo de fotossíntese e permitirá o cálculo da taxa de transporte

de elétrons relativa (rETR) (Eq. 3) a qual fornece dados da taxa de elétrons entre o PSI e PSII. Os cálculos da performance fotossintética de um organismo fotossintetizante permitem obter informações sobre o funcionamento do PSII e analisar o estado de estresse a qual está sendo submetido.

$$rETR = \Phi PSII \; x \; PAR \qquad \textbf{(3)}$$

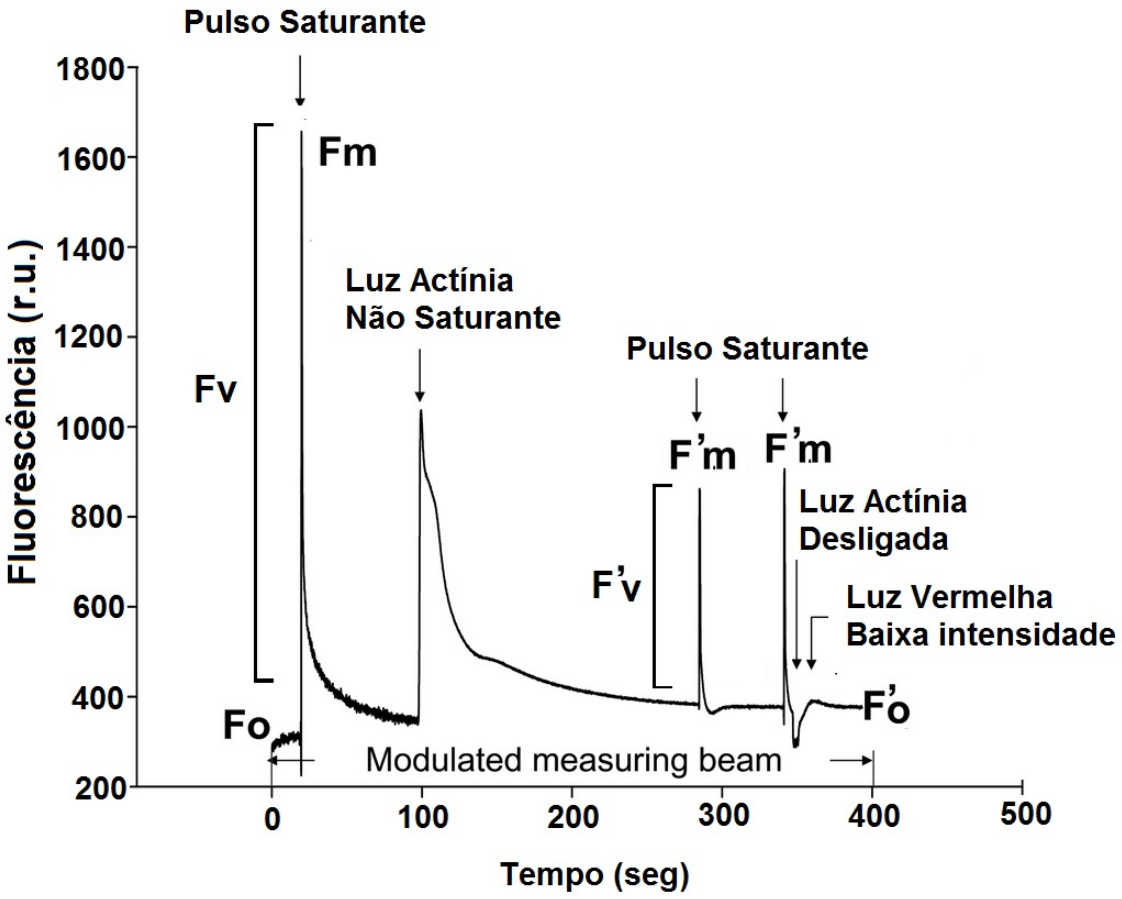

Figura 27 - Exemplo de um gráfico de fluorescência registrado com um fluorômetro PAM. Fluorescência basal ou mínima (F_0); Fluorescência máxima (F_m); Fluorescência máxima adaptada a luz (F'_m), Fluorescência mínima no estado aclimatado à luz vermelha (F'_0); Rendimento máximo da fluorescência variável (F_v), Rendimento de fluorescência variável em luz actínica (F'_v) (Nedbal, Trtìlek, Herppich, 2000).

3.4.2 Performace Potossintética: Análise em PAM (Chile)

Após o período de aclimatação ocorrida em câmara fria no Laboratório LEMAS (Chile), aproximadamente 10 indivíduos de cada uma das seis espécies estudadas em cada estágio de desenvolvimento, foram colocados em uma ponta de fibra ótica e submetidos a curvas de luz de resposta rápida (CLRR) induzidas por PAM. As macroalgas foram submetidas a oito níveis crescentes de irradiâncias de 11, 36, 71, 117, 175, 242, 360 e 490 µmol m^{-2} s^{-1} com intervalos de 30 s após cada análise para medir as curvas de resposta à luz (White, Critchley, 1999) e flash de saturação (0,8 s; ≥ 9000 µmol fótons $m^{-2}.s^{-1}$) (Marambio et al., 2017). Antes da análise das CLRR, as amostras foram colocadas em uma ponta de fibra óptica com um clipe, a fim de manter a fronde no escuro por 20 min (Ralph e Gademann, 2005; Wong et al., 2015) (Fig.28).

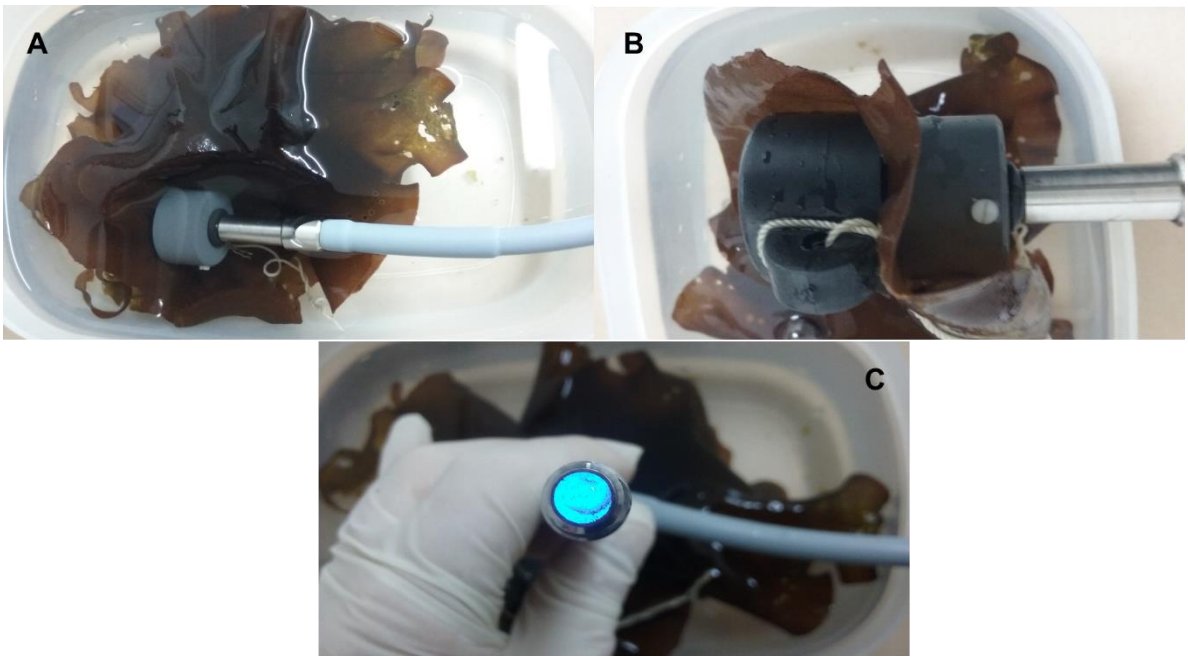

Figura 28 – Detalhe de ponta de fibra óptica com um clipe (escuro) em uma alga da espécie *I. cordata* (A) e (B); Ponta de fibra óptica com detalhe de luz azul (C).

A avaliação quantitativa das CLRR foi realizada utilizando parâmetros de eficiência fotossintética (*α*), fotoinibição (*β*), saturação de irradiância (E_k) e taxa de transferência de elétrons relativa máxima (rETRmax) ajustados à curva seguindo o rETR hiperbólico *vs* curvas *I* que foram ajustadas de acordo com o modelo de Platt et al. (1980) (Eq. 4). Os resultados do desempenho fotossintético foram processados usando o software Kaleida Graph 4.0 (Synergy Software 1986–2005) (Fig. 29).

$$PB(I) = [1 - \exp(-\alpha I / Ps) \exp(-\beta I / Ps) \quad \textbf{(4)}$$

Segundo o modelo Platt et al. (1980), $P^B(I)$ = taxa fotossintética [mg C (mg Chlα)$^{-1}$ h^{-1}] da irradiância *I* (µmol photons m^{-2} s^{-1}); *P* – taxa fototssintética de saturação de luz [mg C (mg Chlα)$^{-1}$ h^{-1}] na ausência da fotoinibição; α – inclinação inicial da curva *P-I* [(mg C (mg Chlα)$^{-1}$ h^{-1}) (µmol photons m^{-2} s^{-1})]; β = indice de fotoinibição [(mg C (mg Chlα)$^{-1}$ h^{-1}) (µmol photons m^{-2} s^{-1})].

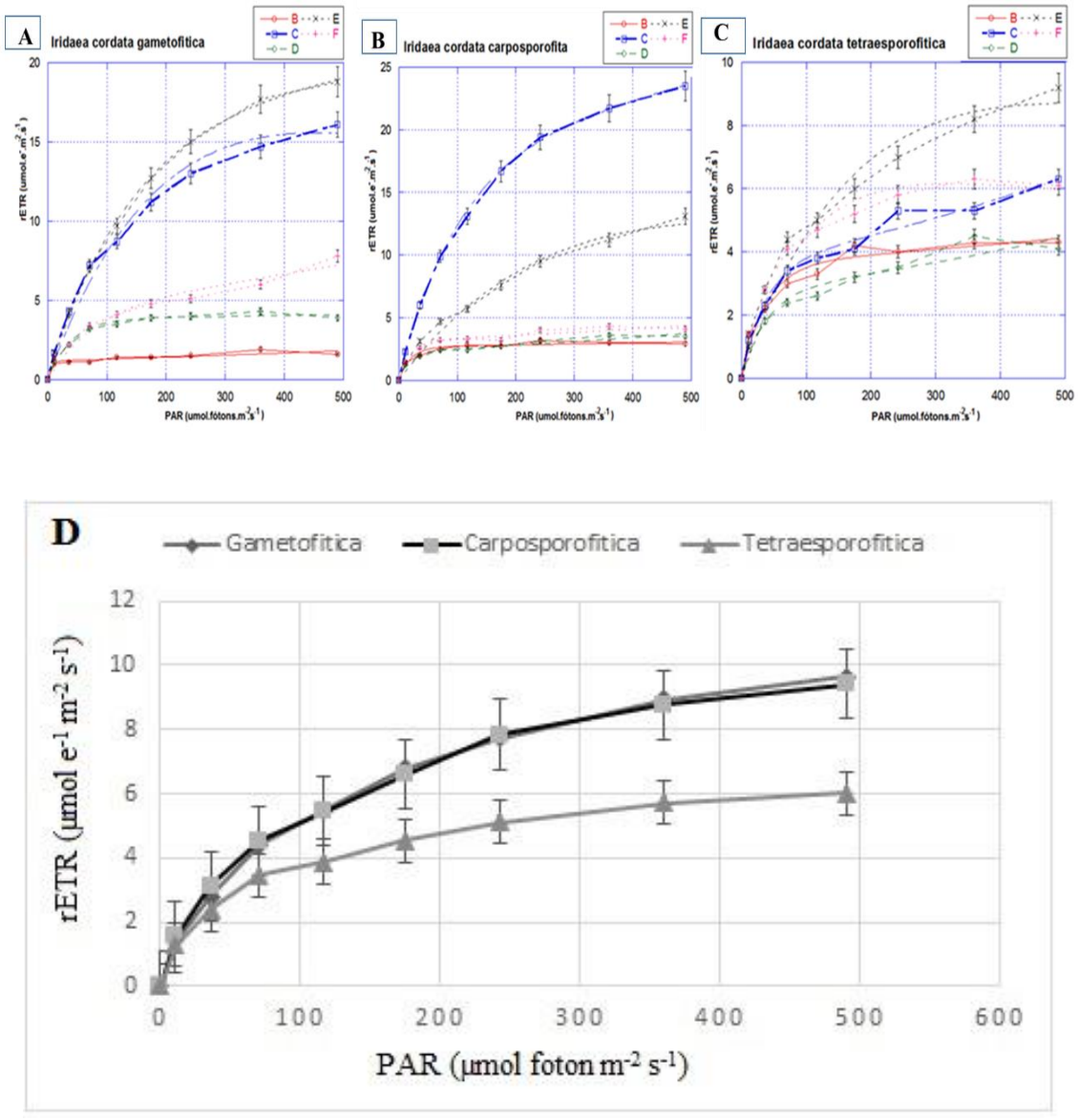

Figura 29 – Representação gráfica taxa de transferência de elétrons relativa (rETR). Dados brutos (A, B e C) da alga *I. cordata*; Dados tabelados segundo modelo de Plat et al., (1980), onde resultados representam média ± DP (onde DP é desvio padrão); (*n* = 5) onde n é o número de amostras independentes.

3.4.3 Análise de Pigmentos Algas Pardas (Chile)

A análise dos pigmentos em algas pardas seguiu a metodologia modificada de Seely et al. (1972) onde aproximadamente 125 mg de alga fresca foram transferidas para um tubo *eppendorf* que continha 1 mL de dimetilsulfóxido (DMSO), posteriromente foram deixadas para descansar por 15 min no escuro (Tait, Hik, 2003; Mansilla et al., 2016; Méndez et al., 2017). Após, a fase superior foi transferida para uma cubeta e analisada em um Espectrofotômetro Hewlett Packard 8452A em comprimento de onda entre 400 a 700 nm. O cálculo da concentração de Chl *a*, Chl *c* e fucoxantina realizado de acordo com as equações (5), (6) e (7) (Seely et al., 1972).

Clorofila *a*

$$\text{Chl}\,a = \text{A665} / 72.8 \quad (\mathbf{5})$$

Clorofila *c*

$$\text{Chl}\,c = (\text{A631} + \text{A582} - 0.297 \times \text{A665}) / 61.8 \quad (\mathbf{6})$$

Fucoxantina

$$\text{Fucox} = (\text{A480} - 0.772\,(\text{A631} + \text{A582} - 0.297 \times \text{A665}) - 0.049 \times \text{A665}) / 130.0 \quad (\mathbf{7})$$

3.4.4 Análise de Pigmentos Algas Vermelhas (Chile)

A análise de pigmento em algas vermelhas foi realizada a partir da maceração de aproximadamente 300 mg de biomassa algal fresca, utilizando nitrogênio líquido até a formação de um pó fino. A amostra foi diluída em 4 mL de tampão fosfato 50 mM, pH 5,5 a 4 °C. A solução resultante foi centrifugada durante 20 min em uma centrífuga marca Genesys 10 a 10.000 rpm (~ 4 °C), onde se obteve um sobrenadante utilizado para análise de alocianinas (AFC), ficocianinas (FC) e ficoeritrinas (FE). O material residual foi diluído em 4 mL de acetona a 90 % (*v/v*) e centrifugado a 12.000 rpm (~ 4 °C) durante 10 min para análise de Chl *a.*

A concentração de ficobiliproteínas seguiram as equações segundo Kursar et al. (1983) (Eqs. 8, 9 e 10) e a quantificaçãpo de Chl *a* seguiu Jeffrey e Humphrey (1975) (Eq. 11).

Aloficocianina

$$AFC = 181{,}3.A651 - 22{,}3.A614 \quad \textbf{(8)}$$

Ficocianina

$$FC = 151{,}1.A614 - 99{,}1.A651 \quad \textbf{(9)}$$

Ficoeritrina

$$FE = 155{,}8.A498{,}5 - 40{,}0.A614 - 10{,}5.A651 \quad \textbf{(10)}$$

Clorofila *a*

$$Chl\ a = 11.85\ A664 - 1.54\ A647 - 0.08\ A630 \quad \textbf{(11)}$$

A figura 30 representa um exemplo de espectro de fluorescência da Chl *a* em uma amostra de *I. cordata* na fase carposporofitica em dois comprimentos de onda, os quais estão relacionados ao estado excitado da molécula, em 662 nm é a banda de absorção no vermelho e corresponde ao primeiro estágio de excitação, subsequente ocorre a banda de absorção no azul em 430 nm e está relacionada ao segundo estado de excitação da molécula.

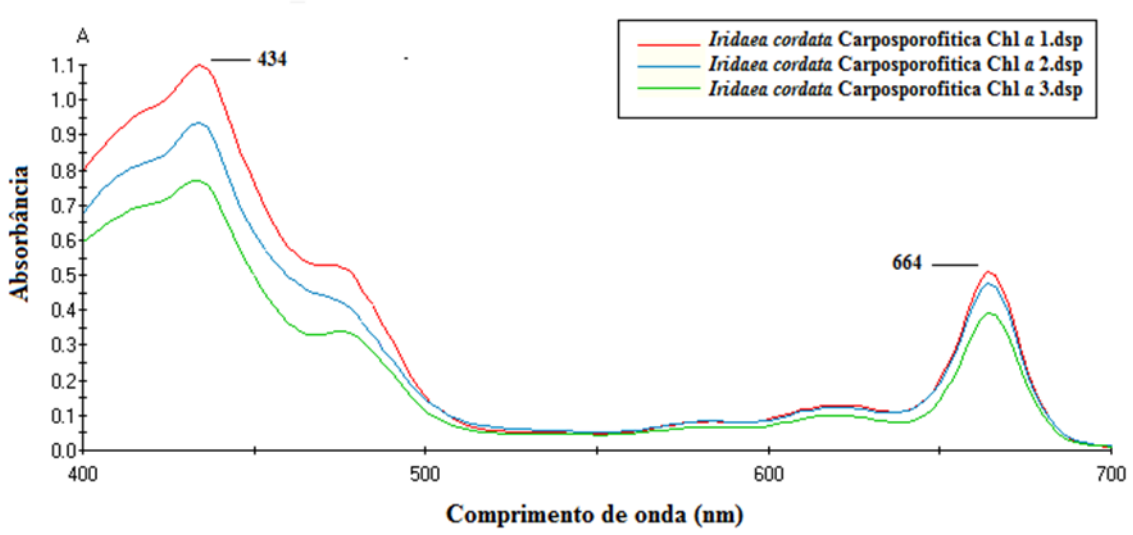

Figura 30 - Espectro de fluorescência e absorção em análise de Chl *a* para amostra de macroalga *Iridaea cordata* no estágio carposporofita de desenvolvimento diluída em acetona.

3.5 Análise bioquímica das macroalgas (Brasil)

3.5.1 Extração de Lipídios e Esterificação dos Ácidos Graxos

A extração de ácidos graxos seguiu o procedimento modificado de Bligh e Dyer (1959) no qual aproximadamente 1 g da biomassa algal seca e pulverizada foram colocadas em um balão de 100 mL, sendo adicionados 10 mL de clorofómio, 20 mL de metanol e 10 mL de uma solução aquosa de sulfato de sódio (1,5%, *p/v*). Posteriormente, houve agitação da mistura em temperatura ambiente, durante 30 min e logo após, foram adicionados ao sistema 10 mL de clorofórmio e 10 mL de uma solução aquosa de sulfato de sódio (1,5%, *p/v*). A solução foi transferida para tubos *falcons* e submetida à centrifugação por 30 min a 5000 rpm. Após a centrifugação, a fase orgânica foi recuperada e o solvente foi evaporado em um evaporador rotativo (Buchi, Suíça) com uma bomba de vácuo V-700 e um refrigerador B-741. O conteúdo lipídico foi obtido em triplicata (n=3) e determinado gravimetricamente.

Os lípidos extraídos da biomassa algal (aproximadamente 20 a 50 mg) foram esterificados e convertidos nos seus respectivos esteres metilicos de ácidos graxos de acordo com o método "*B*" de Moss et al. (1974). O método se baseia na adição de 6 mL de uma solução metanólica de hidróxido de potássio (2%, *w/v*) em um balão de 50 mL, contendo os lipídios extraídos anteriormente, sob agitação e refluxo a 80 °C por 8 min. Posteriormente são adicionados 7 mL de uma solução metanólica de trifluoreto de boro (Aldrich - 14%, *v/v*) sendo agitada sob refluxo por 2 min, sendo após a mistura resfriada a temperature ambiente e adicionados 5 mL de uma solução aquosa de cloreto de sódio (20%, *p/v*). A fase orgânica que contem os ácidos graxos foi recuperada usando 20 mL de hexano, e posteriormente filtrada através de sulfato de sódio anidro, evaporada sob pressão reduzida e seca até peso constante sob fluxo de nitrogênio para posterior análise em GC/DIC.

3.5.2 Cromatografia Gasosa: Análise de Ésteres Metílicos dos Ácidos Graxos

Os ésteres de ácidos graxos foram analisados utilizando uma curva analítica empregando o padrão FAME 37-MIX (Supelco, Bellefonte, Pensilvânia, EUA) em seis concentrações distintas de 0,625 mg mL^{-1} a 20 mg mL^{-1}. O nonadecanoato (C19;0; ≥ 99,0% - Sigma-Aldrich, St. Louis, Missouri, EUA) foi adicionado às amostras e nos padrões da curva em uma concentração de 2 mg mL^{-1}. As análises foram realizadas em Cromatógrafo a Gás com Detector de Ionização por Chama - CG/DIC 2010 (Shimadzu) com injetor split / splitless, autoinjetor AOC-20i e coluna capilar SP®-2560 (100 m × 0,25 mm x 0,20 µm - Supelco) (Tang e Row, 2013)

As condições operacionais utilizadas na análise dos ácidos graxos foram: hidrogênio (H_2) como gás carreador no fluxo de 1,2 mL min^{-1}, modo *split* de 1:100, volume de injeção de 1 µL, temperatura inicial do forno a 100 °C aumentando 3 °C. min^{-1} a 220 ºC. A temperatura do injetor e detector foi de 250 °C. A figura 31 representa um cromatograma do perfil de ésteres do padrão FAME 37-MIX nas condições segundo Santos et al., (2017).

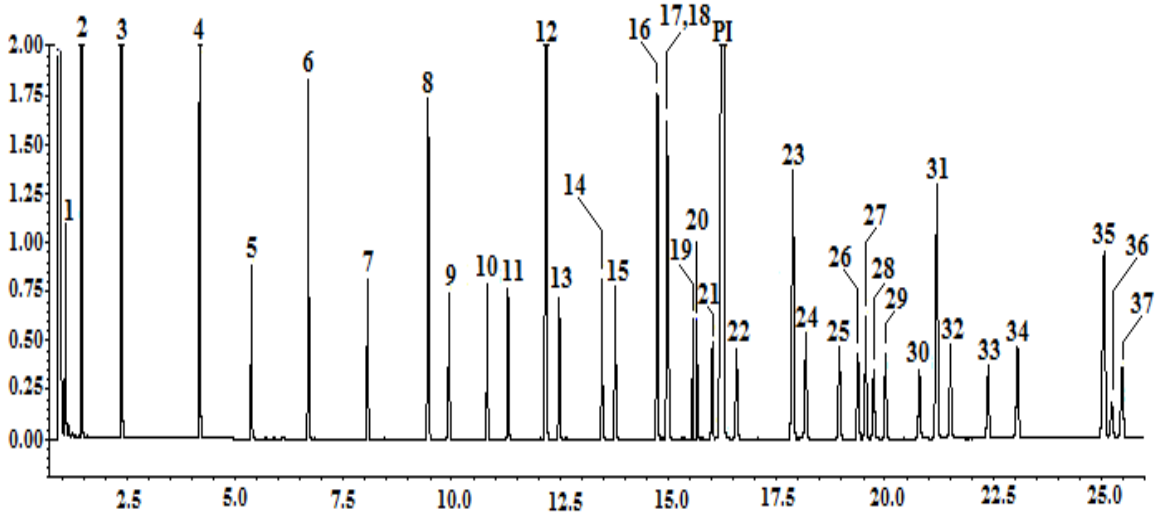

Figura 31 – Cromatograma do Padrão FAME MIX 37 (Sigma-Aldrich). A numeração indica: 1 (C4:0); 2 (C6:0); 3 (C8:0); 4 (C10:0); 5 (C11:0); 6 (C12:0); 7 (C13:0); 8 (C14:0); 9 (C14:1n5); 10 (C15:0); 11 (C15:1*n*-5); 12 (C16:0); 13 (C16:1*n*-7); 14 (C17:0); 15 (C17:1*n*-7); 16 (C18:0); 17 (C18:1*n*-9c); 18 (C18:1*n*-9t); 19 (C18:2*n*-6c); 20 (C18:2*n*-6t); 21 (C18:3*n*-6); PI (C19:0 - padrão interno); 22 (C18:3*n*-3); 23 (C20:0); 24 (C20:1*n*-9); 25 (C20:2*n*-6); 26 (C20:3*n*-6); 27 (21:0); 28 (C20:4*n*-6); 29

(C20:3*n*-3); 30 (C20:5*n*-3); 31 (C22:0); 32 (C22:1*n*-9); 33 (C22:2*n*-6); 34 (C23:0); 35 (C24:0);36 (C22:6*n*-3); 37 (C24:1*n*-9).

3.6 Análise Estatística

A avaliação dos resultados quanto à concentração de pigmentos, parâmetros fotossintéticos, ácidos graxos totais (ΣSFAs, ΣMUFAs e ΣPUFAs) e o perfil de ácidos graxos entre as fases de desenvolvimento foi realizada aplicando a análise de variância two-way (ANOVA). Na análise das variáveis unidirecionais *Fv* / *Fm* foi utilizado ANOVA unidirecional. A análise *post hoc* de médias de HSD de Tukey foi usada para analisar diferenças entre os resultados e para avaliar diferenças significativas em um intervalo de confiança de 95% (p <0,05). Todas as análises estatísticas foram realizadas utilizando o software GraphPad Prism 7 (versão 2017-02, EUA).

7. Considerações Finais

A biopresccção de nove espécies de algas da região Sub-Antártica nos possibilitou ter uma visão da grande diversidade destes organismos que habitam aquela ecoregião, bem como, proporcionou um melhor entendimento sobre seus habitats e as influências dos fatores abióticos como temperatura, radiação solar, salinidade e temperatura no metabolismo de cada alga.

Os resultados também mostraram que estes organismos apresentam um grande potencial de compostos de interesse para alimentação funcional ou nutracêutica, tais como os *n*3, *n*6 e carotenoides, como a fucoxantina que está relacionada, segundo estudos, a atividades antitumoral, antioxidante, hepatoprotetora e anti-inflamatória.

A bioprospecção de pigmentos mostrou altas concentrações de ficoeritrina, juntamente e outras ficobiliproteinas (ficocianinas e alocianinas) que apresentam um grande interesse industrial amplamente utilizado na área alimentícia e cosmética como um corante natural. Na indústria farmacêutica seu uso principal está como antioxidante e surge pesquisas para seu uso no tratamento de Alzheimer.

Todos estes resultados mostram que as algas possuem um grande potencial para os mais variados usos na indústria alimentícia e de fármacos, porém também mostrou que sua utilização deve levar em consideração o seu estágio de

desenvolvimento, pois ocorre diferenciações qualitativas e quantitativas no seu metabolismo, isto é, diferenciam sua constituição de metabolitos.

Com base nas hipoteses propostas no trabalho podemos concluir que a concentração de pigmentos e a performance fotossintética, bem como, as diferenças nos lipídeos totais e ácidos graxos apresentado nos resultados demonstraram que a fase de desenvolvimento influência nestas variáveis e no perfil bioquímico, porém a maior influência ocorre por causa dos fatores abióticos que estas algas estão expostas. Estes fatores, não só influênciam nas concentrações de metabolitos nestes organismos, como também estabelecem as condições para que ocorra os períodos vegetativos e reprodutivos.

8. Referências Introdução

AlgaBase (2018) http://www.algaebase.org/. Acesso em 10 de novembro de 2018.

Appeltans W et al (2012) The Magnitude of Global Marine Species Diversity. Current Biology, 22(23):2189–2202.

Armada del Chile (2018) acesso em 03 de dezembro de 2018. http://meteoarmada.directemar.cl/prontus_meteo/site/edic/base/port/inicio.html

Barsanti l, Coltelli P, Evangelista V, Frassanito AM, Passarelli V, Vesentini N, Gualtieri P (2007) The world of algae. In: Algal toxins: nature, occurrence, effect and detection. Springer Netherlands, Pisa, Italy, pp1-16.

Bartolomeu Santana F, Sena dos Santos PJ (2017) Espectroscopia e modelos atômicos: uma proposta para a discussão de conceitos de Física Moderna no Ensino Médio. Caderno Brasileiro de Ensino de Física, 34(2):555-589.

Billard E, Reyes J, Mansilla A, Faugeron S, Guillemin ML (2015) Deep genetic divergence between austral populations of the red alga *Gigartina skottsbergii* reveals a cryptic species endemic to the Antarctic continente. Polar Biol, 38:2021–2034.

Bishop K, Erdrich S, Karunasinghe N, Han D, Zhu S, Jesuthasan A, Ferguson L (2015) An Investigation into the association between DNA damage and dietary fatty acid in men with prostate cancer. Nutrients, 7(1):405–422.

Bligh EG, Dyer WJ (1959) A rapid method for total lipid extraction and purification. Can J Biochem Physiol, 37:911–917.

Boraso A (2013) Elementos para el estudio de las macroalgas de Argentina. Comodoro Rivadavia. Universitaria de la Patagonia, Chubut, pp 207.

Brothers S, Vadeboncoeur Y, Sibley P (2016) Benthic algae compensate for phytoplankton losses in large aquatic ecosystems. Global Change Biology, 22(12):3865–3873.

Buschmann AH, Moreno C, Vásquez JA, Hernández-González MC (2006) Reproduction strategies of *Macrocystis pyrifera* (Phaeophyta) in Southern Chile: The importance of population dynamics. Developments in Applied Phycology, 349–356.

Cardozo KHM, Marques LG, Carvalho VM, Carignan MO, Pinto E, Marinho-Soriano E, Colepicolo P (2011) Analyses of photoprotective compounds in red algae from the Brazilian coast. Revista Brasileira de Farmacognosia, 21(2):202–208.

Cecere E, Petrocelli A, Verlaque M (2011) Vegetative reproduction by multicellular propagules in Rhodophyta: an overview. Marine Ecology, 32(4):419–437.

Caceres JH, Otaíza R (2015) Manual de una técnica para el repoblamiento de la luga corta, *Mazzaella laminarioides* (Bory) Fredericq (Rhodophyta, Gigartinales), en roqueríos intermareales, Región del Biobío. Editora: Patagonmedia, Chile.

Cheloni G, Slaveykova VI (2018) Photo-oxidative stress in green algae and cyanobacteria. Reactive Oxygen Species 5(14):126–133.

Chen J, Shearer GC, Chen Q, Healy CL, Beyer AJ, Nareddy VB, Gerdes AM, Harris WS, O'connell TD, Wang D (2011) ω-3 fatty acids prevent pressure overload-induced cardiac fibrosis through activation of cGMP/PKG signaling in cardiac fibroblasts. Circulation, 123(6):584–593.

Cifra M, Fields JZ, Farhadi A (2011) Electromagnetic cellular interactions. Progress in Biophysics and Molecular Biology, 105(3):223–246.

Collantes G, Merino A, Lagos V (2002) Fenología de la gametogénesis, madurez de conceptáculos, fertilidad y embriogénesis en *Durvillaea antarctica* (Chamisso) Hariot (Phaeophyta, Durvillaeales). Rev Biol Mar Oceanogr, 37:83–112.

Cunha L, Grenha A (2016) Sulfated seaweed polysaccharides as multifunctional materials in drug delivery applications. Mar Drugs, 14(3):42.

Dromgoole FI (1981) Form and Function of the Pneumatocysts of Marine Algae. Variations in the Pressure and Composition of Internal Gases. Botanica Marina, 24(5).

Dubrasquet H, Reyes J, Sanchez RP, Valdivia N, Guillemin ML (2018) Molecular-assisted revision of red macroalgal diversity and distribution along the Western Antarctic Peninsula and South Shetland Islands. Cryptogamie, Algologie, 39(4):409-430.

Edelman M, Mattoo AK (2008) D1-protein dynamics in photosystem II: the lingering enigma. Photosynthesis Research, 98(1-3):609–620.

Fernando IPS, Nah JW, Jeon, YJ (2016) Potential anti-inflammatory natural products from marine algae. Environmental Toxicology and Pharmacology, 48: 22–30.

Fookes CJR, Jeffrey SW (1989) The structure of chlorophyll c 3, a novel marine photosynthetic pigment. Journal of the Chemical Society, Chemical Communications, 23:1827-1828.

Fu W, Chaiboonchoe A, Khraiwesh B, Sultana M, Jaiswal A, Jijakli K, Nelson DR, Hrout A, Baig B, Amin A, Salehi-Ashtiani K (2017) Intracellular spectral recompositioning of light enhances algal photosynthetic efficiency. Sci Adv, 3:1-11.

Gantt E, Grabowski B, & Cunningham FX (2003) Antenna systems of red algae: phycobilisomes with photosystem ll and chlorophyll complexes with photosystem I. In: Green BR, Parson WW (eds) Light-harvesting antennas in ´photosynthesis. Advances in Photosynthesis and Respiration, Springer, Dordrecht,13:307–322.

Giros, A, Grzybowski M, Sohn VR, Pons E, Morales JF, Xicola RM, Sethi G, Przybowski J, Goel A, Boland R, Gassull MA, llor X (2009) Regulation of colorectal cancer cell apoptosis by the n-3 polyunsaturated fatty acid docosahexaenoic and eicosapentaenoic. Cancer Prevention Research, 2(8):732-742.

Guiry MDG, Guiry GM (2011) AlgaeBase. World-wide electronic publication, National University of Ireland, Galway. http://www.algaebase.org. Acessado em 13 janeiro 2018.

Hammond V, O'donnell VB (2012) Esterified eicosanoids: generation, characterization and function. Biochimica et Biophysica Acta, 1818:2403–2412.

Han BP, Virtanen M, Koponen J, Kraba MS (2000) Effect of photoinhibition on algal photosynthesis: a dynamic model. Journal of Plankton Research, 22(5):865–885.

Hansen JE (1977) Ecology and natural history of *Irdaea cordata* (Gigartinales, Rhodophyta) growth. Journal of Phycology, 13(4):395–402.

Harper MA, Cassie-Cooper V, Chang FH, Nelson WA, Broady PA (2012) Phylum Ochrophyta: brown and golden-brown algae, diatoms, silicoflagellates and kin. New Zealand inventory of biodiversity. Kingdoms Bacteria, Protozoa, Chromista, Plantae, Fungi, pp114-163.

Heldt HW, Piechulla B (2011) Photosynthesis is an electron transport process. Plant Biochemistry, Massachusetts, EUA, pp65–112.

Howell J, Menguc M, Siegel R (2015) Thermal radiation heat transfer, 6 Ed. Boca Raton: CRC Press, pp 1016.

Jakobsen MU, O'reilly EJ, Heitmann BL, Pereira MA, Bälter K, Fraser GE, Goldbourt U, Hallmans G, Knekt P, Liu S, Pietinen P, Spiegelman D, Stevens J, Virtamo J, Willett WC, Ascherio A (2009) Major types of dietary fat and risk of coronary heart disease: a pooledanalysis of 11 cohort studies. American Journal Clinical Nutrition, 89(5):1–8.

Jeffrey SW, Humphrey GF (1975) New spectrophotometric equations for determining chlorophylls *a*, *b*, *c1* and *c2* in higher plants, algae and natural phytoplankton. Biochem Physiol Pflanz, 167:191–194.

Jeffrey SW (1976) The occurrence of chlorophyll c1 and c2 in algae. Journal of Phycology, 12(3):349–354.

Kannan N, Vakeesan D (2016) Solar energy for future world. Renewable and Sustainable Energy Reviews, 62:1092–1105.

Kim HJ, Kim WJ, Koo BW, Kim DW, Lee JH, Nugroho WSK (2016) Anticancer activity of sulfated polysaccharides isolated from the Antarctic red seaweed *Iridaea cordata*. Ocean and Polar Research, 38(2):129-137.

Khotimchenko SV, Kulikova IV (2000) Lipids of different parts of the lamina of *Laminaria japonica* Aresch. Botanica Marina, 43(1):87-91.

Khotimchenko SV, Vaskovsky VE, Titlyanova TV (2002) Fatty acids of marine algae from the Pacific Coast of North California. Botanica Marina, 45(1):17- 22.

Khotimchenko SV (2006) Variations in lipid composition among diferente developmental stages of Gracilaria verrucosa (Rhodophyta). Bot Mar, 49:34–38.

Kuckenberg J, Tartachnyk I, Noga G (2008) Evaluation of fluorescence and remission techniques for monitoring changes in peel chlorophyll and internal fruit characteristics in sunlit and shaded sides of apple fruit during shelf-life. Postharvest Biol Technol, 48 (2):231-241.

Kuckenberg J, Tartachnyk I, Noga G (2009) Temporal and spatial changes of chlorophyll fluorescence as a basis for early and precise detection of leaf rust and powdery mildew infections in wheat leaves. Precision Agric, 10(1):34-44.

Kursar TA, van der Meer JP, Aberte RS (1983) Light harvesting system of the red alga *Gracilaria tikvahiae*. I. Biochemical analyses of pigment mutations. Plant Physiol, 73:353–360.

Lamote M, Johnson LE, Lemoine Y (2012) Photosynthetic responses of an intertidal alga to emersion: The interplay of intertidal height and meteorological conditions. Journal of Experimental Marine Biology and Ecology, 428:16–23.

Larkum AWD, Douglas SE, Raven JA (2003) Photosynthesis in Algae. In: Govindjee (Ed.) Advances in Photosynthesis and Respiration, Springer-Science Business Media, Illinois, U.S.A, v14, pp 498.

Larkum, A. W. (2016). Photosynthesis and Light Harvesting in Algae. In: Borowitzka MA, Beardall J, Raven JA (Eds.). The Physiology of Microalgae, Academic Press, Cambridge, EUA, pp67–87.

Lee RE (2008) Phycology. 4 ed. Colorado, USA: Cambridge University Press, pp 561.

Leonardi RJ, Niizawa I, Irazoqui HA, Heinrich JM (2018) Modeling and simulation of the influence of fractions of blue and red light on the growth of the microalga Scenedesmus quadricauda. Biochemical Engineering Journal, 129:16–25.

Lira MLF, Lopes R, Gomes AP, Barcellos G, Verícimo M, Osako K, Ortiz-Ramirez FA, Ramos CJB, Cavalcanti DN, Teixeira VL, Amaral V (2016) Anti-leishmanial activity of Brazilian green, brown, and red algae. J Appl Phycol 28:591–598.

López-Cristoffanini C, Zapata J, Gaillard F, Potin P, Correa JA, Contreras-Porcia, L (2015) Identification of proteins involved in desiccation tolerance in the red seaweed Pyropia orbicularis (Rhodophyta, Bangiales). Proteomics, 15:3954–3968.

MacDougall K, McNichol J, McGinn P, O'Leary SB, Melanson J (2011) Triacylglycerol profiling of microalgae strains for biofuel feedstock by liquid chromatography–highresolution mass spectrometry. Anal Bioanal Chem, 401:2609–2616.

Mansilla A, Méndez F, Murcia S, Rodríguez JP, Marambio J, Rosenfeld S, Bischof K (2016) Adjustment of pigment composition in *Desmarestia* (Desmarestiaceae) species along a sub-Antarctic to Antarctic latitudinal gradient. Polar Res, 35(1):29383.

Marambio J, Mendez F, Ocaranza P, Rodriguez JP, Rosenfeld S, Ojeda J, Mansilla A (2016) Seasonal variations of the photosynthetic activity and pigment concentrations in different reproductive phases of *Gigartina skottsbergii* (Rhodophyta, Gigartinales) in the Magellan region, sub-Antarctic Chile. Journal of Applied Phycology, 29(2):721–729.

Marambio J, Rodriguez JP, Mendez F, Ocaranza P, Rosenfeld S, Ojeda J, Rautenberger R, Bischof K, Terrados J, Mansilla A (2017) Photosynthetic performance and pigment composition of *Macrocystis pyrifera* (Laminariales, Phaeophyceae) along a gradient of depth and seasonality in the ecoregion of Magellan, Chile. J Appl Phycol, 29(5):2575-2585.

Martín A, Miloslavich P, Díaz Y, Ortega I, Klein E, Troncoso J, Carbonini AK (2015) Intertidal benthic communities associated with the macroalgae Iridaea cordata and Adenocystis utricularis in King George Island, Antarctica. Polar Biology, 39(2):207–220.

Méndez F, Tala F, Rautenberger R, Ojeda J, Rosenfeld S, Rodríguez JP, Marambio J, Ocaranza P, Mansilla A (2017) Morphological and physiological differences between two morphotypes of *Durvillaea antarctica* (Phaeophyceae) from the sub-Antarctic e coregion of Magallanes, Chile. Journal of Applied Phycology, 29(5):2557–2565.

Montecinos A, Broitman BR, Faugeron S, Haye PA, Tellier F, Guillemin ML (2012) Species replacement along a linear coastal habitat: phylogeography and speciation in the red alga *Mazzaella laminarioides* along the south east pacific. BMC Evolutionary Biology, 12(1):97.

Moss, C. W., Lambert, M. A. & Merwin, W. H. (1974). Comparison of rapid methods for analysis of bacterial fatty acids. Journal of Applied Microbiology, 28:80–85.

Murchie EH, Lawson T (2013) Chlorophyll fluorescence analysis: a guide to good practice and understanding some new applications. Journal of Experimental Botany, 64(13):3983–3998.

Nanba O, Satoh K (1987) Isolation of a photosystem II reaction center consisting of D-1 and D-2 polypeptides and cytochrome b-559. Botany, 84:109-112.

National Aeronautics and Space Administration - NASA (2019) https://earthobservatory.nasa.gov/world-of-change/Ozone. Acesso em 01 de abril de 2019.

Nedbal L, Trtìlek M, Herppich WB (2000) Methods and equipment for fluorescence imaging on plant material. Bornimer Agrartechnische Berichte, 25:127-135.

Nelson WA (2005) Life history and growth in culture of the endemic New Zealand kelp *Lessonia variegata* J. Agardh in response to differing regimes of temperature, photoperiod and light. J Appl Phycol, 17:23-28.

Niyogi KK (2009) Photoprotection and High Light Responses. In: Elizabeth H. Harris EH, Witman GB, Stern DB (Eds) The Chlamydomonas Sourcebook. Academic Press, pp847–870.

Oncel SS, Kose A, Faraloni C (2015) Genetic optimization of microalgae for biohydrogen production. In: Kim SK (Ed.) Handbook of Marine Microalgae, Academic Press, pp383–404.

Ocaranza-Barrera P, González-Wevar CA, Guillemin ML, Rosenfeld S, Mansilla A (2018) Molecular divergence between Iridaea cordata (Turner) Bory de Saint-Vincent from the Antarctic Peninsula and the Magellan Region. Journal of Applied Phycology. 1-11.

Park YI, Chow WS, Anderson JM (1995) Light inactivation of functional photosystem II in leaves of peas grown in moderate light depends on photon exposure. Planta, 196:401– 411.

Pratama W, Dewi SC, Sari I, Hardiyati A, Wajong AE (2015) Distribution and abundance of macroalgae in intertidal zone of Drini Beach, Gunungkidul. KnE Life Sciences, 2:514-517.

Platt T, Gallegos CL, Harrison WG (1980) Photoinhibition of photosynthesis in natural assemblages of marine phytoplankton. Journal Marine Research, 38:687–70.

Ralph PJ, Gademann R (2005) Rapid light curves: a powerful tool to assess photosyn-thetic activity. Aquat Bot, 82(3):222–237.

Rao PS, Ganesan K, Kurar KS (2009) Seaweeds: a survey of research and utilization. Algal biology and biotechnology. New Delhi: Krishan Makhijanj.

Rastogi RP, Richa, Kumar A, Tyagi MB, Sinha RP (2010) Molecular mechanisms of ultraviolet radiation-induced DNA damage and repair. J. Nucleic Acids, Article ID 592980, 1-32.

Raven JA (2011) The cost of photoinhibition. Physiologia Plantarum, 142(1): 87–104.

Rodríguez JP, Terrados J, Rosenfeld S, Méndez F, Ojeda J, Mansilla A (2018) Effects of temperature and salinity on the reproductive phases of *Macrocystis pyrifera* (L.) C. Agardh (Phaeophyceae) in the Magellan region. Journal of Applied Phycology. doi:10.1007/s10811-018-1693-x

Sahoo D, Baweja P (2015) General Characteristics of Algae. In: Sahoo D., Seckbach J (eds) The algae world. Cellular origin, life in extreme habitats and astrobiology. Springer, Dordrecht, pp1-27.

San Giovanni JP, Chew EY (2005) The role of omega-3 long-chain polyunsaturated fatty acids in healthand disease of the retina. Progress in Retinal and Eye Research, 24:87–138.

Santos MAZ, Colepicolo P, Pupo D, Fujii MT, Pereira CMP, Mesko MF (2017) Antarctic red macroalgae: a source of polyunsaturated fatty acids. Journal of Applied Phycology, 29(2):759-767.

Sarmiento JL, Gruber N (2006) Ocean Biogeochemical Dynamics. Published by Princeton University Press: William Street, Princeton, New Jersey, pp526.

Satyam K, Thiruchitrambalam G (2018) Habitat ecology and diversity of rocky shore fauna. In: Sivaperuman C, Velmurugan A, Singh AK, Jaisankar I (Eds) Biodiversity and Climate Change Adaptation in Tropical Islands, Academic Press, pp187–215.

Sawicki A, Willows RD, Chen M (2019) Spectral signatures of five hydroxymethyl chlorophyll a derivatives chemically derived from chlorophyll b or chlorophyll f. Photosynthesis Research. On line 1-13.

Schwarz AM, Hawes I, Nelson W, Andrew N (2006) Growth and reproductive phenology of the kelp *Lessonia variegata* in central New Zealand. Mar Freshw Res 40:273-84.

Seely GR, Duncan MJ, Vidaver WE (1972) Preparative and analytical extraction of pigments from brown algae with dimethyl sulfoxide. Mar Biol, 12:184–188.

Sharif N, Munir N, Naz S, Iqbal R, Rauf W (2017) Origin of algae and their plastids. Algae Based Polymers, Blends, and Composites. Chemistry, Biotechnology and Materials Science, Elsevier, 77–113.

Silva PRD (2016) Fotorreações da fotossíntese. São Carlos. Acesso em 10 novembrode2018.https://edisciplinas.usp.br/pluginfile.php/2080019/mod_resource/content/1/Aula10BioqII_Fotoss%C3%ADntese.pdf

Singhal GS, Renger G, Sopory SK, Irrgang KD, Govindjee (1999) Concepts in Photobiology: Photosynthesis and Photomorphogenesis. Springer Netherlands, Narosa Publishing House, New Delhi, India, pp1018.

Smith Colleen et al. (2009) Marks' basic medical biochemistry: a clinical approach. 3 ed. Philadelphia: Ed. Lippincott Williams & Wilkins, pp1011.

Stevens CL, Hurd CL, Smith MJ (2002) Field measurement of the dynamics of the bull kelp *Durvillaea antarctica* (Chamisso) Hariot. J Exp Mar Biol Ecol, 269:147–171.

Szymański N, Dąbrowski P, Zabochnicka-świątek M, Panchal B, Lohse D, Kalaji HM (2017) Taxonomic classification of algae by the use of chlorophyll a fluorescence. Sci Rev Eng Env Sci, 26(4):470–480.

Tait MA, Hik DS (2003) Is dimethylsulfoxide a reliable solvent for extracting chlorophyll under field conditions?. Photosynth Res, 78(1):87–91.

Tala F, Edding M (2004) Growth and loss of distal tissue in blades of *Lessonia nigrescens* and *Lessonia trabeculata* (Laminariales). Aquat Bot, 82:39-54.

Thakur S, Sharma B, Verma A, Chaudhary J, Tamulevicius S, Thakur VK (2018) Recent progress in sodium alginate based sustainable hydrogels for environmental applications. Journal of Cleaner Production, 198:143–159.

The Earth Observatory is part of the EOS Project Science Office at NASA Goddard Space Flight Center (2009). Acesso 20 dezembro de 2018. https://earthobservatory.nasa.gov/features/EnergyBalance/page4.php.

Vance DE, Vance JE (2008) Biochemistry of lipids, lipoproteins and membranes, 5nd. Ed. Elsevier Science, pp638.

White AJ, Critchley C (1999) Rapid light curves: A new fluorescence method to assess the state of the photosynthetic apparatus. Photosynth Res, 59:63–72.

Wong CY, Teoh ML, Phang SM, Lim PE, Beardall J (2015) Interactive effects of temperature and UV radiation on photosynthesis of *Chlorella* strains from polar, temperate and tropical environments: differential impacts on damage and repair. PLoS One 10(10): e0139469. https://doi.org/10.1371/journal.pone.0139469

Yokoya NS, Necchi Júnior O, Martins AP, Gonzalez SF, Plastino EM (2007) Growth responses and photosynthetic characteristics of wild and phycoerythrin-deficient strains of Hypnea musciformis (Rhodophyta). J Appl Phycol, 19:197–205.

Yunoki K, Sato M, Seki K, Ohkubo T, Tanaka Y, Ohnishi M (2009) Simultaneous quantification of plant glyceroglycolipids including sulfoquinovosyldiacylglycerol by HPLC–ELSD with binary gradient elution. Lipids, 44:77–83.

Xue L, Zhang Y, Zhang T, An L, Wang X (2005) Effects of Enhanced Ultraviolet-B Radiation on Algae and Cyanobacteria. Critical Reviews in Microbiology, 31(2):79–89.

Zubia M, Freile-Pelegrín Y, Robledo D (2014) Photosynthesis, pigment composition and antioxidant defences in the red alga Gracilariopsis tenuifrons (Gracilariales, Rhodophyta) under environmental stress. Journal of Applied Phycology, 26(5):2001–2010.

Capitulo 2 – Pigment concentration, photosynthetic performance and fatty acid profile of Sub-Antarctic brown macroalgae in different phases of development from the Magellan Region, Chile

Aceito em Journal of Applied Phycology

ISSN 0921-8971

J Appl Phycol

DOI 10.1007/s10811-019-01777-x

Pigment concentration, photosynthetic performance and fatty acid profile of Sub-Antarctic brown macroalgae in different phases of development from the Magellan Region, Chile

[1]Marco Aurélio Ziemann dos Santos*, [1] Samantha Coelho de Freitas, [1]Lucas Moraes Berneira, [2] Andres Mansilla, [2] Maria Soledad Astorga-España, [3] Pio Colepicolo, [1]Claudio Martin Pereira de Pereira

[1] Center for Chemical, Pharmaceutical and Food Sciences, Federal University of Pelotas, University Campus, S / N - CEP 96160-000, Capão do Leão, RS – Brazil

[2] Laboratory of Antarctic and Sub-Antarctic Marine Ecosystems, University of Magallanes, 01855 Bulnes Ave., Punta Arenas 6200000. Instituto de Ecología y Biodiversidad (IEB), Chile

[3] Department of Biochemistry, Chemistry Institute, Av. Prof. Lineu Prestes, 748 – Butantã, University of São Paulo, SP, Brazil

*Corresponding author: marcziemann@gmail.com

Telephone number: +55053981184936

ORCID: 0000-0002-3776-3701

Abstract

Macroalgae *Durvillaea antarctica*, *Lessonia flavicans* and *Macrocystis pyrifera* in distinct development phases from the ecoregion of Magellan (Chile) were analyzed by Pulse Amplitude Modulated Fluorometry under eight irradiation conditions (11 to 490 µmol photons m^{-2} s^{-1}). Pigmentation was assessed by UV/VIS Spectrophotometry (400 to 700 nm) and fatty acid (FA) profile was determined by Gas Chromatography using standards of their respective methyl esters (0.625 to 20 mg mL^{-1}). Photosynthetic efficiency had significant differences for *L. flavicans* (0.31 ± 0.01 to 0.38 ± 0.01 µmol e^- m^{-2} s^{-1}. µmol photons m^{-2} s^{-1}) and *M. pyrifera* (0.26 ± 0.02 to 0.31 ± 0.03 µmol e^- m^{-2} s^{-1}. µmol photons m^{-2} s^{-1}) for reproductive and vegetative phases, respectively. The relative maximum electron transfer rate varied significantly for *L. flavicans* (8.10 ± 0.84 to 12.40 ± 1.57 µmol e^- s^{-1}) and *M. pyrifera* (6.49 ± 1.30 to 12.89

± 1.53 µmol e^{-} s^{-1}) in distinct development phases. Saturation irradiance analysis showed significant differences for *D. antarctica*, varying from 166.18 ± 14.33 (vegetative) to 132.98 ± 18.43 µmol photon m^{-2} s^{-1} (reproductive). The highest concentrations of pigments were found in reproductive *M. pyrifera* with 35.36 ± 0.21 of Chl *a*, 7.04 ± 0.93 of Chl *c* and 15.75 ± 1.42 µg g^{-1} of fucoxanthin. Finally, the highest concentrations of total FAs were 35.24 ± 2.38% (saturated) and 22.02 ± 1.95% (monounsaturated) in *M. pyrifera* and 63.53 ± 3.36% (polyunsaturated) in *D. antarctica*. Therefore, the study showed significant differences for photosynthetic parameters and FA profiles correlating these results to the development phases of macroalgae.

Keywords: Polyunsaturated – Fatty Acids – Brown Algae - Photosynthetic Activity, Sub-Antarctic Region

Acknowledgement

This study had logistic support from the University of Magallanes and the Laboratory of Antarctic and Sub-Antarctic Marine Ecosystems - Instituto de Ecología y Biodiversidad (IEB), Chile. The authors are grateful for the financial and fellowship support from the Brazilian research funding agencies National Program for Post-Doctoral Studies - Coordination for Improvement of Higher Level Personnel (PNPD-CAPES - General Program of International Cooperation PGCI -99999.002378/2015) and National Council for Scientific and Technological Development (CNPq).

1. Introduction

The region of the Strait of Magellan has a particular benthic marine ecosystem due to marine currents present between the Pacific and Atlantic Oceans (Ríos et al., 2010). According to Mansilla et al., (2012), there are 395 seaweeds species that inhabit the coasts of the Strait of Magellan, Beagle Channel and Cape Horn that can be divided within the phyla Rhodophyta (230), Chlorophyta (75) and Ochrophyta (86). It is worth noting that 11 species are common to the Magellan region and the Antarctic continent (Mansilla et al., 2013b). Among the organisms that inhabit the sub-Antarctic region, *M. pyrifera* of the phylum

Ochrophyta can be found in abundant occurrence since it has an increased tolerance to the adverse conditions found in this habitat.

Periods of solar irradiation reaching 12 h, air temperature between 7 to 12 °C (Sanchez et al., 2012), increased ultraviolet radiation (UV) due to the depletion of the ozone layer over the region (Rowland, 2006), water temperature between 7 to 10 °C and salinity from 30 to 32 PSU are conditions found in the summer of the sub-Antarctic region of the Strait of Magellan (Mansilla et al., 2013a; Servicio Hidrográfico y Oceanográfico de la Armada de Chile, 2018). High levels of UV radiation, mainly as UV-B, can act as a stressing factor causing irreparable damages to the photosystem and DNA of algae (Franklin and Forster, 1997; Bischof et al., 2006).

According to Long et al. (1994), the main target of UV-B is the D1 protein found in the electron transport chain of photosystem II (PSII), which can be damaged by the excess radiation, resulting in photoinhibition. Moreover, UV-B can damage the synthesis of D1 protein and the accessory pigments which are light-absorbing compounds important for optimizing the efficiency of PSII (Häder et al., 2015). In this sense, defense mechanisms of macroalgae are mainly associated to the production of phenolic compounds (phlorotannins) (Gómez and Huovinen, 2015), pigments including fucoxanthin that act as photoprotectors and antioxidants (Pangestuti et al., 2018) as well as differentiated concentrations of lipids in vegetative and reproductive tissues that prevent cellular damages (Freile - Pelegrín and Robledo, 2013; Galindo et al., 2017).

Since the appearance of algae in the pre-Cambrian period (541 million years ago) (Dawes, 2016) their photosynthetic system had to adapt to diverse places that can vary from desert zones to regions of extremely cold weather (Morgan-Kiss et al., 2006). Physiological functions of these organisms are influenced mainly by abiotic parameters such as solar irradiance, light distribution and environmental seasonality (Titlyanov et al., 2014; Gomez et al., 2018). Production of energy in these organisms is influenced by daily fluctuations of nutrients available to algae (Jones et al., 1996; Juneja et al., 2013).

Photosynthetic processes in brown algae are influenced significantly by the concentration of inorganic carbon available in the environment (Nygárd and Dring, 2008). In addition to the diffuse use of CO_2, many algae require an extra amount of carbon uptake that is usually absorbed in the form of bicarbonate (HCO^{3-}). This

exogenous inorganic carbon source is abundant in seas and can assist macroalgae in their growth and development (Bi and Zhou, 2016).

Brown algae can be found in several environments that include tropical waters as well as the sub-Antarctic and Antarctic regions (Pellizzari et al., 2017; Astorga-España and Mansilla et al., 2014). The infralittoral region is known for being the main zone where these organisms can inhabit, submitting them directly under the influence of tidal cycles (Lin et al., 2017; Batista et al., 2018). This is an important factor in the development of brown algae as tidal cycles expose organisms to higher radiation rates for long periods of time (Connan et al., 2007). Moreover, abiotic parameters such as temperature and exposure time to solar irradiance directly affect vegetative and reproductive stages of macroalgae (Hannach and Santelices, 1985). Representatives from the Laminariales orders, for instance, have an enhanced development in cold waters where temperatures are maintained below 20 °C (Wiencke et al., 1993).

In spring and summer seasons when the photoperiod is at relatively higher levels, algae capture higher amounts of light for their photosynthetic process and, thus, increase their reserve of nutrients and growth rate. These mechanisms are important to maintain the metabolism in optimum conditions in the autumn and winter seasons when the photoperiod is decreased (Marambio et al., 2017a). Moreover, the differentiated cellular structure of algae cells, morphology, accessory pigments and structural components of membranes such as lipids are essential constituents related to their evolutionary and adaptive processes (Khotimchenko and Yakovleva, 2005). Brown algae have chlorophyll *a* (Chl *a*) and *c* (Chl *c*) and accessory pigments such as fucoxanthin that are responsible for their typical brown color (Mikami and Hosokawa, 2013).

According to Mikami and Murata (2003), polyunsaturated fatty acids (PUFAs) are responsible for the membrane fluidity in cold temperatures. Nonetheless, this biochemical mechanism is very complex and may not be completely related to the fluctuation of temperature, but to other stress factors such as variations of solar irradiance and hyperosmotic stress that can modulate concentrations of PUFAs in membranes (Kumar et al., 2014). Physiological aspects including photosynthetic performance and chemical information such as the concentration of pigments and the lipid profile associated to the phases of development of marine macroalgae have been remotely studied, even less in organisms from the sub-Antarctic region of the Magellan Strait. In this sense, the aim of this study was to investigate the difference of

the concentration of pigments, fatty acids and photosynthetic performance in vegetative and reproductive phases of brown macroalgae *Durvillae antarctica* (Chamisso) Hariot, *Lessonia flavicans* Bory and *Macrocystis pyrifera* (Linnaeus) C. Agardh of the Magellan region (Chile).

2. Materials and Methods

2.1 Algae collection

2.1.1 Sampling and sample preparation

Samples of seaweeds were collected between December 2016 and March 2017 in the region of the Strait of Magellan (Punta Arenas, Chile) (Figure 1). The analyzed species are from the Phylum Ochrophyta of the order Fucales *D. antarctica* (53° 08S, 71° 30W) and the order Laminariles *L. flavicans* (53° 36S, 70° 55W) and *M. pyrifera* (53° 36S, 70° 55 W) in the vegetative and reproductive phases of development. Approximately 6 individuals of each phase of *D. antarctica* were manually collected at low tide in the intertidal zone and in the lower littoral zone. Approximately 10 individuals of *M. pyrifera* in the vegetative and reproductive phases were collected at sea level and in the infralittoral zone (around 5 m of depth), respectively. In the infralittoral zone, 10 individuals of each phase of *L. flavicans* were collected. Middle and margin tissue of the fronds were used for pigment and photosynthetic activity analyses. The general information of algae collection, stages of development, individuals stored for exsiccate and subsequent morphological identification under specified numbering were carried out in the Herbarium of the Laboratory of Antarctic Marine Ecosystems and Antarctic Submarines (LEMAS), and are indicated in Table 1.

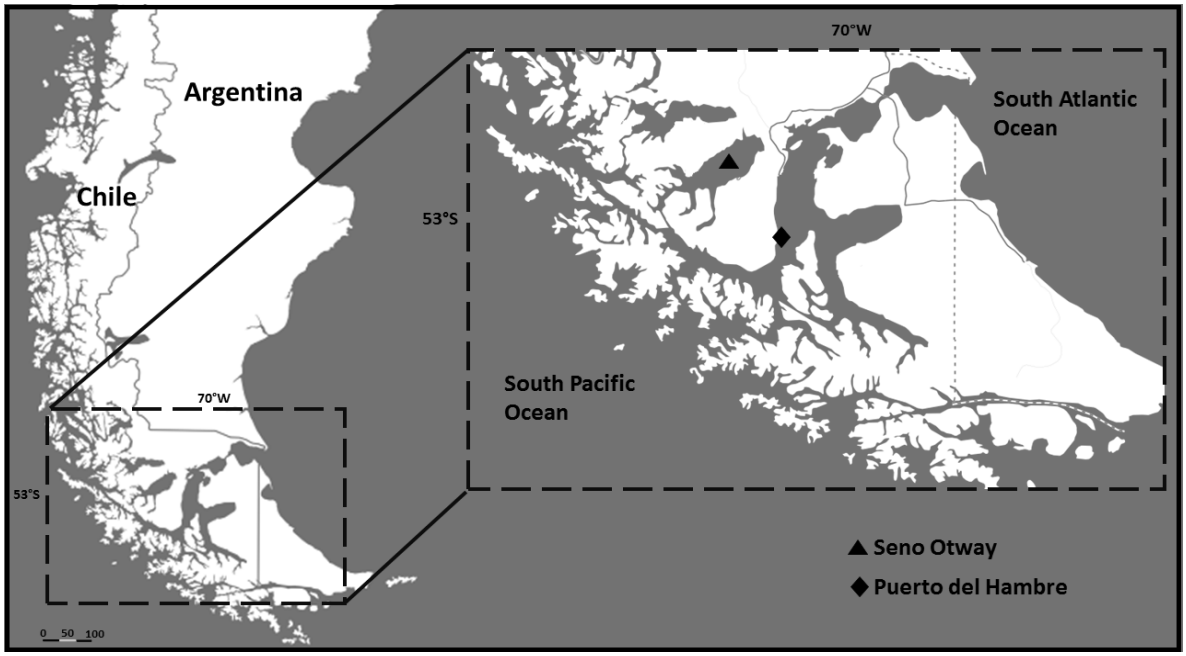

Figure 1 - Sampling site in Seno Otway (53°.08'.52.0S,71°.30'.32.6W) and Puerto del Hambre (53°.36'.46.6S, 70°.55'.46.6W) Strait of Magellan, Sub-Antarctic Chilean region where (a) *D. antarctica*, (b) *M. pyrifera* and *L. flavicans* were collected in the vegetative and reproductive phases.

Table 1 – Collection data, development phase, place location, marine zonation and herbarium number of brown macroalgae collected in the Magellan Region, Chile (2016 – 2017)

Species	Development Phase	Collect Date	Collection Location	Marine Zonation	Herbarium Number
L. flavicans	Veg	21.12.16	Puerto del Hambre	INLT	522p
L. flavicans	Rep	15.02.17	Puerto del Hambre	INLT	523p
M. pyrifera	Veg	15.12.16	Puerto del Hambre	SLL	518p
M. pyrifera	Rep	15.12.16	Puerto del Hambre	INLT	520p
D.antarctica	Veg	23.03.17	Seno Otway	MLLW	582p
D.antarctica	Rep	23.03.17	Seno Otway	MLLW	583p

Infralittoral – INLT; Lower Mesolittoral (MLLW); Sea Level - SLL; Veg - vegetative phase; Rep - reproductive phase

The collected material was placed in a cooler box filled with seawater and sent to the laboratory to be conditioned in a culture chamber with aeration for 24 h acclimatization at 5 ± 1 °C, with artificial radiation of 20 µmol photons m^{-2} s^{-1} PAR, provided by one true light natural daylight fluorescent tube (Osram, Germany) and under a standard photoperiod of 12 h. After a settling period, the collected algae were classified and Pulse Amplitude Modulated Fluorometer (PAM) analysis was conducted.

Before freezing, the material was washed with running and distilled water in order to remove dirt. The species were properly identified, placed in dark plastic bags and put in a horizontal freezer at -20 °C. The remaining algae were weighed and frozen at -20 °C in an air circulation oven to dry. After freezing, the algal biomass was cooled and dried in a JOSF 700T air circulation oven at 35 °C (± 1 °C) for 24 to 30 h and were pulverized in a Lucadema model 226/2 knife mill. After drying, the material was packed in dark plastic bags and frozen at -20 °C until fatty acid analysis was taken. Dry Weight determination (DW) in algae was performed following the Brazilian Pharmacopeia (2010) which is based on the loss of moisture and volatiles eliminated by desiccation. Approximately 2 g of the material was weighed in triplicate (n=3) and desiccation was carried out in a DeLeo model A58EAF stove at 105 °C for 5 h until a constant weight was achieved. The moisture content was calculated by the difference between the initial and final weights of the samples and expressed as a percentage.

2.1.2 Chemicals and Instrumentation

For the identification and quantification of the fatty acids, a mixture of 37 fatty acid methyl esters (F.A.M.E. MIX, C4-C24 - Product Number: 18919-1, Supelco, USA) was used with an internal standard of nonadecanoate (19:0 – Sigma-Aldrich, USA). Chromatographic analysis was carried out in a GC 2010 Gas Chromatograph with a Flame Ionization Detector (GC/FID – Shimadzu) (Tang and Row, 2013) and a Capillary GC Column SP®-2560 (100 m × 0.25 mm x 0.20 µm. Pulse Amplitude Modulated analysis was conducted in a subaquatic equipment DIVING PAM (Walz, Germany). Pigmentation was analyzed with a spectrophotometer (Hewlett Packard 8452A) in wavenumbers ranging from 400 to 700 nm.

2.1.3 Pigmentation Analysis

Pigmentation analysis in brown algae followed the modified methodology of Seely et al. (1972) in which approximately 125 mg of fresh algae were transferred to Eppendorf tubes that contained 1 mL of dimethyl sulfoxide (DMSO) and left to rest for 15 min in the dark (Tait and Hik, 2003; Mansilla et al., 2016; Méndez et al., 2017). Subsequently, the upper phase was transferred to cuvettes and analyzed in a Spectrophotometer Hewlett Packard 8452A in wavenumbers ranging from 400 to 700 nm. No further dilutions were necessary. The calculation of the Chl *a*, Chl *c* and fucoxanthin concentration were done according to equations (1), (2) and (3) **(**Seely et al., 1972)**.**

Chlorophyll *a*

$$\text{Chl}\,a = \text{A665} / 72.8 \quad \textbf{(1)}$$

Chlorophyll *c*

$$\text{Chl}\,c = (\text{A631} + \text{A582} - 0.297 \times \text{A665}) / 61.8 \quad \textbf{(2)}$$

Fucoxanthin

$$\text{Fucox} = (\text{A480} - 0.772\,(\text{A631} + \text{A582} - 0.297 \times \text{A665}) - 0.049 \times \text{A665}) / 130.0 \quad \textbf{(3)}$$

2.1.4 Photosynthetic performance

After the acclimation period, approximately 5 to 6 individuals of each of the three studied species in each stage of development (vegetative or reproductive) were placed on a tip of an optic fiber and subjected to fast response light curves induced by an underwater fluorometer DIVING-PAM (Walz, Germany). Macroalgae were subjected to eight increasing levels of irradiance from 11, 36, 71, 117, 175, 242, 360 and 490 µmol m^{-2} s^{-1} with intervals of 30 s after each analysis in order to measure light response curves (White e Critchley, 1999) and saturation flash (0.8 s; ≥ 9000 µmol photons m^{-2} s^{-1}) (Marambio et al., 2017b). Before analysis of RLCs, samples were placed in a tip of optic fiber with a clip in order to maintain the frond in the dark for 20 min (Ralph e Gademann, 2005; Wong et al., 2015). The spectral composition of underwater irradiances were used from the studies conducted by Rautenberger et al. (2009) and Rautenberger and Bischof (2016). The terminology used to describe the various components of variable chlorophyll fluorescence was in accordance Cosgrove and Borowitzka (2011).

Adaptation to the dark allowed the determination of maximum photochemical efficiency (quantum yield; φPSII$_{max}$ or F_v / F_m), determined by the following Eq. 4, where F_0 is minimum fluorescence yield and F_m is maximum fluorescence yield at the PSII measured under a strong saturation pulse of actinic light in the dark.

$$\varphi\mathrm{PSIImax} = (Fm - F0) / Fm' \quad \textbf{(4)}$$

Relative electron transfer rate (rETR) was determined by the following Eq. 5, where PAR is the irradiance produced by actinic light from the equipment (µmol m^{-2} s^{-1}) (Ralph e Gademann, 2005). The effective photochemical efficiency in actinic light (φPSII) was determined by the following Eq. 6, were F_m' is maximum fluorescence yield in actinic light and *Ft* is fluorescence yield in actinic light (fluorescence yield at time *t*).

$$\mathrm{rETR} = \varphi\mathrm{PSII} \times \mathrm{PAR} \quad (\textbf{5})$$

$$\varphi\mathrm{PSII} = (Fm' - Ft) / Fm' \quad (\textbf{6})$$

Quantitative evaluation of the rapid response to light curves (RLCs) was made using parameters of photosynthetic efficiency (*α*), photoinhibition (*β*), irradiance saturation (E_k) and relative maximum electron transfer rate (rETR$_{max}$) adjusted to the curve following the hyperbolic rETR vs *E* curves that were fitted according to the model of Platt et al. (1980) (Eq. 7). Results of photosynthetic performance were processed using the software Kaleida Graph 4.0 (Synergy Software 1986–2005).

$$PB(I) = [1 - \exp(-\alpha I / Ps) \exp(-\beta I / Ps) \quad (\textbf{7})$$

Where according to the model of Platt et al. (1980), $P^B(I)$ = photosynthetic rate [mg C (mg Chl*α*)$^{-1}$ h^{-1}] at irradiance *I* (µmol photons m^{-2} s^{-1}); P – light saturated photosynthetic rate [mg C (mg Chl*α*)$^{-1}$ h^{-1}] in the absence of photoinhibition; *α* - initial slope of the *P-I* curve [(mg C (mg Chl*α*)$^{-1}$ h^{-1}) (µmol photons m^{-2} s^{-1})]; *β* = an index of photoinhibition [(mg C (mg Chl*α*)$^{-1}$ h^{-1}) (µmol photons m^{-2} s^{-1})].

2.1.5 Lipid extraction and fatty acid methyl esterification

Extraction of fatty acids followed the modified procedure of Bligh and Dyer (1959) in which one gram of the algal biomass was dried and pulverized in a knife mill (A 11 basic-IKA Works, Brazil). Samples were put in a 100 mL flask, where 10 mL of chloroform, 20 mL of methanol and 10 mL of an aqueous solution of sodium sulfate (1.5%, *w/v*) were added. Subsequently, the mixture was agitated at ambient temperature for 30 min and, after this period, 10 mL of chloroform and 10 mL of an aqueous solution of sodium sulfate (1.5%, *w/v*) were added to the system. The solution was transferred to falcon tubes and submitted to centrifugation for 30 min under 5000 rpm (2800 g). After centrifugation, the organic phase was retrieved and the solvent was evaporated in a rotary evaporator (Buchi, Switzerland) with a V-700 vacuum pump and a B-741 cooler. The lipid content was obtained in triplicate (n=3) and determined gravimetrically.

The extracted lipids from the algal biomass (approximately 20 to 50 mg) were esterified and converted to their respective fatty acid methyl esters (FAMEs) according to the method “B” of Moss et al. (1974). Briefly, 6 mL of a methanolic solution of potassium hydroxide (2%, *w/v*) were added to a 50 mL flask that contained the previous extracted lipids, under agitation and reflux at 80 °C for 8 min. Afterwards, 7 mL of a methanolic solution of boron trifluoride (Aldrich - 14%, *v/v*) were added and the solution was stirred under reflux for 2 min. Subsequently, the mixture was cooled and 5 mL of an aqueous solution of sodium chloride (20%, *w/v*) were added. The organic phase that contained the FAMEs was retrieved using 20 mL of hexane, filtered through anhydrous sodium sulfate, evaporated under reduced pressure and dried until constant weight under nitrogen flow.

2.1.6 Gas chromatography Analysis of Fatty Acid Methyl Esters

FAMEs were analyzed based on an analytical calibration employing FAME 37-MIX (Supelco, Bellefonte, Pennsylvania, USA) in six distinct concentration ranging from 0.625 mg mL^{-1} to 20 mg mL^{-1}. Nonadecanoate (≥ 99.0% - Sigma-Aldrich, St. Louis, Missouri, USA) was added to the samples and to the analytical calibration in a concentration of 2 mg mL^{-1}. Analysis were performed in a Gas Chromatograph with a Flame Ionization Detector – GC/FID 2010 (Shimadzu) with a split/splitless injector,

autoinjector AOC-20i and capillary column (SP®-2560 (100 m × 0.25 mm, df 0.20 µm - Supelco). The operational conditions of the analysis were hydrogen as a carrier gas with a flow of 1.2 mL min^{-1}, split mode of 1:100, injection volume of 1 µL, initial temperature of the oven at 100 °C increasing 3 °C.min^{-1} to 220 °C. The temperature of the injection port and the detector were 250 °C (Santos et al., 2017). All reagents used were of analytical grade (≥ 99.0%).

3. Statistical Analysis

Evaluation of the results regarding pigment concentration, photosynthetic parameters, total fatty acids (ΣSFAs, ΣMUFAs and ΣPUFAs) and the fatty acid profile among the phases of development was performed applying two-way analysis of variance (ANOVA). One-way ANOVA was used for univariate variables such as *Fv / Fm* and the major fatty acids distributed among SFAs, MUFAs and PUFAs. After ANOVA, Tukey's HSD post hoc analysis of means was used to analyze differences among the results and to assess significant differences at a confidence interval of 95% ($p<0.05$). All statistical analyses were performed using GraphPad Prism 7 software (Version 2017-02, USA).

4. Results

4.1 Pigmentation Analysis

D. antarctica did not have significant differences between mean concentrations (n=5) found in the vegetative and reproductive phases regarding Chl *a*, Chl *c* and fucoxanthin. On the other hand, *L. flavicans* had accessory pigments in higher concentrations found in the reproductive phase reaching 12.64 ± 2.19, 4.50 ± 0.94 and 10.48 ± 1.16 µg g^{-1} (< 0.05; ANOVA Tukey's HSD), respectively, to Chl *a*, Chl *c* and fucoxanthin with significant differences between Chl *a* and fucoxanthin among the development phases as shown in the Online Resource Table 2. Results with significant differences of Chl *a*, Chl *c* and fucoxanthin were also observed for *M. pyrifera* among vegetative and reproductive phases. This seaweed had the greatest concentration of pigments among the three studied species. The major concentrations of pigments were observed in the vegetative phase, which was the opposite of the observed

for *D. antarctica*, additional data are given in Online Resource Table 3. All results were calculated and expressed in dry weight.

4.2 Photosynthetic performance

Photosynthetic activity analysis of brown macroalgae *D. antarctica*, *L. flavicans* and *M. pyrifera* showed significant differences in photosynthetic efficiency (*α*) for species *L. flavicans* and *M. pyrifera* in their vegetative and reproductive phases. Results for *L. flavicans* varied from 0.31 ± 0.02 µmol e^- m^{-2} s^{-1}. µmol photons m^{-2} s^{-1} in the reproductive phase to 0.38 ± 0.01 µmol e^- m^{-2} s^{-1}. µmol photons m^{-2} s^{-1} in the vegetative stage (< 0.05; ANOVA Tukey's HSD). The seaweed *M. pyrifera* had significant differences with values of 0.26 ± 0.04 and 0.33 ± 0.03 µmol e^- m^{-2} s^{-1}. µmol photons m^{-2} s^{-1} (< 0.05; ANOVA Tukey's HSD) for the reproductive and vegetative phases. On the other hand, *D. antarctica* did not show differences in the results having 0.24 ± 0.01 and 0.23 ± 0.02 (µmol e^- m^{-2} s^{-1}. µmol photons m^{-2} s^{-1}) in vegetative and reproductive stages, respectively (Figure 2a).

The $rETR_{max}$ were significantly different for *L. flavicans* with 12.40 ± 1.57 and 8.10 ± 0.84 µmol m^{-2} s^{-1} as well as for *M. pyrifera* with 12.89 ± 1.53 and 6.49 ± 1.30 µmol m^{-2} s^{-1} (< 0.05; ANOVA Tukey's HSD) in the vegetative and reproductive phases of both species. *D. antarctica* did not show significant differences in $rETR_{max}$ with a value of 40.66 ± 3.63 µmol m^{-2} s^{-1} in the vegetative phase and 30.81 ± 4.68 µm µmol m^{-2} s^{-1} in the reproductive phase (Figure 2b).

Saturation irradiance (E_k) analysis of the studied species had only significant differences for *D. antarctica*, which had values of 166.18 ± 14.33 µmol photon. m^{-2} s^{-1} in the vegetative phase and 132.98 ± 18.43 µmol photon m^{-2} s^{-1} in the reproductive stage (< 0.05; ANOVA Tukey's HSD). *L. flavicans* and *M. pyrifera* did not show differences in E_k and the results obtained, respectively, in the vegetative and reproductive phases of both species were 32.81 ± 4.44 µmol photon m^{-2} s^{-1}, 27.17 ± 3.67 µmol photon m^{-2} s^{-1}, 52.48 ± 10.79 µmol photon m^{-2} s^{-1} and 31.69 ± 14.12 µmol photon m^{-2} s^{-1} (Figure 2c). Statistical data of photosynthetic efficiency (*α*), $rETR_{max}$ and saturation irradiance (E_k) are given in Online Resource Table 2.

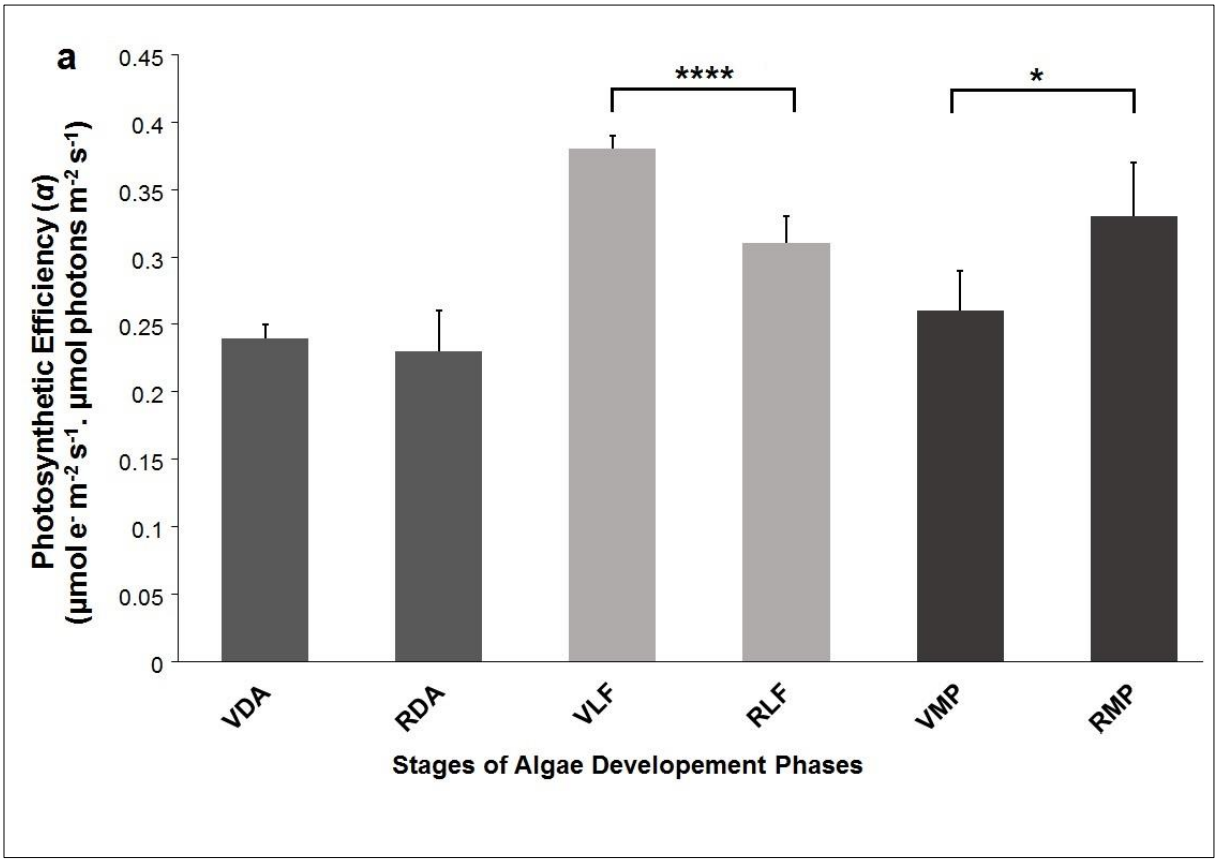
a
Photosynthetic Efficiency (α)
(µmol e⁻ m⁻² s⁻¹. µmol photons m⁻² s⁻¹)
0.45
0.4
0.35
0.3
0.25
0.2
0.15
0.1
0.05
0
****
*
VDA
RDA
VLF
RLF
VMP
RMP
Stages of Algae Developement Phases

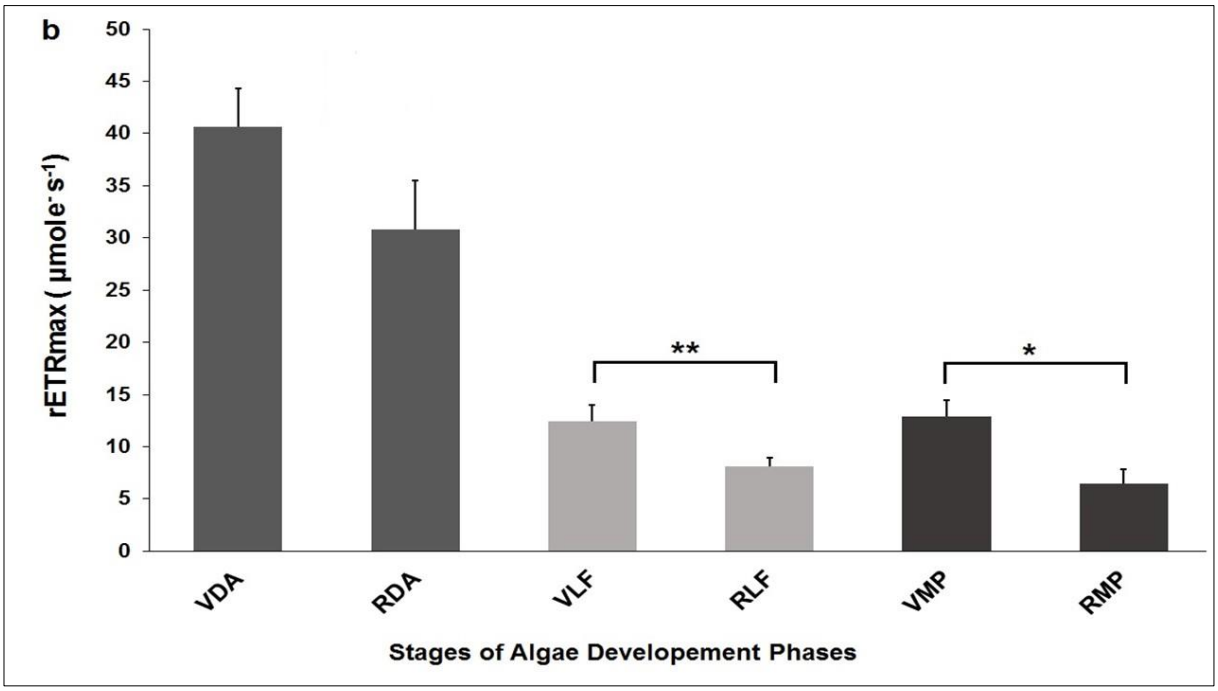
b
rETRmax (µmole⁻ s⁻¹)
50
45
40
35
30
25
20
15
10
5
0
**
*
VDA
RDA
VLF
RLF
VMP
RMP
Stages of Algae Developement Phases

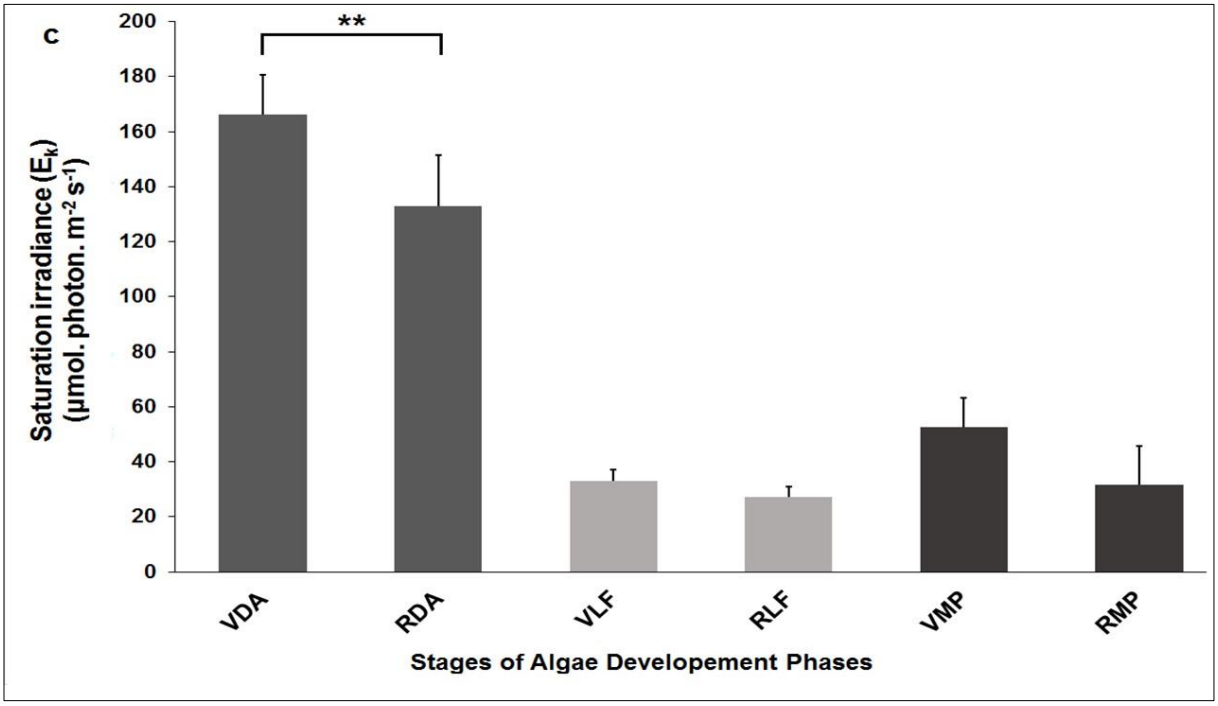

Figure 2 – Photosynthetic parameters of *D. antarctica, L. flavicans* and *M. pyrifera* in vegetative and reproductive phases in the Region de Magellan, Chile. (a) Photosynthetic Efficiency (*α*) in µmol e^- m^{-2} s^{-1}. µmol photons m^{-2} s^{-1}; (b) Relative Maximum Electron Transfer Rate ($rETR_{max}$) in µmol e^- s^{-1}; (c) Saturation Irradiance (E_k) in µmol photon. m^{-2} s^{-1}; VDA (vegetative *D. antarctica*); RDA (reproductive *D. antarctica*); VLF (vegetative *L. flavicans*); RLF (reproductive *L. flavicans*); VMP (vegetative *M. pyrifera*); RMP (reproductive *M. pyrifera*); mean value ± SD (where SD is standard deviation); (n = 5) where *n* is number of independent samples. Values without a common superscript in the same species are significantly different (< 0.05 One-way ANOVA; Tukey's HSD).

The results of maximum quantum yield of PSII (*Fv / Fm*) for the macroalgae *D. antarctica, L. flavicans* and *M. pyrifera* in the vegetative and reproductive phases are shown in Figure 3, in which it can be observed that the highest average results for *Fv / Fm* in the vegetative phase were for *L. flavicans* and *D. antarctica* with 0.722 ± 0.00 and 0.697 ± 0.01, respectively. Seaweeds in the reproductive stage with the best results were *L. flavicans* and *M. pyrifera* with results of 0.679 ± 0.02 and 0.673 ± 0.02, respectively. The lowest results for *Fv / Fm* were for *D. antarctica* (reproductive phase) with 0.575 ± 0.05 and *M. pyrifera (*vegetative

phase) with 0.642 ± 0.02. Analysis of *Fv / Fm* had significant differences between vegetative ad reproductive phases of *D. antarctica* (< 0.05; ANOVA Tukey's HSD) while analysis of *L. flavicans* and *M. pyrifera* did not have significant differences among development phases with *p*= 0.1793 e *p*= 0.5298, respectively. Statistical data are given in Online Resource Table 4.

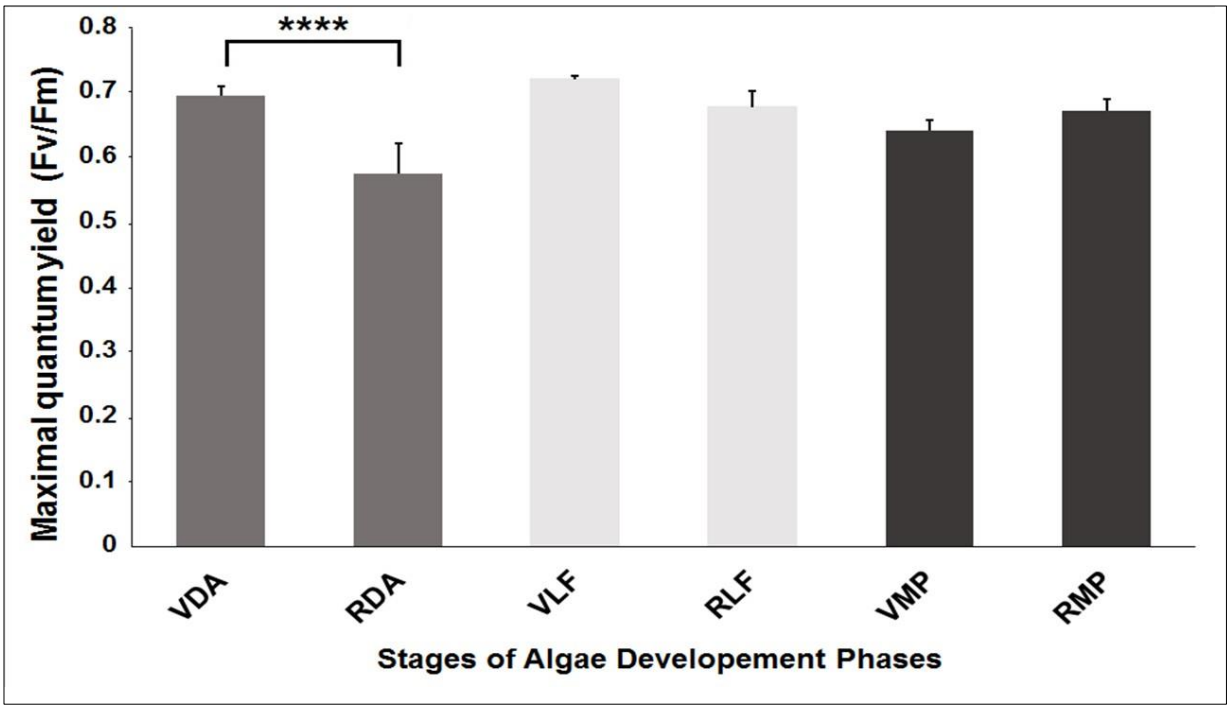

Figure 3 - Maximum quantum yield of PSII (*Fv/Fm*) of species *D. antarctica, L. flavicans* and *M. pyrifera* in the vegetative and reproductive development phases in the Region de Magellan, Chile. Values without a common superscript in the same species are significantly different (< 0.05 One-way ANOVA; Tukey's HSD).

4.3 Total Lipids and Fatty Acids Analysis

Total lipids (% DW) found in the vegetative and reproductive phases of the studied algae had significant difference in the species *D. antarctica* and *M. pyrifera* (Online Resource Table 4). The lowest value found was for vegetative *D. antarctica* with 1.82 ± 0.35%, while the greatest lipid concentration was observed for reproductive *M. pyrifera* with 6.71 ± 1.0% (Online Resource Table S5).

The total concentration of FAMEs did not have significant variations in the development phases of *D. antarctica* as 3.3 ± 0.04 mg g^{-1} and 3.9 ± 0.07 mg g^{-1} were determined in the vegetative and reproductive phases, respectively. *M. pyrifera* and *L. flavicans* had significant variations among the phases with *M. pyrifera* having 7.67 ± 0.56 mg g^{-1} in the vegetative phase and 23.73 ± 0.38 mg g^{-1} in the reproductive phase. Moreover, *L. flavicans* had 4.10 ± 0.13 mg g^{-1} and 5.47 ± 0.24 mg g^{-1} in the vegetative and reproductive phases, respectively. Statistical data are given in Online Resource Table 4.

The Table 6 (Online Resource) displays the fatty acid composition of *D. antarctica, L. flavicans* and *M. pyrifera* in their vegetative and reproductive stages. It can be noted that myristic (14:0), palmitic (16:0) and stearic acid (18:0) were the SFAs found in major concentrations in all the species in both phases of development. 16:0 was the most representative fatty acid among SFAs varying from 13.05 ± 0.11% (vegetative *D. antarctica*) to 24.19 ± 0.46% (reproductive *M. pyrifera*). The sum of the major SFAs (14:0, 16:0 and 18:0) corresponded to 91.7 and 93% in *D. antarctica*, 88.7 and 94.1% in *L. flavicans* as well as 95.7 and 96.6% in *M. pyrifera* for the reproductive and vegetative phases, respectively.

Results showed that there were not significant differences between the sum of the major SFAs for the species and stages of development studied. However, when the total SFAs was analyzed, statistical differences between the vegetative and reproductive phases of *M. pyrifera* could be observed as higher concentrations of lauric (12:0), palmitic (16:0), heptadecanoic (17:0) and araquidic acid (20:0) were found in its vegetative stage.

Fatty acid analysis showed that palmitoleic (16:1*n*7) and oleic acid (18:1*n*9c) were the monounsaturated fatty acids (MUFAs) found in greater concentrations. Palmitoleic acid varied from 1.15 ± 0.01 to 5.09 ± 0.04% (reproductive *M. pyrifera*) while 18:1*n*9c varied from 7.53 ± 0.04 (reproductive *L. flavicans*) and 20.8 ± 0.44% (reproductive *M. pyrifera*). The total MUFAs did not have significant differences among the stages of development of the same species. However, there was a significant difference when these fatty acids were analyzed separately for each species, in which 16:1*n*7 and *cis*-10-heptadecaenoic acid (17:1*n*7) showed significant differences among the phases of *D. antarctica* and *M. pyrifera*,

while 18:1*n*9c only had differences in *M. pyrifera* (< 0.05; ANOVA Tukey's HSD).

Among the PUFAs that can be highlighted in the analyzed macroalgae, *cis*-5,8,11,14,17 eicosapentaenoic acid (20:5*n*3) showed values of 8.58 ± 0.03% (vegetative *D. antarctica*) and 14.93 ± 0.04% (reproductive *L. flavicans*) while arachidonic acid (20:4*n*6) varied from 16.00 ± 0.24% (reproductive *M. pyrifera*) to 30.83 ± 0.49% (vegetative *D. antarctica*). Disparities in the total fatty acids content of PUFAs were verified only for *L. flavicans* and *M. pyrifera.* Profile fatty acids and statistical data of SFAs, MUFAs and PUFAs are given in Online Resource Table 2 and Table 6. Individually, significant variations can be observed among the vegetative and reproductive phases for linoleic acid (18:2*n*6c) and *γ*-linolenic acid (18:3*n*6c) in *D. antarctica*, *L. flavicans* and *M. pyrifera* (< 0.05; ANOVA Tukey's HSD), additional data are given in Online Resource Table 7.

Fatty acids of the C20 class had a significant difference to *cis*-11,14 eicosadienoic acid (20:2*n*6) as it can be noted in *M. pyrifera* (< 0.05; ANOVA Tukey's HSD) among vegetative and reproductive phases; 20:3*n*3 varied in *D. antarctica* and *M. pyrifera* (< 0.05; ANOVA Tukey's HSD) among the development phases; 20:5*n*3 varied in *D. antarctica* and *M. pyrifera*); *cis*-8,11,14 eicosatrienoic acid (20:3*n*6) had significance in the results in *D. antarctica, L. flavicans* and *M. pyrifera* among vegetative and reproductive phases. In the C22 class, only *cis*-13,16 docosadienoic acid (22:2*n*6) had differences among vegetative and reproductive phases of *D. antarctica* and *M. pyrifera* (< 0.05; ANOVA Tukey's HSD). Arachidonic acid (20:4*n*6) that had the greatest concentration in all the species and phases of development did not have a significant variation in results obtained among the phases of development of the studied species (Online Resource Table 7).

The total percentage of saturated (∑SFAs) and monounsaturated fatty acids (∑MUFAs) of the studied samples varied from 23.92 to 35.24% and from 12.55 to 22.02%, respectively, without significant differences among the phases (Figure 4). The greatest concentrations of total polyunsaturated fatty acids (∑PUFAs) were found in vegetative *D. antarctica* (63.53 ± 3.36%), reproductive*D. antarctica* (61.72 ± 4.74%) and reproductive *L. flavicans* (62.77 ± 1.35%) (Figure 4). Diminished concentrations of ∑PUFAs were observed in reproductive *M. pyrifera* reaching 42.74 ± 1.41%. The supplementary files as Online Resource Table 2 shows that there was a significant

difference of ∑PUFAs among vegetative and reproductive phases of *L. flavicans* at 55.32 and 62.77%, respectively, and among the vegetative and reproductive stages of development of *M. pyrifera* with 50.09 and 42.74% (< 0.05; ANOVA Tukey's HSD). All results were calculated and expressed in dry weight of the extracted FAMEs that were subsequently converted and expressed in molar percentage of fatty acids (molar %).

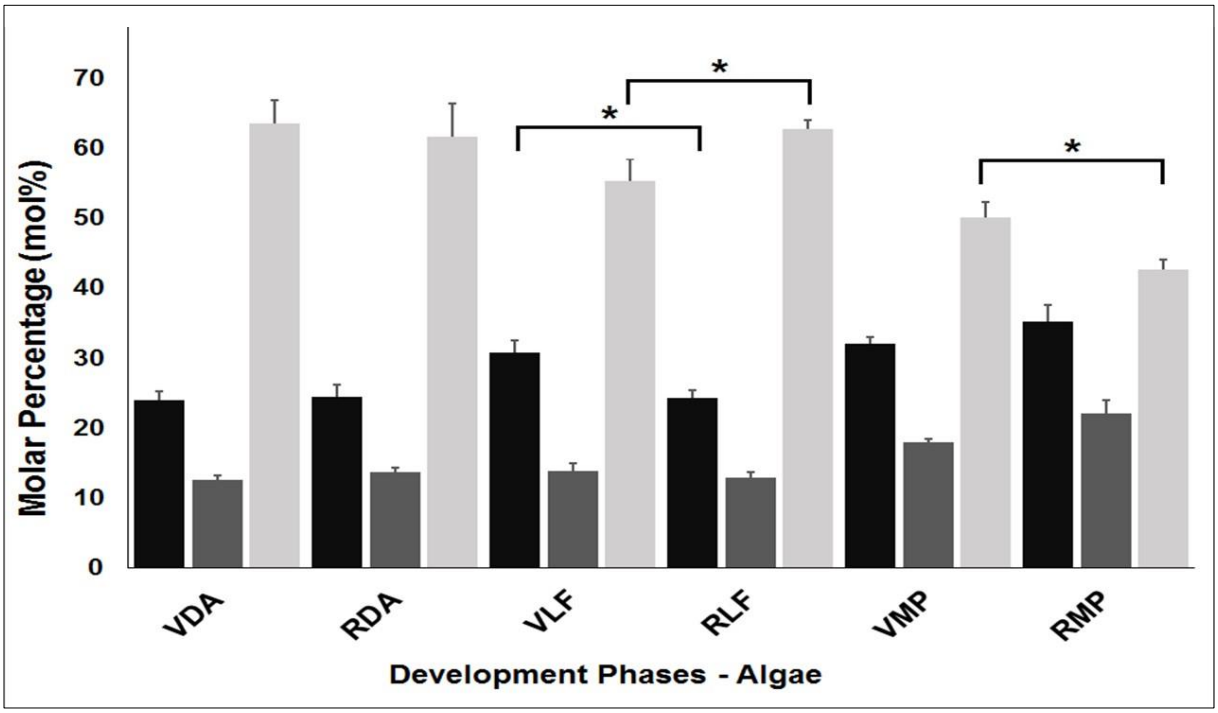

Figure 4 - Variation of the total fatty acid content of three species of brown macroalgae in their distinct stages of development: VDA (vegetative *D. antarctica*); RDA (reproductive *D. antarctica*); VLF (vegetative *L. flavicans*); RLF (reproductive *L. flavicans*); VMP (vegetative *M. pyrifera*); RMP (reproductive *M. pyrifera*). The results represent mean ± SD (where SD is standard deviation); (n = 3) where *n* is number of independent samples. Values without a common superscript in the same species are significantly different (< 0.05 One-way ANOVA; Tukey's HSD).

5. Discussion

The obtained results showed that, in distinct phases of development, *D. antarctica, L. flavicans* and *M. pyrifera* had significant differences regarding pigments and photosynthetic parameters. The concentration of pigments increased in the

reproductive stage of *D. antarctica* and *L. flavicans*, while the opposite was found for *M. pyrifera* since the majority of pigments were observed in the vegetative phase.

Few research works have focused in the influence of abiotic parameters in distinct stages of development of macroalgae. According to Mansilla et al. (2016), conditions of light are the primordial factor for the photosynthetic development and the concentrations of pigments in macroalgae. Rodríguez et al. (2018) reported that conditions of temperature and salinity in the Magellan region affect the development of the reproductive phase of *M. pyrifera* as variations of the values of salinity from 17.3 ± 0.58 PSU (winter) to 33.4 ± 0.40 PSU (summer) increased the germination of spores, while temperatures above 6 °C did not influence germination negatively.

Analysis of pigments in the studied samples indicated that fucoxanthin and Chl *a* were found in greater concentrations than Chl *c* in the macroalgae among their phases of development. These results were superior than the reported by Koch et al. (2015), who reported the analysis of Lessonia berteroana and Lessonia spicata of the order Laminariales collected in Coquimbo (Chile) in full latitudinal range, with values of 1.57 and 1.29 μg g^{-1} DW for Chl *a*, 0.11 and 0.09 μg g^{-1} DW for Chl *c* as well as 0.49 and 0.38 μg g^{-1} DW for fucoxanthin.

The highest concentrations of Chl *a*, Chl *c* and fucoxanthin were observed in the vegetative phase of *M. pyrifera*. The depth of the collection site of the reproductive phase could be one of the factors that could have influenced the distinct concentration of pigments among the phases of developments, which was retrieved approximately 5 m below sea level. In this depth, there was a partial obstruction of solar irradiance caused by surface fronds of the vegetative phase of *M. pyrifera*. In this sense, increased levels of Chl *a* and accessory pigments such as Chl *c* and fucoxanthin could have assisted in the process of luminous energy capture and been directed to metabolic activities of the macroalgae. The results found in the current study agree with Colombo-Pallotta et al. (2006), who showed that the depth of specimens of *M. pyrifera* influenced directly in the concentration of pigments, since fronds collected at 18 m below sea level had increased concentrations of Chl *a*, Chl *c* and fucoxanthin compared to surface fronds. It is worth noting that these organisms developed an efficient system for luminous capitation in which a protein-antenna complex (LHC) known as fucoxanthin-chlorophyll proteins of a/c ligation (FCPs) connects fucoxanthin to Chl *a* and Chl *c* (Fujii et al., 2012; Khoroshyy et al., 2018).

The vegetative phase of M. pyrifera can be found in long extensions of length and in high quantity of biomass (giant kelp) having a prolonged exposure to luminous radiation. In this sense, enhanced intensities of PAR and UV radiation can favor the formation of free radicals and, therefore, lead to an oxidative stress in the macroalgae (Cruces et al., 2017). High levels of fucoxanthin in the vegetative phase compared to the reproductive phase of the studied samples could be associated not only to luminous capture but also to defense mechanisms of the vegetable tissues. According to Dambeck and Sandmann (2014), fucoxanthin can be considered a protecting agent of chlorophyll degradation as well as an antioxidant intermediary in the photosynthetic process and peroxidative stress of macroalgae acting as a natural antioxidant against UV activity (Fariman et al., 2016).

The depth where algae are found can be considered an important factor that influences the incorporation of radiant energy in these organisms since it directly affects dispersion and absorption of luminous energy. Concentrations of CO_2 in water also affect the quantity and quality of the light that reaches a column of water (Häder et al., 2015). In the current study, both phases of development of *L. flavicans* were collected at approximately 1 m of depth, although the reproductive phase was covered by long extensions of the vegetative phase of *M. pyrifera* that obstructed the passage of luminous radiation. This fact can indicate that the obtained results for pigments could be related to the reproductive stage and the decreased luminous intensity which caused an increase in Chl *a* and accessory pigment such as Chl *c* and fucoxanthin. Fertile brown algae require adequate abiotic conditions that include temperature, UV (280 – 400nm) and PAR (400 – 700 nm) levels as well as photoperiod in order to reproduce and develop for the release of the zoospores (Holzinger et al., 2011). Cruces et al. (2017) demonstrated that the exposition of *Lessonia spicata* to PAR and UV radiation for periods of time (from 8 to 20 h) triggered a decrease of 30% and 47% of Chl *c* and Chl *a*, respectively. Moreover, there was a considerable decrease in the concentration of carotenoids, which was associated to periods of exposition to radiation. These results agree with the pigment concentrations found in the current work for *L. flavicans* since there was a decrease in 75.9% of Chl *a*, 41.3% for Chl *c* and 65.3% for fucoxanthin comparing reproductive and vegetative phases.

Analysis of *D. antarctica* showed that the gradient of depth and species were important factors for the obtained concentration of pigments (Fernandes et al., 2016). Both reproductive and vegetative phases of the algae were collected in the low tide of

the intertidal zone, in which concentrations of Chl *a,* Chl *c* and fucoxanthin did not show significant differences among the phases of development.

Both stages of development of *D. antarctica* were collected at the same site so they were subjected to the same ambient adversities such as temperature, luminous radiation, without the influence of dispersion neither absorption of energy by a column of water. These aspects are important since they influence the quantity and length of the antenna that capture the luminous energy (Buschmann et al., 2014). Particularly, concentration of fucoxanthin in *D. antarctica* was higher than Chl *a* indicating that, in this case, the concentration of the accessory pigments can be associated to the protection of algal tissues against the intensity and exposure period to luminous radiation (Simioni et al., 2014; Fariman et al., 2016). Results demonstrated that the site of collection of algae, species and development phase are crucial factors that influence the type and concentration of pigments in these organisms.

The concentration of pigments in photosynthesizing organisms becomes an important factor, mainly in algae that, through the decrease of the antenna, favors the maximization of light capture, proving to be an important strategy to increase their photosynthetic efficiency (Jin et al., 2016).

Analysis of the results of photosynthetic efficiency showed that photosynthetic parameters were different among the phases of development of the studied algae. It could be observed that surface fronds such as vegetative or reproductive *D. antarctica* and vegetative *M. pyrifera* had the highest values for E_k. The increased results for E_k demonstrate that these algae have an enhanced adaptive capacity to tolerate greater levels of solar irradiance and their acclimation is mainly influenced by light intensity and depth of the habitat (Gómez and Huovinen, 2015). Lower values of E_k were observed as depth increases when luminous intensity decreases (Marquardt et al., 2010). These factors are characteristic of algae which are adapted to low levels of solar irradiance as observed by Wiencke et al. (1993) that noted a variation of Ek between 18 a 53 μmol photon. m^{-2} s^{-1} according to changes of these conditions.

Reproductive *M. pyrifera* and *L. flavicans* in both stages of development had values of photosynthetic parameters lower than results previously found in the literature. These outcomes can be related to decreased solar exposure that these algae were subjected to, since these organisms were found under shading caused by a dense canopy at the surface in the form of a giant kelp of vegetative *M. pyrifera*.

Gómez and Huovinen (2011) observed low values of irradiance and photosynthetic saturation for *M. pyrifera* and other sublittoral algae found 1 m below a column of water. The lowest results of the photosynthetic parameters were found in the reproductive phases suggesting that the difference in the values can be directly related to the stages of development (Fukumoto et al., 2018). These results indicate that acclimation in function of irradiation is not associated to the individualization of the studied species and depth, but rather to the phases of development (Marambio et al., 2017b).

Varela et al. (2018) studied the influence of the depth on the photosynthetic parameters of *M. pyrifera* kept at 1 m, 3 m and 6 m of depth, identifying higher values of E_k in the order of 176.8, 77.7 and 33.4 µmol photons m^{-2} s^{-1}, respectively. Similar results for photosynthetic efficiency and $rETR_{max}$ at 3 m of depth could also be observed in this work for the vegetative phase of *M. pyrifera*, while the reproductive stage had lower values for these factors.

In contrast to literature (Graiff et al., 2016; Marambio et al., 2017), the current research work presented low values of $rETR_{max}$ in the vegetative phase of *M. pyrifera* that was exposed to considerable lightness during the day. These low values are typical of algae acclimatized to lower levels of light exposure. Lower values of $rETR_{max}$ in macroalgae exposed to high luminous energy during the day can be explained by factors that include osmotic stress (Kaplan et al., 2013) and algae maturation (Holzinger and Pichrtová, 2016). Moreover, higher radiation intensities can cause damage to the electron transport chain causing less light pickup due to occasional negative regulation of the ability to use energy. Another factor that may be associated with the low $rETR_{max}$ in cases of increased light exposure is the process of heat dissipation or photoprotection made by non-photochemical quenching (NPQ). Algae use this mechanism to dissipate energy in the form of heat after high exposures to luminosity decreasing their levels of energy conversion in the electron transport at the center of the PSII reaction. This mechanism can be considered a defense to high irradiances (Tala et al., 2017). The regulation of PSII energy flow is important to avoid the excessive excitation process of the reaction centers, maintaining an effective process through the transport of electrons between the PSI and PSII photosystems (Roach and Krieger-Liszkay, 2014).

Values of photosynthetic parameters have not been reported for *L. flavicans* in the literature, although other species of the Laminariales order had results of photosynthetic efficiency similar to the ones found in this work. In this sense, Gómez

et al. (2005) observed values of 0.39 ± 0.03, 0.38 ± 0.10 and 0.38 ± 0.10 μmol e^{-} m^{-2} s^{-1}. μmol photons m^{-2} s^{-1} for the strain, frond and holdfast of *Lessonia nigrescens*, respectively. Other research works focused on the temperature of acclimation of Saccharina latíssima, showing results of photosynthetic efficiency of 0.20 and 0.25 μmol e^{-} m^{-2} s^{-1}. μmol photons m^{-2} s^{-1} at 10 °C (Andersen, 2013). Similar results were also found for *D. antarctica* related to photosynthetic efficiency (Gómez and Huovinen, 2011) indicating a pre-acclimation of this algae to high levels of irradiation under low tide.

Koch et al. (2016) showed that abiotic parameters including depth, temperature and irradiation influenced the total lipid concentration and the fatty acid profile of *M. pyrifera* in the sporophytic phase due to its acclimation. In the current work, it can be observed that development phase of an organism seems to be a fundamental aspect that influenced the total concentration of lipids and some classes of fatty acids found in the macroalgae (Gerasimenko et al., 2011). Regarding the total lipids analysis, there were significant differences among the phases of development of the studied species, in which the reproductive stage showed major concentrations of lipids compared to the vegetative phase (Online Resource Table 4)..

The analyzed algae had a distinct morphology of shape, size and coloring among other aspects. However, the qualitative composition of fatty acids was similar between algae and their phases of development. Previous results of the composition of fatty acids of macroalgae showed that innumerous abiotic parameters such as temperature, seasonality and salinity affect the profile of the organisms (Khotimchenko and Yakovleva, 2005; Schmid et al., 2014). However, other studies have shown that some fatty acids are specific of a species and can be used for taxonomical identification (Galloway et al., 2012; Kumari, et al., 2013). In the current research, characteristic results for brown algae were identified including the presence of palmitic acid (16:0) and polyunsaturated fatty acids mainly in the form of cis-5,8,11,14,17 eicosapentaenoic acid (EPA) and arachidonic acid (ARA), agreeing with previous reports of the literature (Schmid, et al.,2014; Tabakaeva and Tabakaev, 2017).

The enhanced levels of radiation to which algae are exposed to in the summer of the sub-Antarctic region (Kirchhoff et al., 1997; Villafañe et al., 2001) associated with the low temperatures of the water (≤ 10 ºC) and air (≤12 ºC) cause a reduction of the fluidity of thylakoid membranes (Cruces et al., 2012). This can be reversed by the presence of PUFAs (Figure 4) which can be responsible for the integrity of the

organism in the period of desiccation (Kumar et al., 2010). The analysis of fatty acids did not reveal the presence of stearidonic acid (18:4n3), which is reported in the literature as a constituent of brown algae (Graeve et al., 2002; Tabakaeva and Tabakaev, 2017) and a component of the biosynthesis of PUFAs. However, Harwood and Guschina (2009) mention that there are alternative routes in this metabolic pathway that employ 11,14,17-eicosatrienoic acid in order to synthesize ARA and EPA. The findings of the current work for total fatty acids (∑FAs) of the vegetative phases of D. antarctica and *M. pyrifera* are in agreement with previous results described by Astorga-España and Mansilla (2014), who found in *M. pyrifera* and *D. antarctica*, respectively, a ∑SFAs of 31.90 and 29.04%, ∑MUFAs of 17.62 and 17.44% and ∑PUFAs of 50.48 and 53.23%. Analysis of fatty acids of D. antarctica collected in the central region of Chile by Ortiz et al. (2006) reached different results with ∑SFAs of 25.84 and 36.38%, ∑MUFAs of 38.11 and 29.21% and ∑PUFAs of 34.42 and 29.23%, for fronds and stems, respectively. These results can be associated to factors including genetic, date of collection and phase of development of the species. In the work of Ortiz et al. (2006), algae were collected in November at temperatures of 13 to 15 °C, while the algae employed in the current research were collected in Punta Arenas in March at temperatures of 7 to 8 °C.

Ortiz et al. (2009) displays similar results for ∑PUFAs and ∑MUFAs for M. pyrifera while for ∑SFAs the concentration was lower (22.78%) than the one found in this work. These results can be related to the difference in the original source since the biomass used was purchased from Marine Cultivation Company Caldera (Caldera, Chile) in the form of a prepared powder. For samples of Lessonia berteroana and Lessonia spicata collected in Coquimbo (Chile) studied by Koch et al. (2015), there were similar results for ∑SFAs, higher concentrations for ∑MUFAs and lower percentages for ∑PUFAs (48.1-51.9%) than what was found in our group for L. flavicans. The difference in the concentration of total fatty acids can be associated to the state of development of the algae, ambient stress, and depth of the collection site and to abiotic parameters (Gerasimenko et al., 2011; Koch et al., 2016).

Brown macroalgae are known for being a source of several compounds of industrial interest such as MUFAs and PUFAs. The use of fatty acids in the pharmaceutical industry has been increasing as this type of lipids can be employed as excipients in medicinal formulations, creams and omega 3 (*n*-3) and 6 (*n*-6) supplements, for instance. As reported in previous studies, n-3 fatty acids were able to

cause apoptosis of tumor cells (Berquin et al., 2008; Vaughan et al., 2013). The ∑*n*-6/∑*n*-3 ratio of the studied algae and their respective phases of development reached 2:1 to 3.2:1, indicating that results are within the recommended parameters, which range from 1:1 to 4:1 of *n*-6 and *n*-3 fatty acids according to Simopoulos (2008). Previous studies have been conducted to determine the presence and concentration of chemical constituents associated to ambient stress and seasonality which algae are subjected to in order to improve information about collection and consumption of these organisms (Schiener et al., 2015; Skriptsova, 2016).

Therefore, this work showed that the distinct phases of development of *D. antarctica, L. flavicans* and *M. pyrifera* had different concentrations of pigments, fluorescence and fatty acids. These physiological and biochemical data revealed information that can lead to a better understanding of the macroalgae behavior in distinct phases of development originated from the sub-Antarctic environment. The results could be important to food, pharmaceutical and nutraceutical fields as stages of development and abiotic parameters were key aspects that influenced the lipid content and the ∑*n*-6/∑*n*-3 ratio. It is worth noting that, under an economic point of view, novel studies are still required in order to increase the knowledge of the influence of abiotic parameters to chemical and biochemical composition as well as nutritional value of macroalgae.

Conflict of Interest: The authors declare that they have no conflict of interest.

6. Reference

Andersen GS, Pedersen MF, Nielsen SL, Harley C (2013) Temperature acclimation and heat tolerance of photosynthesis in Norwegian *Saccharina latissima* (Laminariales, Phaeophyceae). J Phycol. 49: 689-700.

Batista MB, Anderson AB, Sanches PF, Polito PS, Silveira TCL, Velez-Rubio MG, Scarabino F, Camacho O, Schmitz C, Martinez A, Ortega L, Fabiano G, Rothman MD, Liu G, Ojeda J, Mansilla A, Barreto LM, Assis J, Serrão EA, Santos R, Horta PA (2018) Kelps' long-distance dispersal: role of ecological/oceanographic processes and implications to marine forest conservation. Diversity 10(11):1-25.

Berquin IM, Edwards IJ, Chen YQ (2008) Multi-targeted therapy of cancer by ω-3 fatty acids. Cancer Lett 269:363–377.

Bi Y, Zhou Z (2016) Absorption and transport of inorganic carbon in kelps with emphasis on *Saccharina japonica*. In; Mohammad Najafpour (ed) Applied Photosynthesis, IntechOpen. https://www.intechopen.com/books/applied-photosynthesis-new-progress/absorption-and-transport-of-inorganic-carbon-in-kelps-with-emphasis-on-saccharina-japonica; searched on 8 may 2018. doi: 105772/62297

Bischof K, Gómez I, Molis M, Hanelt D, Karsten U, Lüder U, Roleda MY, Zacher K, Wiencke C (2006) Ultraviolet radiation shapes seaweed communities. Rev Environ Sci Biotechnol 5:141-166.

Bligh EG, Dyer WJ (1959) A rapid method for total lipid extraction and purification. Can J Biochem Physiol. 37:911–917.

Brasil (2010) Farmacopeia Brasileira, Agência Nacional de Vigilância Sanitária, Brasília. http://portal.anvisa.gov.br/farmacopeias-virtuais

Buschmann AH, Pereda SV,Varela DA, Rodríguez-Maulén J, López A, González-Carvajal L, Schilling M, Henríquez-Tejo EA, Hernández-González MC (2014) Ecophysiological plasticity of annual populations of giant kelp (*Macrocystis pyrifera*) in a seasonally variable coastal environment in the Northern Patagonian Inner Seas of Southern Chile. J Appl Phycol 26:837–847.

Colombo-Pallotta MF, García-Mendoza E, Ladah LB (2006) Photosynthetic performance, light absorption, and pigment composition of *Macrocystis pyrifera* (Laminariales, Phaeophyceae) blades from different depths. J Phycol 42:1225–1234.

Connan S, Deslandes E, Gall EA (2007) Influence of day–night and tidal cycles on phenol content and antioxidant capacity in three temperate intertidal brown seaweeds. J Exp Mar Biol Ecol 349:359–369.

Cosgrove J, Borowitzka MA (2011) Chlorophyll fluorescence terminology: an introduction. In: Suggett DJ, Borowitzka Michael A, Prášil O (eds) Chlorophyll a fluorescence in aquatic sciences methods and applications. Springer, Dordrecht, pp 1-17.

Cruces E, Huovinen P, Gómez I (2012) Phlorotannin and antioxidant responses upon short-term exposure to UV radiation and elevated temperature in three South Pacific kelps. Photochem Photobiol 88:58–66.

Cruces E, Rautenberger R, Rojas-Lillo Y, Cubillos VM, Arancibia-Miranda N, Ramírez-Kushel E, Gómez I (2017) Physiological acclimation of *Lessonia spicata* to diurnal changing PAR and UV radiation: differential regulation among downregulation of

photochemistry, ROS scavenging activity and phlorotannins photoprotective mechanisms. Photosynth Res 131(2):145-157.

Dambeck M, Sandmann G (2014) Antioxidative activities of algal keto carotenoids acting as antioxidative protectants in the chloroplast. Photochem Photobiol 90:814–819.

Dawes C (2016) Macroalgae Systematics. In: Fleurence J, Levine I (eds) Seaweed in Health and Disease Prevention, Academic Press, pp 107–148.

Fariman GA, Shastan SJ, Zahedi MM (2016) Seasonal variation of total lipid, fatty acids, fucoxanthin content, and antioxidant properties of two tropical brown algae (*Nizamuddinia zanardinii* and *Cystoseira indica*) from Iran. J Appl Phycol 28(2):1323–1331.

Fernandes F, Barbosa M, Oliveira AP, Azevedo IC, Sousa-Pinto I, Valentão P, Andrade PB (2016) The pigments of kelps (Ochrophyta) as part of the flexible response to highly variable marine environments. J Appl Phycol 28:3689–3696.

Franklin LA, Forster RM (1997) The changing irradiance environment: consequences for marine macrophyte physiology, productivity and ecology. Eur J Phycol 32: 207–232.

Freile-Pelegrín Y, Robledo D (2013) Bioactive Phenolic Compounds from Algae. https://onlinelibrary.wiley.com/doi/pdf/10.1002/9781118412893.ch6; searched on 8 may 2018. doi: 10.1002/9781118412893.ch6

Fujii R, Kita M, Doe M, Iinuma Y, Oka N, Takaesu Y, Taira T, Iha M, Mizoguchi T, Cogdell RJ, Hashimoto H (2012) The pigment stoichiometry in a chlorophyll *a*/*c* type photosynthetic antena. Photosynth Res 111:165–172.

Fukumoto R., Borlongan IA, Nishihara GN, Endo H, Terada R (2018) Photosynthetic responses to photosynthetically active radiation and temperature including chilling-light stress on the heteromorphic life history stages of a brown alga, *Cladosiphon okamuranus* (Chordariaceae) from Ryukyu Islands, Japan. Phycol Res 66(3):209–217.

Galindo V, Gosselin M, Lavaud J, Mundy CJ, Else B, Ehn J, Babin M, Rysgaard S (2017) Pigment composition and photoprotection of Arctic sea ice algae during spring. Mar Ecol Prog Ser 585:49–69.

Galloway AWE, Britton-Simmons KH, Duggins DO, Gabrielson PW, Brett MT (2012) Fatty acid signatures differentiate marine macrophytes at ordinal and family ranks. J Phycol 48:956–965.

Gerasimenko NI, Skriptsova AV, Busarova NG, Moiseenko OP (2011) Effects of the season and growth stage on the contents of lipids and photosynthetic pigments in brown alga *Undaria pinnatifida*. Russ J Plant Physl+ 58:885-891.

Gerard VA (1984) The light environment in a giant kelp forest: influence of *Macrocystis pyrifera* on spatial and temporal variability. Mar Biol 84:189-195.

Gómez I, Ulloa N, Orostegui M (2005) Morpho-functional patterns of photosynthesis and UV sensitivity in the kelp *Lessonia nigrescens* (Laminariales, Phaeophyta). Mar Biol 148: 231–240.

Gómez I, Huovinen P (2011) Morpho-functional patterns and zonation of south Chilean seaweeds: the importance of photosynthetic and bio-optical traits. Mar Ecol Prog Ser 422: 77–91.

Gómez I, Huovinen P (2015) Lack of physiological depth patterns in conspecifics of endemic Antarctic brown algae: a trade-off between UV stress tolerance and shade adaptation? PLoS One 10:e0134440. doi: 10.1371/journal.pone.0134440

Gomez I, Navarro NP, Huovinen P (2018) Bio-optical and physiological patterns in Antarctic seaweeds: A functional trait based approach to characterize vertical zonation. Prog Oceanogr. In Press. doi:10.1016/j.pocean.2018.03.013

Graeve M, Kattner G, Wiencke C, Karsten, U (2002) Fatty acid composition of Arctic and Antarctic macroalgae: indicator of phylogenetic and trophic relationships. Mar Ecol Prog Ser 231: 67–74.

Häder DP, Williamson CE, Wängberg SA, Rautio M, Rose KC, Gao K, Helbling EW, Sinhah RP, Worresti R (2015) Effects of UV radiation on aquatic ecosystems and interactions with other environmental factors. Photochem Photobiol Sci 14:108-126.

Han T, Kain JM (1996) Effect of photon irradiance and photoperiod on young sporophytes of four species of the Laminariales. Eur J Phycol 31(3):233-240.

Hannach G, Santelices B (1985) Ecological differences between the isomorphic reproductive phases of two species of *Iridaea* (Rhodophyta: Gigartinales). Mar Ecol Prog Ser 22: 291-303.

Harwood, JL, Guschina IA (2009) The versatility of algae and their lipid metabolismo. Biochimie 91:679-684.

Holzinger A, Di Piazza L, Lütz C, Roleda MY (2011) Sporogenic and vegetative tissues of *Saccharina latissima* (Laminariales, Phaeophyceae) exhibit distinctive sensitivity to experimentally enhanced ultraviolet radiation: photosynthetically active radiation ratio. Phycological Research 59: 221–235.

Jin H, Li M, Duan S, Fu M, Dong X, Liu B, Wang HB (2016) Optimization of light-harvesting pigment improves photosynthetic efficiency. Plant Physiol 172(3):1720–1731.

Jones AB, Dennison WC, Stmart GR (1996) Macroalgal responses to nitrogen source and availability: amino acid metabolic profiling as a bioindicator using *Gracilaria edulis* (Rhodophyta). J Phycol 32:757-766.

Juneja A, Ceballos RM, Murthy GS (2013) Effects of environmental factors and nutrient availability on the biochemical composition of algae for biofuels production: a review. Energies 6:4607-4638.

Pangestuti R, Siahaan EA, Kim SK (2018) Photoprotective substances derived from marine algae. Mar Drugs 16:1-16.https://www.ncbi.nlm.nih.gov/pmc/articles/PMC6265938; searched 28 november 2018. doi: 10.3390/md16110399

Khoroshyy P, Bína D, Gardian Z, Litvín R, Alster J, Pšenčík J (2018) Quenching of chlorophyll triplet states by carotenoids in algal light-harvesting complexes related to fucoxanthin-chlorophyll protein. Photosynth Res 135:213–225.

Khotimchenko SV, Yakovleva IM (2005) Lipid composition of the red alga *Tichocarpus crinitus* exposed to different levels of photon irradiance. Phytochemistry 66:73–79.

Kirchhoff VWJH, Sahai Y, Casiccia CARS, Zamorano BF, Valderrama VV (1997) Observations of the 1995 ozone hole over Punta Arenas, Chile. J Geophys Res 102:16.109-16.120.

Koch K, Thiel M, Tellier F, Hagen W, Graeve M, Tala F, Laeseke P, Bischof K (2015) Species separation within the *Lessonia nigrescens* complex (Phaeophyceae, Laminariales) is mirrored by ecophysiological traits. Bot Mar 58(2): 81–92.

Koch K, Thiel M, Hagen W, Graeve M, Gómez I, Jofre D, Hofmann LC,Tala F, Bischof K (2016) Short- and long-term acclimation patterns of the giant kelp *Macrocystis pyrifera* (Laminariales, Phaeophyceae) along a depth gradient. J Phycol 52:260–273.

Kumar M, Kumari P, Gupta V, Reddy CRK, Jha B (2010) Biochemical responses of red alga *Gracilaria corticata* (Gracilariales, Rhodophyta) to salinity induced oxidative stress. J Exp Mar Biol Ecol 391:27–34.

Kumar M, Kumari P, Reddy CRK, Jha B (2014) Salinity and desiccation induced oxidative stress acclimation in seaweeds. In: Bourgougnon N (ed) Advances in Botanical Research. Academic Press pp. 91–123.

Kumari P, Bijo AJ, Mantri VA, Reddy CRK, Jha B (2013) Fatty acid profiling of tropical marine macroalgae: an analysis from chemotaxonomic and nutritional perspectives. Phytochemistry 86:44–56.

Lin SM, Huang R, Ogawa H, Liu LC, Wang YC, Chiou Y (2017) Assessment of germling ability of the introduced marine brown alga, *Sargassum horneri*, in Northern Taiwan. J Appl Phycol 29:2641–2649.

Long SP, Humphries S, Falkowski PG (1994) Photoinhibition of photosynthesis in nature. Annu Rev Plant Physiol Plant Mol Biol 45: 633-662.

Mansilla A, Ávila M, Yokoya NS (2012) Current knowledge on biotechnological interesting seaweeds from the Magellan Region, Chile. Rev Bras Farmacog 22(4):760-767.

Mansilla A, Rodriguez JP, Souza JMC, Rosenfeld S, Ojeda J, Yokoya NS (2013a). Growth responses to temperature, salinity and nutrient variations, and biomass variation and phenology of *Ahnfeltia plicata* (Rhodophyta, Ahnfeltiales): a commercially interesting agarophyte from the Magellanic Region, Chile. J Appl Phycol, 26(2):1133–1139.

Mansilla A, Ávila M, Ramírez ME, Rodriguez JP, Rosenfeld S, Jaime O, Marambio J (2013b) macroalgas marinas bentónicas del submareal somero de la ecorregión subantártica de Magallanes, Chile. An Inst Patagon 41(2):51-64.

Mansilla A, Méndez F, Murcia S, Rodríguez JP, Marambio J, Rosenfeld S, Bischof K (2016) Adjustment of pigment composition in *Desmarestia* (Desmarestiaceae) species along a sub-Antarctic to Antarctic latitudinal gradient. Polar Res 35(1):29383. https://www.tandfonline.com/doi/pdf/10.3402/polar.v35.29383/needAccess/true; searched on 8 may 2018. doi:10.3402/polar.v35.29383

Marambio J, Mendez F, Ocaranza P, Rodriguez JP, Rosenfeld S, Ojeda J, Murcia S, Terrados J, Bischof K, Mansilla A (2017a) Seasonal variations of the photosynthetic activity and pigment concentrations in different reproductive phases of *Gigartina skottsbergii* (Rhodophyta, Gigartinales) in the Magellan region, sub-Antarctic Chile. J Appl Phycol 29(2):721-729.

Marambio J, Rodriguez JP, Mendez F, Ocaranza P, Rosenfeld S, Ojeda J, Rautenberger R, Bischof K, Terrados J, Mansilla A (2017b) Photosynthetic performance and pigment composition of *Macrocystis pyrifera* (Laminariales, Phaeophyceae) along a gradient of depth and seasonality in the ecoregion of Magellan, Chile. J Appl Phycol 29(5)2575-2585.

Marquardt R, Schubert H, Varela DA, Huovinen P, Henríquez L, Buschmann AH (2010) Light acclimation strategies of three commercially important red algal species. Aquaculture 299:140–148.

Méndez F, Tala F, Rautenberger R, Ojeda J, Rosenfeld S, Rodríguez JP, Mansilla A (2017) Morphological and physiological differences between two morphotypes of *Durvillaea antarctica* (Phaeophyceae) from the sub-Antarctic ecoregion of Magallanes, Chile. J Appl Phycol 29(5):2557–2565.

Mikami K, Murata N (2003) Membrane fluidity and the perception of environmental signals in cyanobacteria and plants. Prog Lipid Res 42:527–543.

Mikami K, Hosokawa M (2013) Biosynthetic pathway and health benefits of fucoxanthin, an algae-specific xanthophyll in brown seaweeds. Int J Mol Sci 14:13763-13781.

Morgan-Kiss M, Priscu JC, Pocock T, Gudynaite-Savitch L, Huner NPA (2006) Adaptation and acclimation of photosynthetic microorganisms to permanently cold environments. Microbiol Mol Biol R 70(1):222–252.

Morelissen B, Dudley BD, Geange SW, Phillips NE (2013) Gametophyte reproduction and development of *Undaria pinnatifida* under varied nutrient and irradiance conditions. J Exp Mar Biol Ecol 448:197–206.

Moss CW, Lambert MA, Merwin WH (1974) Comparison of rapid methods for analysis of bacterial fatty acids. Appl Microbiol 28:80–85.

Nygård CA, Dring MJ (2008) Influence of salinity, temperature, dissolved inorganic carbon and nutrient concentration on the photosynthesis and growth of *Fucus vesiculosus* from the Baltic and Irish Seas. Euro J Phycol 43(3):253-262.

Ortiz J, Romero N, Robert P, Araya J, Lopez-Hernández J, Bozzo C, Navarrete E, Osorio A, Rios A (2006) Dietary fiber, amino acid, fatty acid and tocopherol contents of the edible seaweeds *Ulva lactuca* and *Durvillaea antarctica*. Food Chem 99:98–104.

Ortiz J, Uquiche E, Robert P, Romero N, Quitral V, Llantén C (2009) Functional and nutritional value of the Chilean seaweeds *Codium fragile*, *Gracilaria chilensis* and *Macrocystis pyrifera*. Eur J Lipid Sci Technol 111:320–327.

Pellizzari F, Silva MC, Silva EM, Medeiros A, Oliveira MC, Yokoy NS, Pupo D, Rosa LH, Colepicolo P (2017) Diversity and spatial distribution of seaweeds in the south Shetland Islands, Antarctica: an updated database for environmental monitoring under climate change scenarios. Polar Biol 40:1671–1685.

Platt T, Gallegos CL, Harrison WG (1980) Photoinhibition of photosynthesis in natural assemblages of marine phytoplankton. J Mar Res 38:687–70.

Ralph PJ, Gademann R (2005) Rapid light curves: a powerful tool to assess photosynthetic activity. Aquat Bot 82(3): 222–237.

Ríos C, Mutschke E, Montiel A (2010) Estructura de la comunidad macrofaunística bentónica en la boca oriental del estrecho de Magallanes, Chile austral. An Inst Patagon 38(1):83-96.

Rautenberger R, Mansilla A, Gómez I, Wiencke C, Bischof K (2009) Photosynthetic responses to UV-radiation of intertidal macroalgae from the Strait of Magellan (Chile). Rev Chil Hist Nat 82(1):43-61.

Rautenberger R, Bischof K (2016) Dynamic summer solar radiation in Antarctic coastal ecosystems and its effects on photosyn thesis of the endemic Antarctic brown macroalga *Desmarestia menziesii* (Phaeophyceae). Algological Studies 151(1):123–150.

Roach T, Krieger-Liszkay AK (2014) regulation of photosynthetic electron transport and photoinhibition. Curr Protein Pept Sc 15(4): 351–362.

Rodríguez JP, Terrados J, Rosenfeld S, Méndez F, Ojeda J, Mansilla A (2018) Effects of temperature and salinity on the reproductive phases of *Macrocystis pyrifera* (L.) C. Agardh (Phaeophyceae) in the Magellan region. J Appl Phycol pp. 1-14 (Online Article). https://doi.org/10.1007/s10811-018-1693-x

Rowland FS (2006) Stratospheric ozone depletion. Phil Trans R Soc B 361:769–790.

Sanchez S, Carrasco JF, Fuenzalida H (2012) The Chilean ultraviolet radiation network: monitoring and forecasting UV index for health protection. In: Griffiths J, Rowlands C, Witthaus M (eds) Climate Exchange. http://digital.tudor-rose.co.uk/climate-exchange/index.html; searched 8 may 2018

Santos MAZ, Colepicolo P, Pupo D, Fujii MT, Pereira CMP, Mesko MF (2017) Antarctic red macroalgae: a source of polyunsaturated fatty acids. J Appl Phycol 29(2):759-767.

Schiener P, Black KD, Stanley MS, Green DH (2015) The seasonal variation in the chemical composition of the kelp species *Laminaria hyperborea*, *Saccharina latissima* and *Alaria esculenta*. J Appl Phycol 27:363–373.

Schmid M, Guihéneuf F, Stengel DB (2014) Fatty acid contents and profiles of 16 macroalgae collected from the Irish Coast at two seasons. J Appl Phycol 26:451–463.

Simioni C, Schmidt EC, Felix MRL, Polo LK, Rover T, Kreusch M, Pereira DT, Chow F, Ramlov F, Maraschin M, Bouzon ZL (2014) Effects of ultraviolet radiation

(UVA+UVB) on young gametophytes of *Gelidium floridanum*: growth rate, photosynthetic pigments, carotenoids, photosynthetic performance, and ultrastructure. Photochem Photobiol 90(5):1050-1060.

Simopoulos AP (2008) The importance of the omega-6/omega-3 fatty acid ratio in cardiovascular disease and other chronic diseases. Exp Biol M 233:674-688.

Seely GR, Duncan MJ, Vidaver WE (1972) Preparative and analytical extraction of pigments from brown algae with dimethyl sulfoxide. Mar Biol 12:184–188.

Servicio Hidrográfico y Oceanográfico de la Armada de Chile. http://www.shoa.cl/php/inicio.php/idioma/es; searched 8 may 2018.

Skriptsova AV (2016) Seasonal variations in the fucoidan content of brown algae from Peter the Great Bay, Sea of Japan. Russ J Mar Biol 42:351–356.

Stévant P, Rebours C, Chapman A (2017) Seaweed aquaculture in Norway: recent industrial developments and future perspectives. Aquacult Int 25:1373–1390.

Tabakaeva OV, Tabakaev AV (2017) Compositions of lipids and fatty acids from various parts of the brown alga *Undaria pinnatifida.* Chem Nat Compd 53(5): 843-848.

Tait MA, Hik DS (2003) Is dimethylsulfoxide a reliable solvent for extracting chlorophyll under field conditions?. Photosynth Res, 78(1):87–91.

Tala F, Penna-Díaz MA, Luna-Jorquera G, Rothäusler E, Thiel M (2017) Daily and seasonal changes of photobiological responses in floating bull kelp *Durvillaea antarctica* (Chamisso) Hariot (Fucales: Phaeophyceae). Phycologia 56(3):271–283.

Titlyanov EA, Titlyanova TV, Li X, Hansen GI (2014) Seasonal changes in the intertidal algal communities of Sanya Bay (Hainan Island, China). J Mar Biol AssocUK 94:879-893.

Varela DA, Hernríquez LA, Fernández PA, Leal P, HernándezGonzález MC, Figueroa FL, Buschmann AH (2018) Photosynthesis and nitrogen uptake of the giant kelp *Macrocystis pyrifera* (Ochrophyta) grown close to salmon farms. Mar EnviroN Res 15:93-102.

Vaughan VC, Hassing MR, Lewandowski PA (2013) Marine polyunsaturated fatty acids and cancer therapy. Br J Cancer 108:486–492.

Villafañe VE, Helbling EW, Zagarese HE (2001) Solar ultraviolet radiation and its impact on aquatic systems of Patagonia, South America. Ambio 30(2):112-117.

White AJ, Critchley C (1999) Rapid light curves: A new fluorescence method to assess the state of the photosynthetic apparatus. Photosynth Res 59: 63–72.

Wiencke C, Rahmel J, Karsten U, Weykam G, Kirst GO (1993) Photosynthesis of marine macroalgae from Antarctica: light and temperature requirements. Bot Acta 106:77–87

Wong CY, Teoh ML, Phang SM, Lim PE, Beardall J (2015) Interactive effects of temperature and UV radiation on photosynthesis of *Chlorella* strains from polar, temperate and tropical environments: differential impacts on damage and repair. PLoS One 10(10): e0139469. https://doi.org/10.1371/journal.pone.0139469

Table 2. Results of two-way ANOVA analysis development phase on the seaweed *D. antarctica*, *L. flavicans* and *M. pyrifera* for pigmentation, photoshynthetic parameters, total fatty acids and fatty acid profile

Dependent variable	Factor	*Durvillaea antarctica*					*Lessonia flavicans*					*Macrocystis pyrifera*				
		SS	**d*f***	**MS**	**F**	***p* value**	**SS**	**d*f***	**MS**	**F**	***p* value**	**SS**	**d*f***	**MS**	**F**	***p* value**
Pigmentation	A	17.4	2	8.69	24.78	0.0013	62.22	2	31.11	8.85	0.0162	979.1	2	489.6	211.8	<0.0001
	B	0.20	1	0.20	1.09	0.3368	166.9	1	166.9	86.18	<0.0001	650.2	1	650.2	532.7	<0.0001
	A x B	0.23	2	0.11	0.6516	0.5545	46.03	2	23.01	11.88	0.0082	362.4	2	181.2	148.5	<0.0001
	Error	1.10	6	0.18			11.62	6	1.937			7.323	6	1.221		
Photoshynthetic parameters	C	146096	2	73048	132.9	<0.0001	5468	2	2734	74.35	<0.0001	11540	2	5770	36.92	<0.0001
	B	1855	1	1855	3.989	0.0643	100.1	1	100.1	2.78	0.1162	208	1	208	0.7696	0.3942
	C x B	1742	2	871.2	1.873	0.1879	50.7	2	25.35	0.7039	0.5103	1211	2	605.4	2.24	0.1409
	Error	6976	15	465.1			540.2	15	36.01			4054	15	270.3		
Total fatty acids (∑SFAs, ∑MUFAs and ∑PUFAs)	D	8090	2	4045	187.9	<0.0001	6551	2	3275	351.1	<0.0001	2100	2	1050	428.8	<0.0001
	B	0.00	1	0.00	0.00	>0.9999	0.00	1	0.00	0.00	>0.9999	0.00	1	0.00	0.00	>0.9999
	D x B	7.594	2	3.797	2.17	0.1953	149.3	2	74.64	34.47	0.0005	122.2	2	61.1	7.027	0.0268
	Error	10.49	6	1.74			12.99	6	2.16			52.17	6	8.69		
Fatty acid profile	E	6175	19	325	171.9	<0.0001	5015	18	278.6	313.3	<0.0001	5649	19	297.3	897	<0.0001
	B	0.00	1	0.00	0.00	<0.0001	0.00	1	0.00	0.00	0.9947	0.00	1	0.00	0.00	0.9981
	E x B	37.92	19	1.996	12.5	<0.0001	54.48	18	3.027	13.13	<0.0001	306	19	16.11	17.24	<0.0001
	Error	6.385	40	0.1596			8.759	38	0.2305			37.38	40	0.9346		

Significant effects ($p < 0.05$) are indicated in italics; (SS) sums of squares, (d*f*) degrees of freedom, (MS) mean of the squares, (F) F test statistic; A - Pigmentation; B - Development Phase; C - Photosynthetic parameters; D - Total fatty acids; E - Fatty acid profile.

Table 3 – Pigment concentration of Chl *a*, Chl *c* and fucoxanthin (Fucox) in the vegetative and reproductive phases of *D. antarctica*, *L. flavicans* and *M. pyrifera* collected in the Magellan Region, Chile (2016 – 2017)

Algae	Chl *a*	Chl *c*	Fucox
D. antarctica vegetative	1.26 ± 0.11^{a}	0.74 ± 0.16^{a}	3.12 ± 0.60^{a}
D. antarctica reproductive	1.80 ± 0.61^{a}	0.81 ± 0.04^{a}	3.14 ± 0.33^{a}
L. flavicans vegetative	3.05 ± 0.48^{a}	2.64 ± 0.40^{a}	3.64 ± 0.20^{a}
L. flavicans reproductive	12.64 ± 2.19^{b}	4.50 ± 0.94^{b}	10.48 ± 1.16^{b}
M. pyrifera vegetative	10.99 ± 1.16^{b}	3.73 ± 0.35^{b}	7.37 ± 0.67^{b}
M. pyrifera reproductive	35.36 ± 0.21^{a}	7.04 ± 0.93^{a}	15.75 ± 1.42^{a}

Mean value ± SD in $\mu g.g^{-1}$ DW (dry weight), where SD is standard deviation; (n=5) where *n* is number of independent samples. Values without a common superscript in the same species are significative different (One-way ANOVA $p < 0.05$;Tukey's HSD).

Table 4. Results of one-way ANOVA analysis development phase on the seaweed *D. antarctica, L. flavicans* and *M. pyrifera* for *Fv/Fm*, total lipid content and FAMEs

Dependent variable	Dependent variable	SS	d*f*	MS	F	*p* value
Fv/Fm	Development Phase	0.07894	5	0.01579	16.38	*<0.0001*
	Error	0.02892	30	0.00096		
Total Lipid Content	Development Phase	45.79	5	9.157	16.28	*<0.0001*
	Error	6.75	12	0.5625		
FAMEs	Development Phase	923.6	5	184.7	1033	*<0.0001*
	Error	2.147	12	0.1789		

Significant effects ($p < 0.05$) are indicated in italics; (SS) sums of squares, (d*f*) degrees of freedom, (MS) mean of the squares, (F) F test statistic; *Fv/Fm* maximum quantum yield; FAMEs fatty acid methyl esters

Table 5 - Total lipid contents in macroalgae species *D. antarctica, L. flavicans* e *M. pyrifera* in the vegetative and reproductive phases collected in the Magellan Region, Chile (2016 – 2017)

Macroalgae	Lipid (% DW)
D. antarctica vegetative	1.82 ± 0.35^{a}
D. antarctica reproductive	4.13 ± 0.04^{b}
L. flavicans vegetative	3.63 ± 0.75^{a}
L. flavicans reproductive	5.56 ± 0.32^{a}
M. pyrifera vegetative	3.14 ± 0.30^{a}
M. pyrifera reproductive	6.71 ± 1.00^{b}

Mean values ± SD in % DW (dry weight), where SD is standard deviation; (n=3) where*n* is number of independent samples. Values without a common superscript in the same species of algae are significantly different (p <0.05).

Table 6 – Fatty acid composition (molar %) in the subantarctic macroalgae *D. antarctica*, *L. flavicans* and *M. pyrifera* collected in the Magellan Region, Chile (2016 – 2017)

FAs	VDA	RDA	VLF	RLF	VMP	RMP
12:0	ND	ND	1.14 ± 0.00	ND	0.38 ± 0.01	0.07 ± 0.00
14:0	7.64 ± 0.12	8.20 ± 0.04	6.72 ± 0.03	6.36 ± 0.03	8.44 ± 0.07	7.85 ± 0.11
15:0	0.45 ± 0.01	0.54 ± 0.00	0.75 ± 0.00	0.52 ± 0.00	0.42 ± 0.00	0.41 ± 0.01
16:0	13.05 ± 0.11	13.42 ± 0.11	19.24 ± 0.24	15.86 ± 0.07	20.78 ± 0.08	24.19 ± 0.46
16:1*n*7	2.17 ± 0.01	1.77 ± 0.00	3.75 ± 0.03	3.76 ± 0.00	5.09 ± 0.04	1.15 ± 0.01
17:0	0.70 ± 0.01	0.47 ± 0.02	0.82 ± 0.01	0.49 ± 0.00	0.62 ± 0.00	0.18 ± 0.00
17:1*n*7	0.16 ± 0.00	0.31 ± 0.00	ND	ND	0.23 ± 0.00	0.06 ± 0.00
18:0	1.17 ± 0.01	1.18 ± 0.01	1.38 ± 0.02	0.62 ± 0.00	1.14 ± 0.01	2.02 ± 0.02
18:1*n*9c	10.09 ± 0.08	11.40 ± 0.05	8.16 ± 0.10	7.53 ± 0.04	12.16 ± 0.09	20.80 ± 0.44
18:2*n*6c	7.68 ± 0.07	6.28 ± 0.02	4.02 ± 0.05	3.63 ± 0.01	4.63 ± 0.01	8.14 ± 0.03
20:0	0.54 ± 0.02	0.42 ± 0.00	0.78 ± 0.00	0.42 ± 0.00	0.23 ±0.00	0.53 ± 0.00
18:3*n*6	0.73 ± 0.00	0.40 ± 0.00	1.05 ± 0.01	0.52 ± 0.03	0.38 ± 0.00	0.80 ± 0.00
20:1*n*9	ND	ND	1.94 ± 0.02	1.67 ± 0.01	ND	ND
18:3*n*3	6.37 ± 0.02	5.30 ± 0.01	6.57 ± 0.01	6.25 ± 0.03	4.15 ± 0.01	3.56 ± 0.02
20:2*n*6	6.31 ± 0.04	5.28 ± 0.03	7.26 ± 0.08	8.92 ± 0.02	3.89 ± 0.01	2.38 ± 0.02
22:0	0.30 ± 0.00	0.29 ± 0.00	ND	ND	ND	ND
20:3*n6*	1.53 ± 0.00	0.76 ± 0.00	1.03 ± 0.02	0.88 ± 0.00	1.04 ± 0.01	1.18 ± 0.01
22:1*n*9	0.12 ± 0.01	0.14 ± 0.00	ND	ND	0.42 ± 0.00	ND
20:3*n*3	0.24 ± 0.01	0.16 ± 0.00	ND	0.46 ± 0.00	0.33 ± 0.00	0.11 ± 0.00
20:4*n*6	30.83 ± 0.49	30.21 ± 0.27	23.91 ± 0.26	26.39 ± 0.06	25.19 ± 0.22	16.00 ± 0.24
22:2*n*6	1.19 ± 0.01	0.53 ± 0.00	ND	0.79 ± 0.00	1.20 ± 0.01	0.60 ± 0.04
20:5*n*3	8.58 ± 0.03	12.80 ± 0.09	11.48 ± 0.15	14.93 ± 0.04	9.29 ± 0.02	9.96 ± 0.08

Results expressed in mean ± SD of total fatty acids, where SD is standard deviation; (n=3) where *n* is number of independent samples; ND: non detected; FAs – fatty acids; VDA – vegetative *D. antarctica*; RDA – reproductive *D. antarctica*; VLF – vegetative *L. flavicans*; RLF – reproductive *L. flavicans*; VMP – vegetative *M. pyrifera*; RMP – reproductive *M. pyrifera*. Values without a common superscript in the same species are significative different (One-way ANOVA p< 0.05 ;Tukey's HSD).

Table 7. Results of one-way ANOVA analysis development phase on the seaweed *D. antarctica, L. flavicans* and *M. pyrifera* for individually fatty acids

Dependent variable	**Dependent variable**	**SS**	**d*f***	**MS**	**F**	***p* value**
C16:1*n*7	Development Phase	1433	5	286.6	262.7	<0.0001
	Error	13.09	12	1.091		
C17:1*n*7	Development Phase	9.351	3	3.117	674	<0.0001
	Error	0.037	8	0.004625		
C18:1*n*9	Development Phase	3220	5	644	12.21	0.0002
	Error	632.8	12	52.73		
C18:3*n*3	Development Phase	29.51	5	5.901	86.8	<0.0001
	Error	0.8158	12	0.06798		
C18:3*n*6	Development Phase	454.9	7	64.98	579.4	<0.0001
	Error	1.794	16	0.1121		
C20:2	Development Phase	162.2	5	32.44	92.37	<0.0001
	Error	4.21	12	0.3512		
C20:3*n*3	Development Phase	0.3062	3	0.1021	59.98	<0.0001
	Error	0.0136 1	8	0.001702		
C20:3*n*6	Development Phase	5.154	5	1.031	46.09	<0.0001
	Error	0.2684	12	0.02236		
C20:4*n*6	Development Phase	374.8	5	74.96	2.808	0.0663
	Error	320.3	12	26.7		
C20:5*n*3	Development Phase	210	5	42	16.79	<0.0001
	Error	30.02	12	2.501		
C22:2	Development Phase	3.832	3	1.277	94.04	<0.0001
	Error	0.1087	8	0.01358		

Significant effects ($p < 0.05$) are indicated in italics; (SS) sums of squares, (d*f*) degrees of freedom, (MS) mean of the squares, (F) F test statistic.

Capitulo 3 – Fatty acids of subantarctic red algae at different development stages.

Submetido em Food Chemistry

25.03.2019

Fatty acid profile of Sub-Antarctic red macroalgae in gametophytic, carposporophytic and tetraesporophytic phases of development from the Magellan Region, Chile

[1,a]Marco Aurélio Ziemann DOS SANTOS*, [2,a]Lucas Moraes BERNEIRA, [3,a]Caroline Carapina DA SILVA, [4,a]Carla Rosane Barboza MENDONÇA, [5,b]Andres MANSILLA, [6,a]Claudio Martin Pereira DE PEREIRA

[a]Center for Chemical, Pharmaceutical and Food Sciences, Federal University of Pelotas, University Campus, S / N - CEP 96160-000, Capão do Leão, RS – Brazil

[b]Laboratory of Antarctic and Sub-Antarctic Marine Ecosystems, University of Magallanes, 01855 Bulnes Ave., Punta Arenas 6200000. Instituto de Ecología y Biodiversidad (IEB), Chile

[1,*]Corresponding author: marcziemann@gmail.com
Telephone number: +55053981184936
ORCID: 0000-0002-3776-3701

Acknowledgements

This study had logistic support from the University of Magallanes and the Laboratory of Antarctic and Sub-Antarctic Marine Ecosystems - Instituto de Ecología y Biodiversidad (IEB), Chile. The authors are grateful for the financial and fellowship support from the Brazilian research funding agencies National Program for Post-Doctoral Studies - Coordination for Improvement of Higher Level Personnel (PNPD-CAPES - General Program of International Cooperation PGCI - 99999.002378/2015) and National Council for Scientific and Technological Development (CNPq).

Abstract

The sub-Antarctic region has a vast diversity of red macroalgae composed of several bioactive compounds including fatty acids (FAs). In this sense, the aim of this work was to evaluate the FA composition in gametophytic, carposporophytic and

tetraesporophytic phases of *Gigartina skottsbergii*, *Iridaea cordata* and *Mazzaella laminarioides* collected in the Magellan region (Chile). FA extraction followed the Bligh & Dyer method (1959) and analysis was performed by Gas Chromatography coupled to Flame Ionization Detection. Results showed that total lipids varied between 1.25 to 2.72% while FA classes were distributed from 23.34 to 59.93%, 11.20 to 18.47% and 21.60 to 65.47% for saturated, monounsaturated and polyunsaturated FAs, respectively. Moreover, development phases influenced total lipids and FA profile of the specimens, however samples maintained adequate Σ*n*6/Σ*n*3 ratios. Therefore, sub-Antarctic red macroalgae were a feasible source of FAs essential to human nutrition that could be applied to pharmaceutical and biotechnological areas.

Key-words: Polyunsaturated Fatty Acids; Rhodophyta; Gas Chromatography; Development Phase; Macroalgae; Lipids.

1 Introduction

Macroalgae comprise a complex group of photosynthetic, unicellular or multicellular organisms with specific patterns such as pigmentation, morphology and chemical constitution that characterize and classify each species into distinctive phyla (Lee, 2008). Is it known that several seaweeds modify their biochemical and physiological metabolism under certain conditions that include environmental stress or reproductive mechanisms (Vitova, Bisova, Kawano & Zachleder, 2015). These metabolic changes have still been little studied despite possibly assisting food, pharmaceutical and biotechnological areas since it could assist in the identification of novel compounds of nutritional interest (Kwang, Song & Lee, 2008).

Macroalgae can be an important source of several nutritional compounds that include proteins, carbohydrates, vitamins, fibers, minerals (Astorga-España & Mansilla, 2014). and lipids (Harrysson, Hayes, Eimer, Carlsson, Toth & Undeland, 2018; Vieira, 2018). Their consumption as food resource is still largely unexplored in Western countries, although it is widely explored in several Asian countries including Korea, Japan and China (Ito et al., 2018). Moreover, some of these organisms are commercially used as biofertilizers, cosmetic products and functional foods, for instance. (Paiva, Lima, Patarra, Neto & Baptista, 2014; Michalak, Chojnacka, Dmytryk, Wilk , Gramza & Roj, 2016).

Since lipid fractions of seaweeds generally range from 1 to 7% varying according species their use as energy source is commercially unattractive (Kendel, Wielgosz - Collin, Bertrand, Roussakis, Bourgougnon & Bedoux, 2015). Nonetheless, the lipid fraction could be a source of monounsaturated (MUFAs) or polyunsaturated (PUFAs) fatty acids (FAs) that are important nutraceutical compounds Korzeniowska, Górka, Lipok, & Wieczorek, 2018). Previous studies showed that cold-water macroalgae mainly of the Rhodophyta phylum tend to produce large amounts of PUFAs distributed among omegas 3 (*n*3) and 6 (*n*6). According to Santos et al. (2017), specimens of *Iridaea cordata*, *Palmaria decipiens*, *Plocamium cartilagineum* and *Pyropia endiviifolia* collected in the Antarctic region had on average 11.4 to 44.0% of saturated FAs (SFAs), 2.7 to 7.6% of MUFAs and 43.6 to 81.1% of PUFAs. These components act as signal transductions, energy storage as well as assist in the constitution and fluidity of membranes (Harwood & Guschina, 2009).

Reports of the literature indicate that the consumption of *n*3-PUFAs has a nutraceutical potential preventing diseases that affect the neurological and cardiovascular systems as well as assisting the organism against autoimmune (Adkins, Soulika, Mackey & Kelley, 2019) and cancer conditions (Zhu et al., 2017). In certain cases, the biological action of *n*3-PUFAs originates from the dietary supply of non-human synthesized FAs such as α-linolenic acid (ALA, C18:3*n*3) and linoleic acid that cannot be produced endogenously by humans (C18:2*n*6) (David, Michael & Lehninger, 2013).

It is worth noting that the consumption of macroalgae in Asian countries is not directly associated to the combat against diseases, but to obtain an ideal dietary intake of certain compounds. In this sense, previous reports indicate that the Σ*n*6/Σ*n*3 ratio of eastern countries is approximately 4:1 or less while western diets reach as much as 15:1. Increased Σ*n*6/Σ*n*3 ratios are considered nutritionally inadequate and can promote the pathogenesis of cardiovascular diseases (Simopoulos & Meester, 2009).

In their development, red macroalgae can suffer from considerable metabolic changes influencing the types and concentration of FAs produced among their gametophytic, carposporophytic and tetraesporophytic developmental stages and, thus, potentially affect their nutraceutical potential (Khotimchenko, 2006). Despite the possible biochemical changes in the phases of development of seaweeds, the majority of research works involving the extraction and identification of bioactive compounds in macroalgae use different developmental phases without comparing their life cycles

(Bjarnadóttir et al., 2018; Rahelivao, Gruner, Andriamanantoanina, Andriamihaja, Bauer & Knölker, 2015).

As it can be observed, the particularities of seaweeds should be carefully evaluated in order to maximize their commercial application and nutraceutical purposes (Seca, Gouveia, Barreto, Silva & Pinto, 2018). In this sense, the aim of this work was to evaluate differences in the profile and concentration of FAs in the gametophytic, carposporophytic and tetraesporophytic phases of red macroalgae *Gigartina skottsbergii* Setchell & N.L.Gardner, *Iridaea cordata* (Turner) Bory de Saint-Vincent and *Mazzaella laminarioides* (Bory) Fredericq collected in the sub-Antarctic region of the Magellan Strait (Chile).

2 Materials and Methods

2.1 Sampling

Samples were collected in the sub-Antarctic region of the Magellan Strait (Punta Arenas, Chile) between January and March of 2017. The species analyzed that belong to the Rhodophyta phylum were *Gigartina skottsbergii* Setchell & NL Gardner, *Mazzaella laminarioides* (Bory) Fredericq and *Iridaea cordata* (Turner) Bory de Saint-Vincent in their gametophytic, carposporophytic and tetraesporophytic development phases. Approximately 10 individuals were collected under low tide at distinct stages of development for each species. *G. skottsbergii* was collected at 5 m of depth in the infralittoral area, *M. laminarioides* was harvested in the high mesolithic zone while *I. cordata* was collected in the middle mesolithic zone. After collection, specimens were morphologically identified and their exsiccates were deposited in the Herbarium of the Laboratory of Antarctic and Sub-Antarctic Marine Ecosystems (LEMAS). Information regarding collection site, species, development phase and other general data are indicated in Table 1.

Table 1. Collection data, development phase, collection site, marine zonation and herbarium number of red macroalgae collected in the Magellan Region, Chile (2017)

Species	Development Phase	Collection Site	Marine Zonation	Herbarium Number
G. skottsbergii	Gametophytic	Puerto del Hambre	INLT	1303r
	Carposporophytic	Puerto del Hambre	INLT	1301r
	Tetraesporophytic	Puerto del Hambre	INLT	1302r
I. cordata	Gametophytic	San Juan	MINT	1307r
	Carposporophytic	San Juan	MINT	1308r
	Tetraesporophytic	San Juan	MINT	1306r
M. laminarioides	Gametophytic	San Juan	HINT	1298r
	Carposporophytic	San Juan	HINT	1299r
	Tetraesporophytic	San Juan	HINT	1300r

Infralittoral Zone (INLT); Higher Intertidal Zone (HINT); Middle Intertidal Zone (MINT); San Juan (53° 43'S - 70° 58'W); Puerto del Hambre (53° 36'S - 70° 55'W).

The collected macroalgae were conditioned in thermal boxes in seawater and sent to the laboratory for cleaning with running and distilled water. Subsequently, algal biomass were weighted, introduced in dark bags and frozen at -20 ºC. After the freezing period (~7 days), specimens were dried in a JOSF 700T air circulation oven at 35 ° C (± 1 ° C) for a period between 24 and 36 h, pulverized in mill (Lucadema model 226/2) and again packed in dark bags and frozen at -20 ° C until further analysis. Dry Weight (DW) determination followed the Brazilian Pharmacopeia (2010) using 2 g of algal biomass in triplicate (n=3). Dehydration was carried out in a DeLeo oven (model A58EAF) at 105 °C for 5 h until samples reached constant weight (Brazilian Pharmacopeia, 2010). The moisture content was calculated by the difference of the initial and final weights of the specimens and expressed as percentage of dry weight

(% DW). This method is based on the loss of moisture and volatiles of the samples, which are eliminated by desiccation.

2.2 Chemicals and Standards

Quantification and identification of FAs followed the methodology of Tang & Row (2013) using a Gas Chromatograph with Flame Ionization Detector (GC/FID 2010 - Shimadzu) and a SP®-2560 Capillary GC column (100 m × 0.25 mm x 0.20 µm - Supelco, USA). Quantification of FAs was performed using a mixture of C4-C24 methyl esters of FAs (FAME 37-MIX - Supelco, Bellefonte, Pennsylvania, USA) and an internal standard methyl nonadecanoate (C19:0 - Sigma-Aldrich, USA). HPLC-grade *n*-hexane was purchased from JT Baker (Phillipsburg, USA) while a 14% boron trifluoride (BF_3) methanolic solution was acquired from Sigma Aldrich (St Louis, USA). The remaining chemicals used were analytical grade reagents (CHROMASOLV Plus, ≥98.5 % - Sigma-Aldrich).

2.3 Extraction and Derivatization of Fatty Acids

The lipid fraction of macroalgae was extracted using the modified method of Bligh & Dyer (1959). Briefly, 1 g of algal biomass was weighed in triplicates (*n*=3) and homogenized with 40 mL of methanol: chloroform: 1.5% (*w*/*v*) sodium sulphate solution (1:2:1, *v*/*v*/*v*) for 30 min at room temperature. After this period, 20 mL chloroform: 1.5% (*w*/*v*) sodium sulphate solution (1:1 *v*/*v*) were added to the system and the samples were further centrifuged for 30 min at 800 G Force (Novatecnica). The chloroform layer was retrieved and evaporated using a rotary vacuum evaporator (Büchi, Switzerland) through nitrogen flow (N_2) until constant weight. Total lipids were determined by the gravimetric method in triplicate (*n*=3) (Table 2).

The extracted FAs were converted to their respective methyl esters following the method of Moss, Lambert & Merwin (1974). Briefly, 20 to 50 mg of the extracted lipids and 5 ml of 2% (*w*/*v*) methanolic solution of potassium hydroxide were refluxed for 8 min at 80 °C. After this step, 7 mL of a 14% (*v*/*v*) methanolic solution of BF_3 were added and the samples remained for 3 min under reflux. Subsequently, samples were cooled to room temperature and phase separation occurred with 5 mL of 20% (*w*/*v*) solution of sodium chloride and 20 mL *n*-hexane. The organic phase was separated and the

solvent was evaporated on a rotary vacuum evaporator (Büchi, Switzerland) and N_2. FAMEs were weighed and stored in a freezer before GC/FID analysis.

2.4 Chromatographic Analysis

FAMEs were diluted in *n*-hexane and1 µL of the diluted sample was injected in split mode (1:100) using a nitrogen flow (carrier gas) of 1.2 mL min^{-1}. The capillary column used was a SP® 2560 (100 m × 0.25 mm x 0.20 µm - Supelco). The heating ramp started at 140 °C, maintaining this temperature for 5 min, increasing 4 °C min^{-1} to 240 °C remaining at this temperature for 10 min. The injector port and detector were kept at 280 °C. The results were calculated as mole percent (mol %) using an analytical curve of FAMEs (FAME 37-MIX - Supelco, Bellefonte, Pennsylvania, USA) at concentrations of 0.625 mg mL^{-1} and 20 mg mL^{-1} and methyl nonadecanoate (≥ 99.0% - Sigma-Aldrich, St. Louis, Missouri, USA) as an internal standard at a concentration of 2 mg mL^{-1} (Santos et al., 2017).

3 Statistical Analysis

Evaluation of the results regarding total fatty acids (ΣSFAs, ΣMUFAs and ΣPUFAs) and the fatty acid profile among the phases of development was performed applying two-way Analysis of Variance (ANOVA). One-way ANOVA was used for univariate variables for major FAs distributed among SFAs, MUFAs and PUFAs. After ANOVA, Tukey's HSD post hoc analysis of means was used to analyze differences among the results and to assess significant differences at a confidence interval of 95% (p<0.05). All statistical analyses were performed using GraphPad Prism 7 software (Version 2017-02, USA). The results were also subjected to Principal Component Analysis (PCA) using Minitab (State College, USA) software version 17.

4 Results

4.1 Total Lipid Content

The total lipid (TL) content had significant differences in the development phases of the same species and among the specimens (Table 2). Generally, lipid concentrations varied between 1.25 ± 0.04% for *G. skottsbergii* in the gametophytic

phase and 2.72 ± 0.16% for *M. laminarioides* in tetraesporophytic stage. *G. skottsbergii* had significant differences between the three stages of development whereas *I. cordata* did not present significant differences between the phases. Moreover, *M. laminarioides* had significant differences between the gametophytic and carposporophytic phases as well as gametophytic and tetraesporophytic phases.

Evaluating the same development phase among the specimens it can be observed that the gametophytic phase did not present significant differences between the species for TLs while the carposporophytic phase had significant differences in *I. cordata* and *M. laminarioides*. The tetraesporophytic phase had significant differences (p<0.05) between *G. skottsbergii* and *I. cordata* as well as in *I. cordata* and *M. laminarioides*. Generally, TL concentrations increased from the tetraesporophytic phases to maximum levels at the gametophytic and carposporophytic stages (Table 2).

Table 2. Total lipid contents of the studied Rhodophyta species and their development phases collected in the Magellan Region, Chile (2017)

Species	Development Phase	Lipids (%DW)
G. skottsbergii	Gametophytic	1.25 ± 0.04^{a}
	Carposporophytic	2.13 ± 0.06^{b}
	Tetraesporophytic	2.68 ± 0.27^{c}
I. cordata	Gametophytic	1.48 ± 0.09^{a}
	Carposporophytic	1.67 ± 0.13^{abd}
	Tetraesporophytic	1.94 ± 0.17^{bde}
M. laminarioides	Gametophytic	1.28 ± 0.08^{ade}
	Carposporophytic	2.38 ± 0.07^{bcf}
	Tetraesporophytic	2.72 ± 0.16^{ch}

Results represented as mean ± SD (where SD is standard deviation); (n = 3) where n is number of independent samples. Values without a common superscript in the same species are significantly different (p< 0.05 One-way ANOVA; Tukey's HSD); DW - dry weight.

4.2 Fatty Acid Analysis

Specimens of *G. skottsbergii* and *I. cordata* had on average 10 and 18 FAs, respectively, in their constitution while carposporophytic *M. laminarioides* was

composed of 22 FAs. As it can be observed in Table 3, the FA profile of *I. cordata* and *M. laminarioides* increased in the order PUFAs > SFAs > MUFAs which was the opposite found in *G. skottsbergii* that had the proportion SFAs > PUFAs > MUFAs.

The FA profile of the sub-Antarctic red macroalgae revealed that the most predominant SFAs were myristic (C14:0), palmitic (C16:0) and stearic (C18:0) acid. Among SFAs, C16:0 had the highest concentrations varying from 17.87 ± 0.36% in *M. laminarioides* (gametophytic phase) to 39.74 ± 0.57% in *G. skottsbergii* (carposporophytic phase). Significant differences in the amounts of C16:0 were observed for *G. skottsbergii* between gametophytic and carposporophytic phases as well as carposporophytic and tetraesporophytic phases. In the case of *M. laminarioides*, differences occurred between the gametophytic and carposporophytic phases (<0.05; Tukey's ANOVA HSD). It is worth noting that there were no significant differences in the concentration of 16:0 in the specimens of *I. cordata*.

Table 3. Fatty acid composition (mol %) of the studied Rhodophyta species and their development phases collected in the Magellan Region, Chile (2017).

Fatty Acid	*Gigartina skottsbergii*			*Iridaea cordata*			*Mazaella laminarioides*		
	GSG	**CGS**	**TGS**	**GIC**	**CIC**	**TIC**	**GML**	**CML**	**TML**
C12:0	1.07 ± 0.03[a]	nd	0.07 ± 0.00[a]	nd	0.65 ± 0.04[a]	0.46 ± 0.02[a]	nd	0.39 ± 0.01[a]	nd
C14:0	5.52 ± 0.22[a]	6.53 ± 0.09[a]	5.51 ± 0.04[a]	1.90 ± 0.02[a]	2.64 ± 0.15[a]	2.55 ± 0.05[a]	3.40 ± 0.28[a]	2.73 ± 0.03[a]	3.54 ± 0.67[a]
C14:1	1.14 ± 0.05[a]	nd	Nd	nd	nd	nd	nd	nd	nd
C15:0	1.40 ± 0.06[a]	nd	Nd	nd	0.55 ± 0.04[a]	nd	nd	0.45 ± 0.00[a]	nd
C16:0	34.46 ± 2.84[a]	39.74 ± 0.57[b]	36.47 ± 0.41[a]	24.46 ± 0.23[a]	23.92 ± 1.54[a]	24.71 ± 0.37[a]	17.87 ± 0.36[a]	20.93 ± 0.19[b]	20.33 ± 2.08[b]
C16:1	2.56 ± 0.19[ab]	4.45 ± 0.19[a]	1.86 ± 0.08[b]	1.64 ± 0.01[a]	4.06 ± 0.10[b]	2.16 ± 0.08[a]	2.61 ± 0.12[a]	2.07 ± 0.08[a]	1.75 ± 0.43[a]
C17:0	1.65 ± 0.24[a]	nd	nd	nd	0.48 ± 0.06[a]	nd	nd	0.50 ± 0.02[a]	nd
C17:1	Nd	nd	nd	nd	nd	nd	nd	0.34 ± 0.02[a]	0.35 ± 0.8[a]
C18:0	6.19 ± 0.07[a]	13.65 ± 0.16[b]	4.77 ± 0.24[a]	1.23 ± 0.03[a]	3.10 ± 0.29[b]	2.36 ± 0.04[b]	2.06 ± 0.11[a]	2.08 ± 0.12[a]	1.65 ± 0.28[a]
C18:1*n*9c	11.62 ± 0.78[a]	14.03 ± 0.18[b]	15.40 ± 0.27[b]	11.45 ± 0.13[a]	10.08 ± 0.59[b]	9.48 ± 0.15[b]	6.75 ± 0.42[a]	8.38 ± 0.08[a]	7.25 ± 0.07[a]
C18:2*n*6t	Nd	nd	nd	0.76 ± 0.03[a]	2.20 ± 0.15[b]	1.19 ± 0.03[ab]	0.27 ± 0.03[a]	0.51 ± 0.02[a]	0.17 ± 0.04[a]
C18:2*n*6c	2.15 ± 0.19[a]	6.59 ± 0.41[b]	3.36 ± 0.11[a]	3.38 ± 0.10[a]	4.52 ± 0.08[b]	3.71 ± 0.08[ab]	1.79 ± 0.02[a]	2.05 ± 0.06[a]	2.49 ± 0.64[a]
C18:3*n*3	Nd	nd	nd	1.87 ± 0.08[a]	5.21 ± 0.15[b]	3.42 ± 0.25[c]	2.33 ± 0.09[a]	1.14 ± 0.04[a]	0.53 ± 0.15[a]
C18:3*n*6	Nd	nd	nd	0.50 ± 0.01[a]	0.53 ± 0.01[a]	0.73 ±0.04[a]	1.44 ± 0.01[a]	0.82 ± 0.08[a]	0.82 ± 0.21[a]
C20:0	Nd	nd	nd	0.15 ± 0.01[a]	nd	nd	nd	0.25 ± 0.02[a]	nd
C20:1*n*9c	Nd	nd	nd	0.22 ± 0.01[a]	0.51 ± 0.06[a]	0.65 ± 0.00[a]	nd	0.33 ± 0.01[a]	nd
C20:2	nd	nd	nd	0.95 ± 0.52[a]	2.17 ± 0.01[b]	2.16 ± 0.02[b]	nd	0.47 ± 0.03[a]	nd
C20:3*n*6	2.22 ± 0.20[a]	nd	1.29 ± 0.04[a]	1.44 ± 0.04[a]	1.99 ± 0.16[a]	1.60 ± 0.07[a]	2.19 ± 0.12[a]	1.90 ± 0.02[a]	2.26 ± 0.60[a]
C20:4*n*6	15.50 ± 0.70[a]	6.86 ± 0.24[b]	15.58 ± 0.16[a]	24.88 ± 0.24[a]	17.29 ± 0.48[b]	21.92 ± 0.21[c]	19.28 ± 0.58[a]	16.79 ± 0.13[a]	19.24 ± 2.81[a]

C20:5*n*3	14.56 ± 0.82^{a}	8.15 ± 0.19^{b}	15.08 ± 0.24^{a}	23.22 ± 0.29^{a}	17.50 ± 0.40^{b}	21.45 ± 0.50^{c}	38.11 ± 1.06^{a}	35.82 ± 0.34^{a}	37.77 ± 4.37^{a}
C22:1*n*9c	nd	nd	nd	0.40 ± 0.02^{a}	0.77 ± 0.02^{a}	0.54 ± 0.01^{a}	nd	0.47 ± 0.04^{a}	0.52 ± 0.12^{a}
C22:2	nd	nd	nd	nd	nd	nd	nd	0.54 ± 0.06^{a}	nd
C22:6*n*3	nd	nd	nd	0.37 ± 0.02^{a}	nd	nd	nd	nd	nd
C24:0	nd	nd	nd	0.19 ± 0.00^{a}	0.53 ± 0.06^{a}	nd	nd	nd	nd
C24:1*n*9	nd	nd	0.61 ± 0.00^{a}	0.98 ± 0.02^{a}	1.15 ± 0.07^{a}	0.90 ± 0.07^{a}	1.89 ± 0.07^{a}	1.05 ± 0.02^{a}	1.34 ± 0.33^{a}
∑C18	19.96 ± 0.91^{a}	34.27 ± 0.41^{b}	23.52 ± 0.39^{a}	19.19 ± 0.14^{a}	25.63 ± 0.62^{b}	20.89 ± 0.30^{a}	14.65 ± 0.62^{a}	14.87 ± 0.36^{a}	12.90 ± 1.40^{a}
∑C20	32.28 ± 1.45^{a}	15.01 ± 0.30^{b}	31.95 ± 0.29^{a}	50.86 ± 0.36^{a}	39.56 ± 0.81^{b}	47.80 ± 0.45^{a}	59.58 ± 1.02^{a}	55.92 ± 0.53^{a}	59.26 ± 0.96^{a}
∑SFA	50.30 ± 2.32^{a}	59.93 ± 0.57^{b}	46.83 ± 0.25^{a}	27.83 ± 0.23^{a}	31.93 ± 1.50^{b}	30.08 ± 0.36^{ab}	23.34 ± 0.50^{a}	27.88 ± 0.73^{b}	25.53 ± 1.13^{ab}
∑MUFA	15.28 ± 0.95^{a}	18.47 ± 0.29^{a}	17.87 ± 0.23^{a}	14.70 ± 0.18^{a}	16.56 ± 0.64^{a}	13.72 ± 0.16^{a}	11.24 ± 0.53^{a}	12.53 ± 0.25^{a}	11.20 ± 1.04^{a}
∑PUFA	34.43 ± 1.64^{a}	21.60 ± 0.72^{b}	35.30 ± 0.29^{a}	57.37 ± 0.37^{a}	51.51 ± 0.86^{b}	56.10 ± 0.52^{a}	65.42 ± 0.92^{a}	59.58 ± 0.48^{b}	61.65 ± 0.95^{b}
∑PUFA/∑SFA	0.69 ± 0.06	0.36 ± 0.02	0.75 ± 0.01	2.05 ± 0.03	1.62 ± 0.10	1.87 ± 0.06	2.81 ± 0.09	2.14 ± 0.07	2.42 ± 0.07
∑*n*3	14.56 ± 0.82^{a}	8.15 ± 0.19^{b}	15.08 ± 0.24^{a}	25.47 ± 0.28^{a}	22.72 ± 0.51^{a}	24.88 ± 0.55^{a}	40.44 ± 0.98^{a}	36.68 ± 0.50^{b}	38.29 ± 4.22^{ab}
∑*n*6	19.86 ± 0.89^{a}	13.45 ± 0.60^{b}	20.23 ± 0.25^{a}	31.90 ± 0.41^{a}	28.79 ± 0.54^{a}	31.32 ± 0.13^{a}	24.98 ± 0.59^{a}	22.90 ± 0.21^{a}	24.98 ± 4.30^{a}
∑*n*6/∑*n*3	1.36 ± 0.04	1.65 ± 0.07	1.34 ± 0.03	1.25 ± 0.03	1.27 ± 0.02	1.26 ± 0.03	0.62 ± 0.01	0.62 ± 0.01	0.68 ± 0.02

Saturated fatty acid (SFA); Monounsaturated fatty acid (MUFA); Polyunsaturated Fatty Acid (PUFA); Mazaella laminarioides gametophytic (GML), carposporophytic (CML) and tetraesporophytic (TML); Gigartina skottsbergii gametophytic (GGS), carposporophytic (CGS) and tetraesporophytic (TGS); Iridaea cordata gametophytic (GIC), carposporophytic (CIC) and tetraesporophytic (TIC); nd (no detected). Data presented as molar percentage area (mol%) of total fatty acids; Results represented as mean ± SD (where SD is standard deviation); (n = 3) where n is number of independent samples. Values without a common superscript in the same species are significantly different ($p < 0.05$ Two-way ANOVA; Tukey's HSD).

The C14:0 was other SFA found in noticeable amounts in the samples varying from 1.90 ± 0.02% to 6.53 ± 0.09%, respectively, in *G. skottsbergii* (gametophytic phase) and *I. cordata* (carposporophytic phase). Nonetheless, there were no significant differences of C14:0 between the development stages of the specimens. Moreover, C18:0 had concentrations that ranged from 1.23 ± 0.03% to 13.65 ± 0.16% in *G. skottsbergii* (gametophytic phase) and *I. cordata* (carposporophytic phase), respectively. Comparing the amounts of C18:0 to C14:0 it can be observed that C18:0 was only prevalent in carposporophytic *I. cordata* (3.09 ± 0.29%) as well as gametophytic and carposporophytic *G. skottsbergii* (6.20 ± 0.07% and 13.65 ± 0.16%, respectively).

The two main identified MUFAs were palmitoleic (C16:1) and oleic (C18:1*n*9c) acid. C16:1 had concentrations between 1.64 ± 0.01% and 4.45 ± 0.19% in *I. cordata* (gametophytic phase) and *G. skottsbergii* (carposporophytic phase). Moreover, C18:1*n*9c had the higher amounts among MUFAs, reaching 6.75 ± 0.45% and 15.40 ± 0.27% in *M. laminarioides* (gametophytic phase) and *G. skottsbergii* (tetraesporophytic phase).

Linolelaidic acid (C18:2*n*6t) was the only trans-FA found in the studied species occurring in *I. cordata* and *M. laminarioides* in all developmental stages reaching concentrations of 0.76 ± 0.03% and 2.20 ± 0.15% with significant differences between gametophytic and carposporophytic phases of *I. cordata*, respectively. The essential FA to the human diet linoleic acid (C18:2*n*6c) was found in all species and stages of development, but α-linolenic acid (18:3*n*3), another essential FA, was only found in *M. laminarioides* and *I. cordata*. Results of C18:2*n*6c varied between 1.79 ± 0.02% and 6.59 ± 0.41% reaching higher concentrations in the carposporophytic phase of *G. skottsbergii*. For C18:3*n*3, the most expressive result was in *I. cordata* (carposporophytic phase) with 5.21 ± 0.15%.

Arachidonic (ARA, C20:4*n*6) and eicosapentaenoic (EPA, C20:5*n*3) acid were the PUFAs found in highest concentration in the studied macroalgae and their respective development phases. As it can be seen in Table 3, despite proximate amounts of both C20:4*n*6 and C20:5*n*3, *G. skottsbergii* and *I. cordata* had significant differences among their stages of development whereas *M. laminarioides* did not significant differences. The sum of these two PUFAs represented

on average 81%, 76% and 87% of the total concentration of PUFAs in *G. skottsbergii*, *I. cordata* and *M. laminarioides*, respectively (Figure 1).

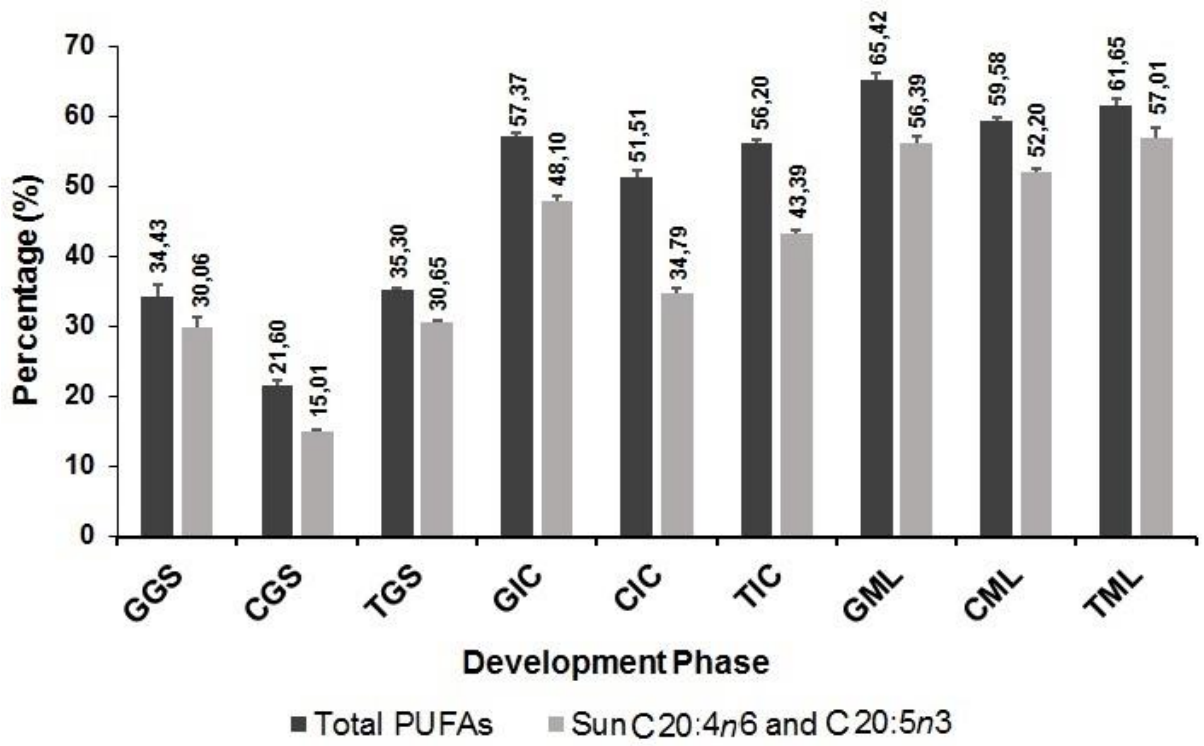

Figure 1. Comparison between the sum of C20:4n6 and C20:5n3 against the sum of PUFAs in gametophytic (GGS), carposporophytic (CGS) and tetraesporophytic (TGS) Gigartina skottsbergii; gametophytic (GIC), carposporophytic (CIC) and tetraesporophytic (TIC) Iridaea cordata; gametophytic (GML), carposporophytic (CML) and tetraesporophytic (TML) Mazaella laminarioides. Results represented as mean ± SD (where SD is standard deviation); (*n* = 3) where n is number of independent samples.

Comparing the classes of FAs, it can be observed that *M. laminarioides* and *I. cordata* had a predominance of PUFAs over SFAs, which influenced their ∑PUFA/∑SFA ratios to levels that ranged from 2.14 ± 0.07 to 2.81 ± 0.09 and 1.62 ± 0.10 to 2.05 ± 0.08, respectively. On the other hand, *G. skottsbergii* was mainly constituted of SFAs than PUFAs contributing to ∑PUFA/∑SFA ratios from 0.36 ± 0.02 to 0.75 ± 0.01. It is worth noting that each macroalgae had distinct concentrations of the classes of PUFAs that were generally found in higher amounts in the gametophytic and tetraesporophytic phases.

Although dominated by n6 PUFAs, *G. skottsbergii* and *I. cordata* maintained a good had ∑*n*6/∑*n*3 ratio according the indicated by the World Health Organization (WHO) reaching values of 1.34 ± 0.03 to 1.65 ± 0.07 and 1.25 ± 0.03 to 1.27 ± 0.02, respectively. Among the studied macroalgae, *M. laminarioides* had a predominance of *n*3-PUFAs, which increased its overall ratio to levels that fluctuated from 0.62 ± 0.01 to 0.68 ± 0.02. It is worth noting that there was no significant difference of ∑*n*6/∑*n*3 ratio among the phases of development of the samples.

PCA was conducted in order to further verify the influence of the phase of development and species regarding the overall FA composition. In this sense, variables that generally had significant difference among the samples that include ∑SFAs, ∑MUFAs, ∑PUFAs, ∑C18, ∑C20, ∑C22, ∑PUFAs/∑SFAs, ∑*n*3, ∑*n*6 and ∑*n*6/∑*n*3 (**Fig 2b**) were chosen for the multivariate evaluation. The resulting score plot (**Fig 2a**) had Principal (PC1) and Second (PC2) Components explained 75.74% and 13.50% of the variations between the FAs profile of the studied sub-Antarctic macroalgae, respectively.

Multivariate analysis could cluster and distinguish samples based on the distinct influences of the variables. Parameters that included ∑SFAs, ∑MUFAs, ∑*n*6/*n*3 and ∑C18, for instance, were associated to the negative axis of PC1 while the other variables were placed at the positive axis of PC1. It is worth noting that each parameter had also distinct contributions to PC2 as ∑*n*3 and ∑*n*6 contributed to positive or negative axis of PC2, respectively. In this sense, it can be observed that the phases of development of the studied macroalgae clustered in distinct regions of the score plot. *G. skottsbergii* and *M. laminarioides* were found in the upper quadrants of PCA differencing in the position along PC1 axis. On the other hand, *I. cordata* was placed in the lower quadrants of PCA varying between the negative and positive axis of PC1.

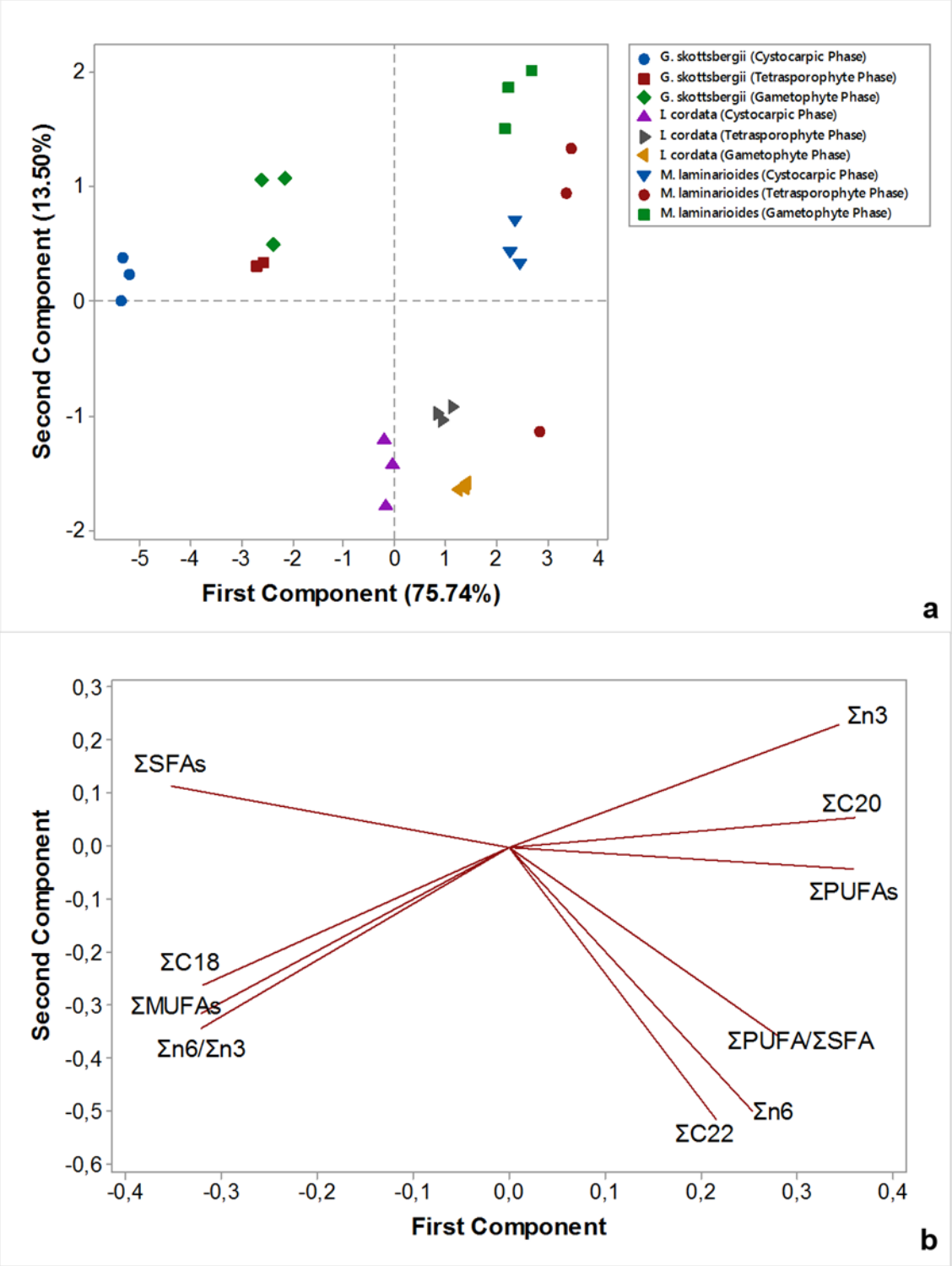

Figure 2. PCA of the score plot (**a**) of red sub-Antarctic macroalgae and their respective development phases and loading plot (**b**) of the FAs used as variables in the evaluation.

5 Discussion

In the present study, results were evaluated concerning changes in the biosynthesis of FAs in function of algal development phases. Since the specimens had the same population and were collected short time other variables that could affect the results including seasonality and habitat were minimized. It is worth noting that further comparisons with reports of the literature were made at similar order or phylum of the studied samples since there are few data regarding the species in distinct development phases.

Analysis showed that the samples had an increase in TLs from the gametophytic to the tetraesporophytic stage indicating that the concentration of lipids is directly related to the development phase. According to Kendel, Wielgosz-Collin, Bertrand, Roussakis, Bourgougnon & Bedoux (2015) *Solieria chordalis* (Gigartinales, Rhodophyta) collected at the Atlantic coast (France) had TLs on average concentrations of 2.96 ± 0.04%. Analyzing specimens of the Gigartinales order of the Tasmanian coast, Schmid et al.,(2018) found values of TLs for *Dasyphloea insignis*, *Gigartina recurva*, *Rhodoglossum gigartinoides* and *Callophyllis rangiferine* of 1.4 ± 0.2%, 0.9 ± 0.0%, 1.9 ± 0.1% and 0.6 ± 0.0%, respectively. Moreover, red seaweeds collected from different locations of Diu and Saurashtra (coast of Gujarat, India) by Kumari, Kumar, Gupta, Reddy & Jha (2010) had TLs that ranged from 1.0 ± 0.20% to 1.5 ± 0.30%. Santos et al. (2017) reported amounts of TLs for *Iridaea cordata* collected in the Antarctic region of 2.4 ± 0.5%, which was above the results found in the current study for the same species. Since the evaluated red macroalgae had TLs that varied from 1.25 ± 0.04% to 2.72 ± 0.16% the results corroborated with previous reports for species of Gigartinales order.

The main MUFAs detected in the studied red macroalgae were C16:1*n*7 (palmitoleic acid) and C18:1*n*9 agreeing with previous reports of the literature. Concerning development phases, C18:1*n*9 was the main MUFA found in the samples and their respective life cycles comprehending more than 65% of the total concentration of MUFAs. These results were above the reported for the gametophytic phases of *Tichocarpus crinitus* collected in Sea of Japan (Khotimchenko & Yakovleva, 2005) and *Iridaea cordata* collected in Antarctica (Santos et al., 2017). Nonetheless, developmental phases of *M. laminarioides* collected in the upper infralittoral zone had

similar results to *Chondrus crispus* collected in lower infralitoral zone by Koch, Hagen, Graeve and Bischof (2017). *G. skottsbergii* had the highest concentrations of MUFAs with the results for the tetraesporophytic phase (15.40%) reaching higher concentrations than the reported by Graeve et al. (2002) that determined 10.7% of MUFAs for the same species and development phase collected in Antarctica.

Specimens of *G. skottsbergii* had the highest concentrations of SFAs in comparison to *I. cordata* and *M. laminarioides* being C16:0 the main SFA representing more than 70% of the total concentration of SFAs in *G. skottsbergii*. Concerning development phases, the tetraesporophytic stage of *I. cordata* and *M. laminarioides* had concentrations for C16:0 of 24.71 ± 0.37% and 20.33 ± 0.37%, respectively. Results were below the reported by Graeve et al. (2002) and Koch et al. (2017) that determined 29.4% and 27.2% - 30.4% of C16:0 for *Gymnogongrus turquetii* (Gigartinales) and *C. crispus* with values between 27.2 and 30.4%, respectively. However, *G. skottsbergii* had higher amounts of C16:0 compared to the same species in the tetraesporophytic phase reaching 36.47 ± 0.41% (Graeve et al., 2002).

The obtained results for ΣSFAs and ΣMUFAs showed that the carposporophytic phase of the studied algae presented the highest concentrations of these FAs. According to Liu, Bogaert, Engelen, Leliaert, Roleda & De Clerck (2017), the carposporophytic phase is the stage in which algae releases spores making the organisms to store large reserves of triacylglycerols (TAGs) to supply energy expenditures related to the reproductive process. TAGs comprehend neutral lipids found in large amounts in seaweeds as storage product or energy reservoir for the algal metabolism having mainly SFAs and MUFAs bound to their structure (Guschina & Harwood, 2013).

Increased concentrations of PUFAs found in *I. cordata* and *M. laminarioides* agree with previous reports of cold environment Rhodophyta species (Santos et al., 2017; Pacheco et al. al., 2018). On the other hand, *G. skottsbergii* had values of 35.30 ± 0.29%, which were below the amount found by Graeve et al., (2002) for the same species in the tetraesporophytic phase. The PUFA C18:3*n*3 acid that was not detected in *G. skottsbergii* and appears at low concentrations in *M. laminarioides* (tetraesporophytic phase) was also not detected by Graeve et al. (2002) in six Rhodophyta species of the 15 macroalgae analyzed. In the report, the samples that had C18:3*n*3 presented concentrations ranging from 0.2% to 4.1%. Tasende (2000)

reported 2.85% and 5.77% of C18:3*n*3 in *Chondrus crispus* in the gametophytic and tetraesporophytic phases, respectively, corroborating with the results found in the current work for *M. laminarioides* (gametophytic phase).

The main PUFAs found in the samples were C20:4*n*6 and C20:5*n*3 acids, which had decreased concentrations in the carposporophytic phase compared to the other evaluated life cycles in the studied species. According to Guschina & Harwood (2013), the large amount of TAGs in the carposporophytic phase can be possibly related to the lower concentrations of PUFAs in this stage since, unlike SFAs and MUFAs, these molecules bind in small proportions to TAGs.

It is worth noting that the high concentrations of C18-FAs and C20-FAs in *I. cordata* and *M. laminarioides* agree with the literature with C20-FAs being reported in several studies as characteristic of Rhodophyta species (Kumari, Kumar, Reddy & Jha, 2013). Analyzing the results, it can be observed that the carposporophytic phase had lower amounts of C20-FAs and increased concentrations of C18-FAs in the specimens compared to the other life cycles. We suggest that this outcome can be associated to higher concentrations of C18-SFAs (e.g. C18:0) and C18-MUFAs (e.g. C18:1*n*9c) in the carposporophytic phase that were linked to the R_1, R_2 and R_3 positions of glycerol skeleton of TAGs as energy reserves for this phase in the species studied.

Lower amounts of C20-FAs in the specimens of *G. skottsbergii* differ from the results of red macroalgae and can be associated to certain types of glycolipids in the photosynthetic membranes. Differently than *I. cordata* and *M. laminarioides, G. skottsbergii* was not exposed during the day to large amounts of solar radiation since its collection site had approximately 10 m of depth.

Photosynthetic membranes are responsible for the capture of sunlight and for the distribution of energy to thylakoids. These membranes are mainly formed by monogalactosyldiacylglycerol (MGDG) and digalactosyldiacylglycerol (DGDG), which mainly binds to PUFAs in the forms of C20:4*n*6 and C20:3*n*3 in the *sn-1* and *sn-2* positions. Despite lower amounts of C20-FAs, *G. skottsbergii* had higher concentrations of C16-FAs and C18-FAs that are associated to TAGs in processes of energy formation required for reproduction and maintenance of metabolism in low light zones (Kalisch, Dörmann & Hölzl, 2016; Li-Beisson, Thelen, Fedosejevs & Harwood, 2019).

Regarding Σ*n*3 and Σ*n*6, results showed that generally there were no significant differences between the developmental phases. Exceptions occurred in *G. skottsbergii*

and *I. cordata* that had differences between the carposporophytic phases compared to the other life cycles. Moreover, results of Σ*n*6/Σ*n*3 ratio for *G. skottsbergii* and *I. cordata* were higher than those previously reported while *M. laminarioides* had results below or similar to literature (Graeve et al., 2002; Kumari et al., 2010 & Santos et al. 2017).

Adequate Σ*n*6/Σ*n*3 ratios below 10:1 are essential in order to obtain a healthy and ideal diet which is not currently observed in Western nutrition due to the consumption of industrialized food that have increased amounts of *n*6-PUFAs (Simopoulos & Meester, 2009). The evaluated macroalgae in their respective development phase had adequate Σ*n*6/Σ*n*3 ratios indicating that the constituents MUFAs and PUFAs could be interesting feeding agents for a healthy diet in human nutrition.

PCA showed that the differences in the FA profile of red sub-Antarctic macroalgae allowed their discrimination. Similarly, distinct concentrations of FAs differentiated the development phases of the studied seaweeds. Among the reasons that could explain this behavior was the higher concentration of SFAs in *G. skottsbergii* specimens which shifted the samples to the positive and negative axis of PC1 and PC2, respectively. For *M. laminarioides*, increased amounts of n3-PUFAs, C20-FAs and ∑PUFAs allowed its differentiation from *I. cordata* that had higher concentrations of n6-PUFAs, C22-FAs and ∑PUFAs/∑SFAs. Moreover, fluctuations in the amounts of the variables also can explain differentiation among development phases.

Differentiation of species and phyla of macroalgae have been previously indicated in the literature at where Kumari et al. (2010) analyzed 27 brown, green and red seaweeds from the coast of India and could distinguish samples using FAs as variables. Further statistical evaluations also showed that FAs could be used to assess taxonomical similarities among the specimens. Boulom, Robertson, Hamid, Ma & Lu (2014) sed PCA to analyze the influence of seasons in the production of FAs from *Undaria pinnatifida* and showed that samples from summer, spring and winter could be differenced based on their profile of FAs.

Summarizing, the current research work presented important results showing that seaweeds and their developmental phases had differentiated qualitative and quantitative FA content. Moreover, the study provided one of the first in-depth investigations regarding FA concentrations in gametophytic, carposporophytic and tetraesporophytic phases of red seaweeds from the sub-Antarctic region. Therefore,

the evaluation of the life cycles of macroalgae should be carefully assessed in order to optimize the nutraceutical potential of macroalgae.

Conflict of Interest: The authors declare that they have no conflict of interest.

6 References

Adkins, Y., Soulika, A. M., Mackey, B., & Kelley, D. S. (2019). Docosahexaenoic acid (22:6n-3) ameliorated the onset and severity of experimental autoimmune encephalomyelitis in mice. Lipids, 54(1), 13-23. https://doi.org/10.1002/lipd.12130.

Astorga-España, M. S. & Mansilla A. (2014). Sub-Antarctic macroalgae: opportunities for gastronomic tourism and local fisheries in the region of Magallanes and Chilean Antarctic territory. Journal of Applied Phycology, 26:973–978. http://doi.org/10.1007/s10811-013-0141-1.

Bjarnadóttir, M., Aðalbjörnsson, B. V., Nilsson, A., Slizyte, R., Roleda, M. Y., Hreggviðsson, G. Ó., Jónsdóttir, R. (2018). *Palmaria palmata* as an alternative protein source: enzymatic protein extraction, amino acid composition, and nitrogen-to-protein conversion factor. Journal of Applied Phycology, 30(3), 2061–2070. http//doi.org/10.1007/s10811-017-1351-8.

Bligh, E.G. & Dyer, W. J. (1959). A rapid method for total lipid extraction and purification. Canadian Journal Biochemistry Physiology, 37, 911–917. https://doi.org/10.1139/o59-099.

Boulom, S., Robertson, J., Hamid, N., Ma, Q., & Lu, J. (2014). Seasonal changes in lipid, fatty acid, α-tocopherol and phytosterol contents of seaweed, Undaria pinnatifida, in the Marlborough Sounds, New Zealand. Food Chemistry, 161, 261–269. http//doi.org/10.1016/j.foodchem.2014.04.007

Brazil (2010) Brazilian Pharmacopoeia, National Health Surveillance Agency, Publishing Company FioCruz, Brasília, pp.91. http://portal.anvisa.gov.br/farmacopeias-virtuais. searched on 8 may 2018.

Guschina, I. A. & Harwood, J. L. (2013). Algal lipids and their metabolism. In: Borowitzka M., Moheimani N. (eds) Algae for biofuels and energy. Developments in Applied Phycology, v.5. Springer, Dordrecht.

Graeve, M., Kattner, G., Wiencke, C. & Karsten, U. (2002). Fatty acid composition of Arctic and Antarctic macroalgae: indicator of phylogenetic and trophic relationships. Marine Ecology Progress Series, 231, 67-74. http//doi.org. 10.3354/meps231067.

Harwood, J. L., Guschina, I. A. (2009). The versatility of algae and their lipid metabolism. Biochimie, 91(6):679–684. https://doi.org/10.1016/j.biochi.2008.11.004.

Harrysson, H., Hayes, M., Eimer, F., Carlsson, N. G., Toth, G. B., & Undeland, I. (2018). Production of protein extracts from Swedish red, green, and brown seaweeds, *Porphyra umbilicalis* Kützing, *Ulva lactuca* Linnaeus, and *Saccharina latissima* (Linnaeus) J. V. Lamouroux using three different methods. Journal of Applied Phycology, 30(6), 3565-3580. https://doi.org/10.1007/s10811-018-1481-7.

Ito M., Koba, K., Hikihara, R., Ishimaru, M., Shibata, T., Hatate, H., & Tanaka, R. (2018). Analysis of functional components and radical scavenging activity of 21 algae species collected from the Japanese coast. Food Chemistry, 255, 147–156. https://doi.org/10.1016/j.foodchem.2018.02.070.

Kalisch B., Dörmann P. & Hölzl G. (2016) DGDG and glycolipids in plants and algae. In: Nakamura Y., Li-Beisson Y. (eds) Lipids in plant and algae development. Subcellular Biochemistry, v 86 (pp. 51-83). Switzerland:Springer International Publishing.

Kendel, M., Wielgosz-Collin, G., Bertrand, S., Roussakis, C., Bourgougnon, N., & Bedoux, G. (2015). Lipid composition, fatty acids and sterols in the seaweeds *Ulva armoricana*, and *Solieria chordalis* from Brittany (France): an analysis from nutritional, chemotaxonomic, and antiproliferative activity perspectives. Marine Drugs, 13(9), 5606–5628. https://doi.org/10.3390/md13095606.

Khotimchenko, S. V. & Yakovleva I. M. (2005) Lipid composition of the red alga *Tichocarpus crinitus* exposed to different levels of photon irradiance. Phytochemistry, 66, 73–79.http://doi.org/ 10.1016/j.phytochem.2004.10.024.

Khotimchenko, S. V. (2006). Variations in lipid composition among diferente developmental stages of *Gracilaria verrucosa* (Rhodophyta). Botanica Marina, 49, 34–38. http//doi.org/10.1515/bot.2006.004.

Korzeniowska, K., Górka, B., Lipok, J. & Wieczorek, P. P. (2018) Algae and their extracts in medical treatment. In: Chojnacka K., Wieczorek P., Schroeder G., Michalak I. (eds) Algae biomass: characteristics and applications. Developments in Applied Phycology, v. 8. Springer, Cham

Koch, K., Hagen, W., Graeve, M. & Bischof, K. (2017). Fatty acid compositions associated with high-light tolerance in the intertidal rhodophytes *Mastocarpus stellatus* and *Chondrus crispus*. Helgoland Marine Research, 71(1), 1-16. http//doi.org/10.1186/s10152-017-0495-x.

Kumari, P., Kumar, M., Gupta, V., Reddy, C. R. K. & Jha, B. (2010). Tropical marine macroalgae as potential sources of nutritionally important PUFAs. Food Chemistry, 120(3), 749–757. http//doi.org/10.1016/j.foodchem.2009.11.006.

Kumari, P., Kumar, M., Reddy, C. R. K., & Jha, B. (2013). Algal lipids, fatty acids and sterols. In H. Dominguez (Ed.), Functional Ingredients from Algae for Foods and Nutraceuticals (pp. 87–134). Cambridge:Woodhead Publishing.

Lee, R. (2008). Basic characteristics of the algae. In Phycology (pp. 3-30). Cambridge: Cambridge University Press.

Li-Beisson, Y., Thelen, J. J., Fedosejevs, E. & Harwood, J. L. (2019). The lipid biochemistry of eukaryotic algae. Progress in Lipid Research, 74, 31-68. http//doi.org/10.1016/j.plipres.2019.01.003.

Liu, X., Bogaert, K., Engelen, A. H., Leliaert, F., Roleda, M. Y. & De Clerck, O. (2017). Seaweed reproductive biology: environmental and genetic controls. Botanica Marina, 60, 89–108. http//doi.org/ 10.1515/bot-2016-0091.

Michalak, I., Chojnacka, K., Dmytryk, A., Wilk, R., Gramza, M., & Rój, E., (2016). Evaluation of supercritical extracts of algae as biostimulants of plant growth in field trials. Frontiers in Plant Science, 7 (1591), 1-11. https://doi.org/10.3389/fpls.2016.01591.

Moss, C. W., Lambert, M. A. & Merwin, W. H. (1974). Comparison of rapid methods for analysis of bacterial fatty acids. Journal of Applied Microbiology, 28, 80–85.

Pacheco, B. S., Dos Santos, M., Schultze, E., Martins, R. M., Lund, R. G., Seixas, F. K., Colepicolo, P., Collares, T., Paula, F. R. & De Pereira, C. (2018). Cytotoxic activity of fatty acids from Antarctic macroalgae on the growth of human breast cancer cells. Frontiers in Bioengineering and Biotechnology, 6, 1-10. http//doi.org/10.3389/fbioe.2018.00185.

Paiva, L., Lima, E., Patarra, R. F., Neto, A. I., & Baptista, J., (2014). Edible Azorean macroalgae as source of rich nutrients with impact on human health. Food Chemistry, 164, 128–135. https://doi.org/10.1016/j.foodchem.2014.04.119.

Nelson, D. L., Cox, M. M. & Lehninger A. L., (2013). Lehninger principles of biochemistry. (6 ed). New York: Ed. W.H. Freeman.

Rahelivao, M. P., Gruner, M., Andriamanantoanina, H., Andriamihaja, B., Bauer, I. & Knölker, H (2015). Red algae (Rhodophyta) from the coast of Madagascar: preliminary bioactivity studies and isolation of natural products. Marine Drugs, 13, 4197-4216. http//doi.org/10.3390/md13074197.

Santos, M. A. Z., Colepicolo, P., Pupo, D., Fujii, M. T., Pereira, C. M. P. & Mesko, M. F. (2017). Antarctic red macroalgae: a source of polyunsaturated fatty acids. Journal of Applied Phycology, 29(2), 759-767. https://doi.org/10.1007/s10811-016-1034-x.

Schmid, M., Kraft, L. G. K., van der Loos, L. M., Kraft, G. T., Virtue, P., Nichols, P. D., & Hurd, C. L. (2018). Southern Australian seaweeds: a promising resource for omega-3 fatty acids. Food Chemistry, 265, 70–77.

Seca, A. M. L., Gouveia, V. L. M., Barreto, M. C., Silva, M. A. S., & Pinto, D. C. G. A. (2018). Comparative study by GC-MS and chemometrics on the chemical and nutritional profile of *Fucus spiralis* L. juvenile and mature life-cycle phases. Journal of Applied Phycology, 30:2539–2548. https://doi.org/10.1007/s10811-018-1447-9.

Simopoulos, A. P. & De Meester, F. (eds) (2009). A Balanced omega-6/ omega-3 fatty acid ratio, cholesterol and coronary heart disease. *World* Review of *Nutrition* and Dietetics, Karger, 100, 1–21. https://doi.org/10.1159/000235706.

Tang, B. & Row, K. H. (2013). Development of gas chromatography analysis of fatty acids in marine organisms. Journal Chromatographic Science, 51, 599-607. http//doi.org/10.1093/chromsci/bmt005.

Tasende, M. G. (2000). Fatty acid and sterol composition of gamtophyte and sporophytes of *Chondrus crispus* (Gigartinacea Rhodophyta). Scientia Marina, 64(4):421 -426. http//doi.org/ 10.3989/scimar.2000.64n4421.

Vieira, E. F., Soares, C., Machado, S., Correia, M., Ramalhosa, M. J., Oliva-Telesa, M. T., Carvalho, A. P., Domingues, V. F., Antunes, F., Oliveira, T. A. C., Morais, S. & Delerue-Matos, C. (2018). Seaweeds from the Portuguese coast as a source of proteinaceous material: Total and free amino acid composition profile. Food Chemistry, 269, 264–275. https://doi.org/10.1016/j.foodchem.2018.06.145.

Vitova, M., Bisova, K., Kawano, S., & Zachleder, V. (2015). Accumulation of energy reserves in algae: from cell cycles to biotechnological applications. Biotechnology Advances, 33(6), 1204–1218. https://doi.org/10.1016/j.biotechadv.2015.04.012.

Zhu, S., Jiang, X., Jiang, S., Lin, G., Gong, J., Chen, W. & Chen, Y. Q. (2017). GPR120 is not required for ω-3 PUFAs-induced cell growth inhibition and apoptosis in breast cancer cells. Cell Biology International, 42(2), 180–186.

Capitulo 4 – Photosynthetic performance and pigment concentration of three Rhodophyta species in different development phases of the Magellan Region

Artigo submetido em Photosynthesis Research

05.04.2019

Photosynthetic performance and pigment concentration of three Rhodophyta species in different development phases of the Magellan Region

[1]Marco Aurélio Ziemann dos Santos*, [1]Lucas Moraes Berneira, [2]Andres Mansilla, [2] Fabio Mendez, [2]Silvia Murcia, [1]Claudio Martin Pereira de Pereira

[1] Center for Chemical, Pharmaceutical and Food Sciences, Federal University of Pelotas, University Campus, S / N - CEP 96160-000, Capão do Leão, RS – Brazil
[2] Laboratory of Antarctic and Sub-Antarctic Marine Ecosystems, University of Magallanes, 01855 Bulnes Ave., Punta Arenas 6200000. Instituto de Ecología y Biodiversidad (IEB), Chile

*Corresponding author: marcziemann@gmail.com
Telephone number: +55053981184936
ORCID: 0000-0002-3776-3701

Acknowledgements

This study had logistic support from the University of Magallanes and the Laboratory of Antarctic and Sub-Antarctic Marine Ecosystems - Instituto de Ecología y Biodiversidad (IEB), Chile. The authors are grateful for the financial and fellowship support from the Brazilian research funding agencies National Program for Post-Doctoral Studies - Coordination for Improvement of Higher Level Personnel (PNPD-CAPES - General Program of International Cooperation PGCI - 99999.002378/2015) and National Council for Scientific and Technological Development (CNPq).

Abstract

Studies on photosynthetic parameters and pigment in the development phases of Rodophytas are important in order to evaluate its evolution in the sub-Antarctic region. In this sense, the aims of this work was to investigate the concentration of pigments and the photosynthetic performance in the gametophytic, carposporophytic and tetrasporophytic phases of *Gigartina skottsbergii*, *Iridaea cordata* and *Mazzaella laminarioides* collected in the Magellan. Analysis of allophycocyanin

(APC), phycocyanin (PC), phycoerythrin (PE) and chlorophyll (Chl *a*) were performed in a spectrophotometer using 400 and 700 nm of length. For the analysis of photosynthetic performance, a Pulse Amplitude Modulated Fluorometer was used in eight increasing levels of irradiance. Results showed that *G. skottsbergii* had a maximum quantum yield that varied between 0.320 and 0.392 while *I. cordata* had 0.393 and 0.449 and *M. laminarioides* ranged from 0.357 and 0.516. Photosynthetic efficiency differed between 0.09 to 0.18 µmol e^- m^{-2} s^{-1}. µmol photons m^{-2} s^{-1} in *I. cordata* and *M. laminarioides*, respectively. Moreover, values of relative electron transfer rate and irradiance saturation reached, respectively, values between 8.05 to 33.68 µmol m^{-2} s^{-1} as well as 12.64 to 52.60 µmol photon m^{-2} s^{-1}. There were significant differences for APC in *G. skottsbergii* between 4.86 to 48.91 µg g^{-1} and in *M. laminarioides* from 4.04 to 58.94 µg g^{-1}. Variations for PC occured in *G. skottsbergii* and *M. laminarioides* reaching values of 4.48 to 27.01 µg g^{-1} and 2.92 to 25.77 µg g^{-1}, respectively. Therefore, there were significant differences in photosynthetic parameters and concentration of pigments in the development phases.

Key-words: Pulse Amplitude Modulated Fluorometer; Phycobiliproteins; Maximum Quantum Yield; Red Algae; Sub-Antarctic Region.

1. Introduction

Macroalgae comprehend complex groups of organisms that can be divided into three main phyla including Rhodophyta (red algae), Chlorophyta (green algae) and Ochrophyta (brown algae) according to their morphology and pigmentation. They have worldwide distribution occurring from temperate to tropical zones as well as in inhospitable places such as polar environments (Santos et al., 2017; Ocaranza-Barrera et al., 2018) The sub-Antarctic region is a biogeographic area comprising the southernmost landmass of the American continent known for its extreme environmental conditions that include, for instance, low temperatures, limited photoperiod in the winter and high exposure to ultraviolet light in the summer (Mansilla, Ojeda, 2012)

Marine algae are exposed to considerable environmental influences including high incidence of solar radiation mainly in the form of ultraviolet B (UVB) radiation (Bouchard, Roy & Campbell, 2006) acidification of oceans, rising sea temperatures,

melting of glaciers influencing the salinity of seas (Meredith et al., 2017) as well as the increased level of pollution in coastal regions (Mach et al., 2017).

Changes in abiotic parameters can cause considerable influences in the seaweeds affecting the biosynthesis of primary and secondary metabolites that are used by the organism as a mechanism of response to survive in the environment (Qian et al., 2014; Wang et al., 2019) Ambient factors are also closely related to the reproduction of macroalgae since this stage requires signals that vary according to environment conditions (Dobkowski, Flanagan, Nordstrom, 2019).

Red macroalgae have distinctive life cycles with three-phase generations that allowed these organisms to disperse through several marine habitats and to have an increased biological diversification. In this sense, red seaweeds can be found in upper intertidal to infralittoral zones and, thus, from rocks areas to great depths of sea. The places where these algae are fixated influence directly in their metabolism, as they can receive intense solar irradiation for long periods (Yoon et al., 2017). On the other side, they can be in zones with low or no incidence of solar irradiation at all, which also may influence on the physiological activity of these organisms (Marambio et al., 2017). These parameters, such as the habitat, also affect the structural part of the algae such as the photosynthetic membranes, which are responsible for receiving and distributing energy for the cells' interior metabolic transformations (Kalisch, Dörmann, Hölzl, 2016).

It is known that seaweeds have variable chemical compositions according to species, seasonality and habitat that should be observed at the moment of their harvest since previous studies showed that these variables are directly linked to the development and evolutionary cycle of seaweeds (Tasende, 2000; Khotimchenko, 2006). In this sense, the gametophytic, carposporophytic and tetrasporophytic phases influence the concentration of pigments and the photosynthetic performance of red macroalgae. Studies regarding these parameters in function of development phases are important means to understand the evolution of the species that occur in the sub-Antarctic region as well as to gather information that could further assist in the collection and sustainable cultivation of macroalgae for food consumption.

In this sense, the aim of this work was to evaluate differences in concentrations of pigment and the photosynthetic performance of gametophytic, carposporophytic and tetrasporophytic of red macroalgae *Gigartina skottsbergii* Setchell & N.L.Gardner, *Iridaea cordata* (Turner) Bory de Saint-Vincent and *Mazzaella laminarioides* (Bory) Fredericq collected in the Magellan region (Chile).

2. Materials and Methods

2.1 Sampling and Sample Preparation

Macroalgae *Gigartina skottsbergii* Setchell & N.L.Gardner, *Iridaea cordata* (Turner) Bory de Saint-Vincent and *Mazzaella laminarioides* (Bory) Fredericq of the Gigartinales order and Rhodophyta phylum were collected in the region of Punta Arenas (Chile) between January and April of 2017 in the gametophytic, carposporophytic and tetrasporophytic phases (Table 1). Specimens of *G. skottsbergii* were collected in Puerto del Hambre (53° 36S, 70° 55W) under diving at approximately 5 to 10 m of depth in the infralittoral zone. About 5 to 10 individuals of each development phase were retrieved from the collection site. Specimens from *I. cordata* and *M. laminarioides* were collected in San Juan (53° 43S, 70° 58W) in the medium and superior infralittoral zone, respectively. Approximately 10 individuals of each species and development phase were collected in the process. Subsequent to collection, macroalgae submerged in seawater were sent to the laboratory in coolers and conditioned in culture chambers with aeration for 24 h at 5 ± 1 °C, photosynthetically active radiation (PAR) level of 40 µmol photons m^{-2} s^{-1} and standard photoperiod of 12/12 h. Conditioning of macroalgae was made for further analysis of photosynthetic performance using a Pulse Amplitude Modulated Fluorometer (PAM). Pigment analysis was made afterwards conditioning period with samples that were introduced in dark bags at – 20 °C. For both photosynthetic performance and pigment analysis medium and margin portions of the fronds were used in the procedures. Information regarding collection site, species, development phases, geographical coordinates and morphological identification (Herbarium of Antarctic and Sub-Antarctic Marine Ecosystems Laboratory – LEMAS) are indicated at Table 1.

Table 1 – Collection data, development phase, place location, marine zonation and herbarium number of red macroalgae collected in the Magellan Region, Chile (2017)

Species	Development Phase	Collection Location	Marine Zonation	Herbarium Number
G. skottsbergii	Gametophytic	Puerto del Hambre	INLT	1303r
	Carposporophytic	Puerto del Hambre	INLT	1301r
	Tetrasporophytic	Puerto del Hambre	INLT	1302r
I. cordata	Gametophytic	San Juan	MINT	1307r

	Carposporophytic	San Juan	MINT	1308r
	Tetrasporophytic	San Juan	MINT	1306r
M. laminarioides	Gametophytic	San Juan	HINT	1298r
	Carposporophytic	San Juan	HINT	1299r
	Tetrasporophytic	San Juan	HINT	1300r

Infralittoral Zone – INLT; Higher Intertidal Zone (HINT); Middle Intertidal Zone (MINT); San Juan (53° 43S - 70° 58W); Puerto del Hambre (53° 36S - 70° 55W).

2.2 Pigment Analysis

Briefly, 300 mg of fresh algal biomass was macerated using liquid nitrogen until finely grounded. The samples were diluted in 4 mL of phosphate buffer 50 mM (pH 5.5) at 4 °C. The resulting solution was centrifuged (Genesys 10) for 20 min at 10.000 rpm (~ 4 °C) and the upper layer was used for the analysis of allophycocyanin (APC), phycocyanin (PC) and phycoerythrin (PE). The residual material was diluted in 4 mL of acetone, centrifuged for 10 min at 12.000 rpm (~ 4 °C) and used for the analysis of chlorophyll (Chl *a*). Samples were analyzed at 400 to 700 nm of wavelength using a Spectrophotometer (Hewlett Packard - 8452A). Concentrations of phycobiliprotein (PBP) and chlorophyll *a* (Chl *a*) were quantified following the equations of Kursar et al. (1983) for phycobiliproteins (Eq. 1-3) and Jeffrey e Humphrey (1975) for Chl *a* (Eq. 4).

Allophycocyanin

$$APC = 181.3\,x\,A651 - 22.3\,x\,A614 \quad \textbf{(1)}$$

Phycocyanin

$$PC = 151{,}1\,x\,A614 - 99{,}1\,x\,A651 \quad \textbf{(2)}$$

Phycoerythrin

$$PE = 155.8\,x\,A498{,}5 - 40.0\,x\,A614 - 10.5\,x\,A651 \quad \textbf{(3)}$$

Chlorophyll *a*

$$Chl\ a = 11.85\,x\,A664 - 1.54\,A647 - 0.08\,x\,A630 \quad \textbf{(4)}$$

2.3 Photosynthetic performance

Photosynthetic performance was made in fronds of each development phase (gametophytic, carposporophytic and tetrasporophytic stages) of macroalgae after

acclimation period of 24 h. For the procedure, approximately 7 individuals in each development phase (*n* =7) were analyzed, where *n* is the number of independent samples. Analysis were made in an Pulse Amplitude Modulated Fluorometer - DivingPAM (Walz GmbH, Alemanha). Samples were subjected to rapid light response curves (LCR) at eight increasing levels of irradiance of actinic light (E: 0 - 490 µmol photons m^{-2} s^{-1}) at intervals of 30 s after each analysis in order to measure light response curves (White and Critchley, 1999) and saturation flash (0.8 s; ≥ 9000 µmol photons m^{-2} s^{-1}) (Marambio et al., 2017). Before analysis of LCR, a dark leaf clip (DIVING-LC) was used to maintain the frond in the dark for a period of 20 min without actinic light in order to obtain estimates of F_0 e F_m (Ralph, Gademann, 2005; Wong et al., 2015). Analysis of the spectral composition of subaquatic irradiances could not be measure at the moment of collection so that the data used in the current work were obtained from the previous studies conducted by Rautenberger et al. (2009) and Rautenberger and Bischof (2016).

Adaptation to the dark allowed the determination of maximum photochemical efficiency using Eq. 5, where F_0 is the minimum fluorescence after acclimation to the dark and F_m is the maximum fluorescence after sample saturation by flashes after acclimation to the dark (Maxwell and Johnson 2000).

$$Fv\ /\ Fm\ =\ (Fm\ -\ F0)\ /\ Fm \quad \textbf{(5)}$$

The effective photochemical efficiency under actinic light (ΦPSII) was determined using Eq. 6, where F_m' is the maximum yield o fluorescence under actinic light and *F* is the yield of fluorescence under actinic light.

$$\Phi PSII\ =\ (\ F'm\ -\ F\ )\ /\ F'm \quad \textbf{(6)}$$

The relative electron transfer rate (rETR) at each light intensity was calculated using Eq. 7, where PAR is the produced irradiance by actinic light and ΦPSII represents the effective photochemical efficiency under actinic light (Ralph, Gademann, 2005).

$$rETR\ =\ \Phi PSII\ x\ PAR \quad \textbf{(7)}$$

Results obtained by LCR at eight levels of irradiance under actinic light were adjusted according to Platt et al. (1980) (Eq. 8) in order to determine the parameters of photosynthetic efficiency (*α*), photoinhibition (*β*), irradiance saturation (E_k) and relative maximum electron transfer rate ($rETR_{max}$). Results were processed using the software Kaleida Graph 4.0 (Synergy Software 1986–2005) in order to analyze the results of photosynthetic performance.

$$PB(I) = [1 - exp(-\alpha I / Ps)\, exp(-\beta I / Ps) \quad \textbf{(8)}$$

Where according to the model of Platt et al. (1980), $P^B(I)$ represents the photosynthetic rate at irradiance *I*; P_s – light saturated photosynthetic rate in the absence of photoinhibition; *α* - initial slope of the *P-I* curve; *β* = an index of photoinhibition.

3. Statistical Analysis

Evaluation of the results regarding pigment concentration, photosynthetic parameters between the phases of development was performed applying two-way ANOVA. For univariate variables such as F_v/F_m one-way ANOVA was used. After ANOVA, Tukey's HSD post hoc analysis of means was used to analyze differences among the results and to assess significant differences at a confidence interval of 95% (p<0.05). All statistical analyses were performed using GraphPad Prism 7 software (Version 2017-02, USA).

4. Results

Specimens of *G. skottsbergii*, *I. cordata* and *M. laminarioides* in their gametophytic, carposporophytic and tetrasporophytic phases were retrieved in near collection sites between January and April in order to reduce differences that could be caused by abiotic parameters. Results (Table 2) showed that photosynthetic performance had significant differences (< 0.05; ANOVA Tukey's HSD) for E_k between gametophytic and trasporophytic phases for *I. cordata* and between carposporophytic and tetrasporophytic phases for *I. cordata* and *M. laminarioides*. Parameters including E_k,, *α* and $rETR_{max}$ had similar variations among the results of *I. cordat* and *M.*

laminarioides having increased concentrations in the tetrasporophytic ($rETR_{max}$) and carposporophytic phase (E_k) to *I. cordata* and carposporophytic (E_k) and gametophytic phase ($rETR_{max}$) to *M. laminarioides* in than the other life cycles. On the other hand, *I. cordata* had a distinct behavior for these parameters having lower concentrations in the carposporophytic and tetrasporophytic phase. Photosynthetic efficiency varied between 0.09 ± 0.01 a 0.18 ± 0.03 µmol e^- m^{-2} s^{-1}. µmol photons m^{-2} s^{-1} in *I. cordata* (tetrasporophytic phase) and *M. laminarioides* (carposporophytic phase), respectively. Values of $rETR_{max}$ and E_k fluctuated respectively from 8.05 ± 0.94 to 33.68 ± 2.70 µmol m^{-2} s^{-1} as well as from 12.64 ± 1.06 to 52.60 ± 23.62 µmol photon m^{-2} s^{-1} for *G. skottsbergii* and *M. laminarioides*.

Results for maximum quantum yield of PSII (*Fv/Fm*) can be observed in Figure 1 and indicated that the tetrasporophytic phase had the lowest amounts in the analyzed specimens. For *G. skottsbergii* results varied from 0.320 ± 0.02 (tetrasporophytic phase) to 0.392 ± 0.03 (gametophytic phase), *I. cordata* had values of 0.393 ± 0.02 (tetrasporophytic phase) and 0.449 ± 0.07 (carposporophytic phase) while *M. laminarioides* had 0.357 ± 0.06 (tetrasporophytic phase) and 0.516 ± 0.04 (carposporophytic phase). Significant variations occurred in *M. laminarioides* between the gametophytic and carposporophytic phase compared to the tetrasporophytic stage (< 0.05; ANOVA Tukey's HSD) (Figure 1).

Regarding phycobiliproteins (PBPs), samples had significant differences mainly to allophycocyanin (APC) as it can be observed variations in *G. skottsbergii* of 48.65 ± 5.09 and 489.12 ± 44.25 µg g^{-1} DW as well as in *M. laminarioides* of 40.45 ± 5.45 and 589.44 ± 73.21 µg g^{-1} DW (Fig. 2a). The pigment phycocyanin (PC) also had significant variations for *G. skottsbergii* and *M. laminarioides* having values of 44.89 ± 2.13 and 270.13 ± 19.28 µg g^{-1} DW as well as 29.24 ± 5.61 and 257.70 ± 34.49 µg g^{-1} DW, respectively (Fig. 2b). Phycoerythrin (PE) varied significantly in the three specimens as *G. skottsbergii* had results of 142.35 ± 7.85 and 1467.23 ± 20.32 µg g^{-1} DW, *M. laminarioides* had values of 146.17 ± 53.67 and 739.32 ± 103.53 µg g^{-1} DW and *I. cordata* had 162.24 ± 23.73 and 356.93 ± 103.42 µg g^{-1} DW (Fig. 2c). Chlorophyll *a* (Chl *a*) did not have significant variations in the analyzed specimens (Fig. 2 d).

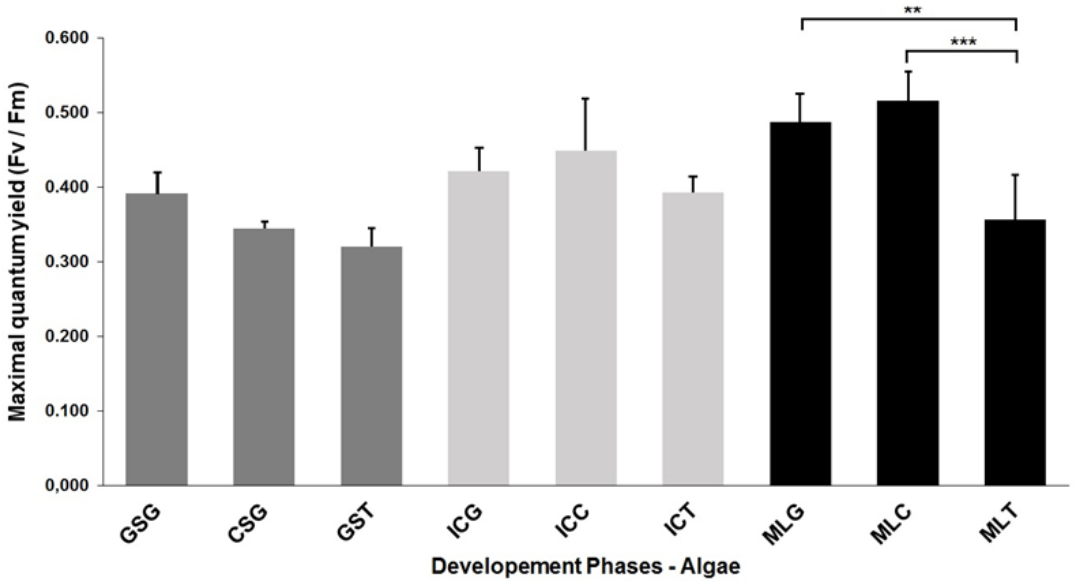

Figure 1 - Maximum quantum yield of PSII (*Fv/Fm*) of species *Gigartina skottsbergii* gametophytic (*GSG*), carposporophytic (*GSC*) and tetrasporophytic (*GST*); *Iridaea cordata* gametophytic (*ICG*), carposporophytic (*ICC*) and tetrasporophytic (*ICT*); *Mazaella laminarioides* gametophytic (*MLG*), carposporophytic (*MLC*) and tetrasporophytic (*MLT*); Values without a common superscript in the same species are significantly different (< 0.05 One-way ANOVA; Tukey's HSD).

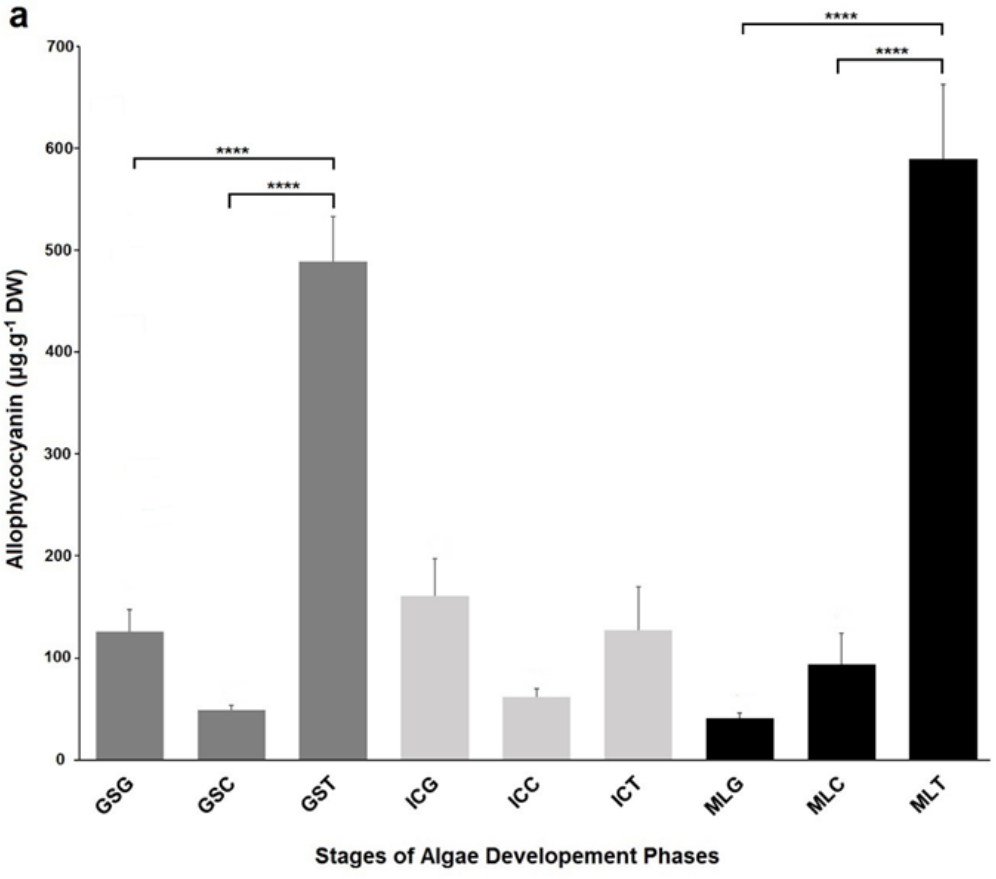

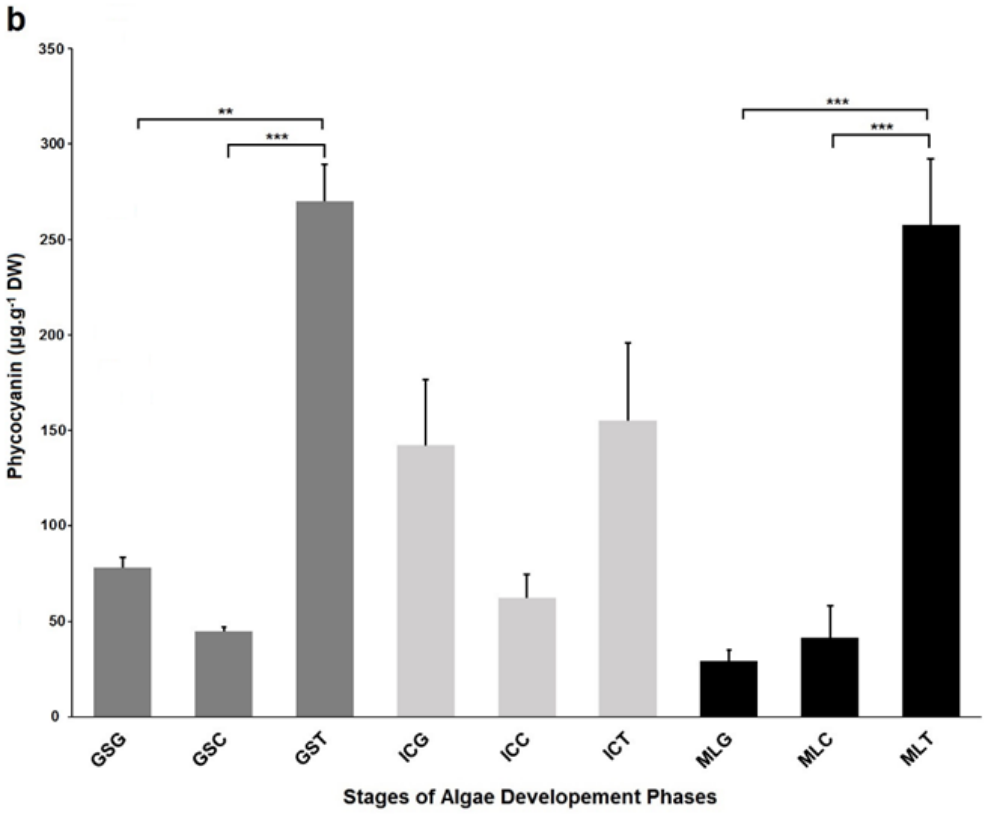
b
Phycocyanin (µg.g-1 DW)
350
300
250
200
150
100
50
0
**
***
***
***
GSG
GSC
GST
ICG
ICC
ICT
MLG
MLC
MLT
Stages of Algae Developement Phases

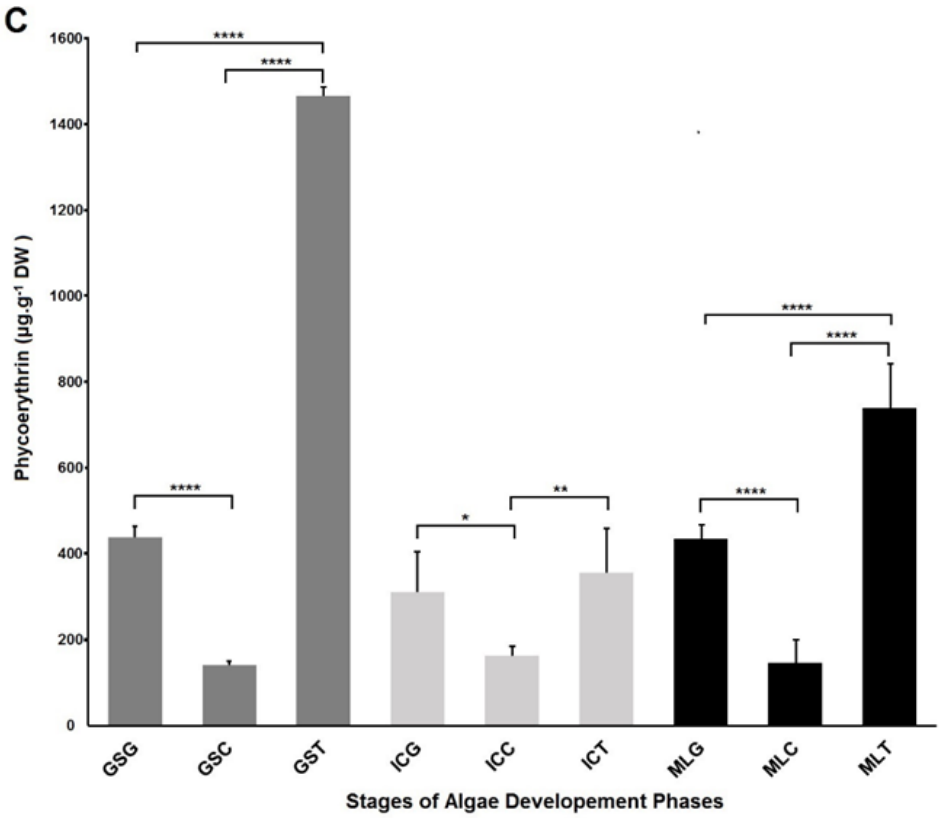
C
Phycoerythrin (µg.g-1 DW)
1600
1400
1200
1000
800
600
400
200
0
****
****
****
*
**
****
****
****
GSG
GSC
GST
ICG
ICC
ICT
MLG
MLC
MLT
Stages of Algae Developement Phases

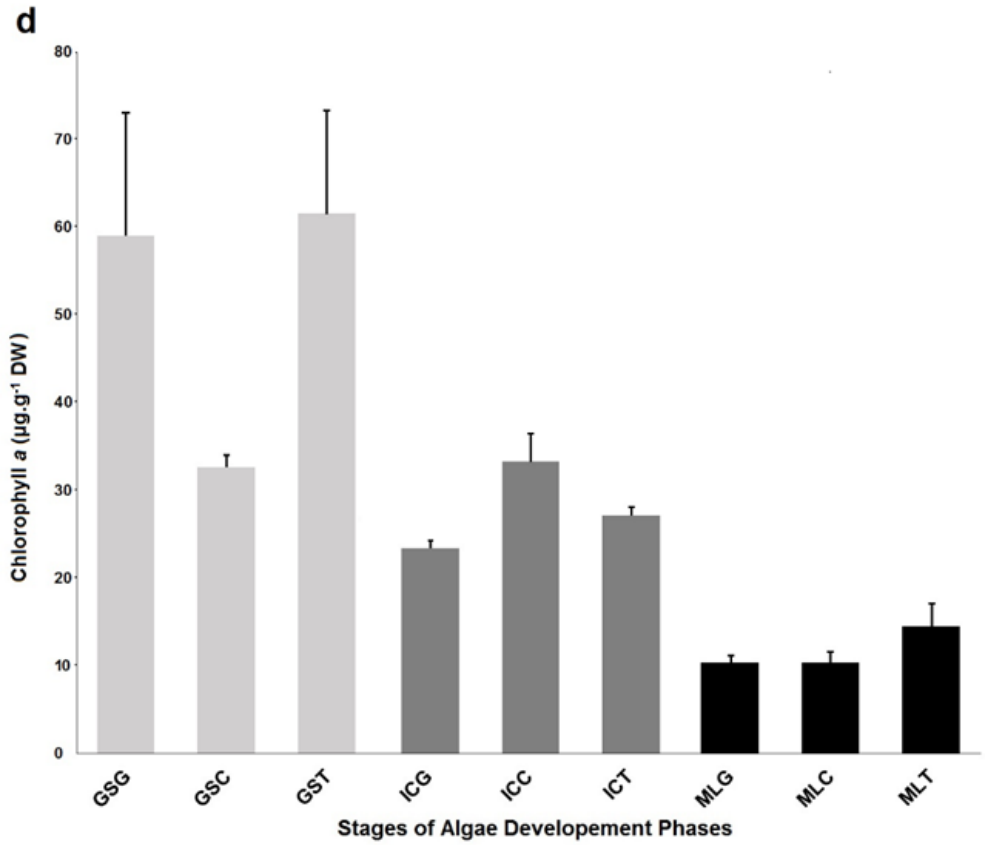

Figure 2- Concentration of chlorophyll (Chl *a*), allophycocyanin (APC), phycocyanin (PC) and phycoerythrin (PE); Pigment concentration in µg g^{-1} DW; *Gigartina skottsbergii* gametophytic (*GSG*), carposporophytic (*GSC*) and tetrasporophytic (*GST*); *Iridaea cordata* gametophytic (*ICG*), carposporophytic (*ICC*) and tetrasporophytic (*ICT*); *Mazaella laminarioides* gametophytic (*MLG*), carposporophytic (*MLC*) and tetrasporophytic (*MLT*). Values without a common superscript in the same species are significantly different (< 0.05 Two-way ANOVA; Tukey's HSD).

As it can be observed, there were significant differences in the ratios of APC/Chl *a*, PE/Chl *a*, PE/PC as well as PE/APC mainly in the development phases *M. laminarioides* which did not occur significantly in the PE/Chl *a* and PC/APC ratio. For *G. skottsbergii* there were significant differences between PE/Chl *a*, however APC/Chl *a*, PC/Chl *a*, PE/PC, PE/ACP and PC/APC ratios did not have singificant variations in the development phases. Concerning *I. cordata* did not occur significantly variations. Ratios of PBP/ Chl *a* had the highest results in the reaching as much as 42.53 ± 9.26 and 53.22 ± 12.14 for tetrasporophytic phases of *M. laminarioides* and 6.05 ± 1.21 in *I. cordata* (gametophytic phase). For PBP/PBP the highest results were 15.89 ± 3.77 and 11.15 ± 2.14 for *M. laminarioides* (gametophytic phase) and 1.24 ± 0.08 in *I. cordata* (tetrasporophytic phase) (Table 2).

Table 2 – Pigment ratios APC/Chl *a*, PC/Chl *a*, PE/Chl *a*, PE/PC, and PC/APC of *G. skottsbergii*, *I. cordata* and *M. laminarioides* in gametophytic, carposporophytic and tetrasporophytic phases

Species	APC/Chl *a*	PE/ Chl *a*	PC/ Chl *a*	PE/PC	PE/APC	PC/APC
G. skottsbergii gametophytic	2.16 ± 0.11^{a}	7.88 ± 1.43^{a}	1.41 ± 0.31^{a}	5.64 ± 0.29^{a}	3.63 ± 0.49^{a}	0.64 ± 0.11^{a}
G. skottsbergii carposporophytic	1.49 ± 0.10^{a}	4.36 ± 0.16^{a}	1.37 ± 0.06^{a}	3.17 ± 0.06^{a}	2.96 ± 0.33^{a}	0.93 ± 0.10^{a}
G. skottsbergii tetrasporophytic	8.28 ± 1.77^{a}	54.75 ± 4.04^{b}	4.53 ± 0.73^{a}	5.46 ± 0.33^{a}	3.03 ± 0.25^{a}	0.55 ± 0.02^{a}
I. cordata gametophytic	6.85 ± 1.41^{a}	13.24 ± 3.38^{a}	6.05 ± 1.21^{a}	2.15 ± 0.11^{a}	2.01 ± 0.33^{a}	0.92 ± 0.21^{a}
I. cordata carposporophytic	1.86 ± 0.21^{a}	4.85 ± 0.26^{a}	1.86 ± 0.21^{a}	2.64 ± 0.16^{a}	2.65 ± 0.39^{a}	1.01 ± 0.17^{a}
I. cordata tetrasporophytic	4.64 ± 1.38^{a}	13.07 ± 3.26^{a}	5.68 ± 1.27^{a}	2.30 ± 0.12^{a}	2.85 ± 0.12^{a}	1.24 ± 0.08^{a}
M. laminarioides gametophytic	3.89 ± 0.23^{a}	42.72 ± 6.32^{a}	0.07 ± 0.01^{a}	15.89 ± 3.77^{a}	11.15 ± 2.14^{a}	0.73 ± 0.10^{a}
M. laminarioides carposporophytic	8.84 ± 2.43^{a}	13.71 ± 3.22^{b}	0.28 ± 0.01^{a}	3.57 ± 0.11^{b}	1.60 ± 0.21^{b}	0.44 ± 0.06^{a}
M. laminarioides tetrasporophytic	42.53 ± 9.26^{b}	53.22 ± 12.14^{a}	0.35 ± 0.01^{a}	2.86 ± 0.06^{b}	1.24 ± 0.03^{b}	0.43 ± 0.00^{a}

Mean value ± SD (where SD is standard deviation); (n = 3) where *n* is number of independent samples. Values without a common superscript in the same species are significantly different (< 0.05 Two-way ANOVA; Tukey's HSD)

5. Discussion

In the current study photosynthetic performance and concentration of pigments were evaluated in function of development phases and their possible variations as a result of their habitat. Based on the obtained results, it can be observed that *G. skottsbergii* had the lowest values for F_v/F_m reaching 0.320 ± 0.02 (tetrasporophytic phase) and 0.392 ± 0.03 (gametophytic phase), which is characteristic of macroalgae adapted to low light environments (Wu et al. al. 2015). In the Magellan region, this seaweed is usually found in depths close to 10 m and lives in the understory formed by the canopy of *Macrocystis pyrifera* receiving little solar radiation. These habitat characteristic and reproductive stage possibly influenced F_v/F_m to lower values than the reported in the literature (Roleda et al., 2008; Navarro, Huovinen, Gómez, 2016).

Specimens of *M. laminarioides* had results of F_v/F_m with significant differences between 0.357 and 0.516 according to the development phase, which was similar to the results found by Varela et al. (2006) for the same species collected in central Chile (Maitencillo and Pucatrihue) in the gametophytes and sporophytes phases. The values of F_v/F_m in summer (January) averaged between 0.400 and 0.600 indicating that photosynthetic performance is directly related to the reproduction phase of seaweeds as well as to daily fluctuations of abiotic parameters in the upper and lower intertidal zones.

Navarro et al. (2016) and Zacher et al. (2009) carried out works with reproductive cells of *I. cordata* reporting results for F_v/F_m in tetraspores of 0.380 ± 0.03 and 0.470 ± 0.04. These values corroborate with the results described in our study that reached 0.422 ± 0.03 (gametophytic phase), 0.449 ± 0.07 (carposporophytic phase) and 0.393 ± 0.02 in (tetrasporophytic phase). According to Navarro et al. (2016), results of the reproductive cells of *I. cordata* differ in their photosynthetic performance, which can be mainly associated to the photosynthetic characteristics of each species, although other facts such as type of reproductive cell, size and mobility also affect the results that express characteristics of species found in the coast.

Photosynthetic performance of *G. skottsbergii* did not have significant differences among development phases for the parameters of $rETR_{max}$, (α) and E_k. Given the results found for F_v/F_m it can be observed that the three life cycles had an adaptation to shading zones. According to Wiencke et al. (2007), macroalgae that inhabit regions below 10 m of depth and have low E_k (<40 µmol photons m^{-2} s^{-1}) are adapted to high

degrees of shading independently to their taxonomical classification. Previous reports in the literature show similar values for $rETR_{max}$ and (α) but higher values to E_k. Analyzing the gametophytic phase of *G. skottsbergii* collected in Puerto del Hambre (Chile) in the summer, Marambio et al (2016) found values of 7.11 ± 1.26 µmol e^{-1} m^{-2} s^{-1} for ^{rETRmax}, 0.16 ± 0.03 µmol e^{-1} m^{-2} s^{-1}. µmol photons m^{-2} s^{-1} for (α) and 48.12 ±13.68 µmol photons m^{-2} s^{-1} for E_k. Moreover, Navarro et al. (2016) and Roleda et al. (2008) reported respectively values of 27.0 ± 9.0 and 54.0 ± 2.0 µmol $e^{-1}m^{-2}$ s^{-1} ($rETR_{max}$); 7.0 ± 2.0 and 6.87 ± 0.18 µmol photons m^{-2} s^{-1} for E_k and 0.27 ± 0.05 and 0.14 ± 0.00 µmol e^{-1} m^{-2} s^{-1}. µmol photons m^{-2} s^{-1} for (α) in carpospores.

According to the obtained results, specimens *I. cordata* and *M. laminarioides* were adapted to higher incidences of solar irradiance. Both species were retrieved in the collection site having the same characteristics of habitat and environmental stress regarding abiotic parameters. In this sense, macroalgae *I. cordata* and *M. laminarioides had* significant differences in the three development phases for E_k having lower values in the tetrasporophytic phase and higher results in the carposporophytic and gametophytic phase, respectively. Weykam, Thomas and Wiencke (1997), analyzing *I. cordata* and *Palmaria decipiens*, showed considerable variations for E_k and (α) when macroalgae were exposed to 6 months of dark and 6 months of light. Fluctuations in these parameters showed that *P. decipiens* was not adapted to rapid changes in luminosity while *I. cordata* maintained the photosynthetic apparatus functioning throughout light/dark periods. Independently to belonging to the same phyla, both species had distinct adaptive characteristics to changes in light conditions. Summarizing, despite belonging to the ecologic niche, *I. cordata* and *M. laminarioides* had distinct results for photosynthetic performance indicating that seaweeds had differentiated adaptations to ambient stress.

Gómez et al. (2004) studied 18 species collected in the platform of Niebla near Valdivia (Chile) and had results for $rETR_{max}$ between 11.4 ± 2.3 and 80.9 ± 10.4 µmol $e^{-1}m^{-2}$ s^{-1} and for (α) of 0.13 ± 0.03 and 0.34 ± 0.03 µmol e^{-1} m^{-2} s^{-1}. µmol photons m^{-2} s^{-1} that agree with results found in the current work for *I. cordata* and *M. laminarioides*. Regarding E_k, results for *M. laminarioides* ranged from 237.2 ± 73.8 µmol photons m^{-2} s^{-1} (Gómez et al. (2004) which were above the values reported in the current work that were 25.93 ± 3.52 and 52.60 ± 23.62 µmol m^{-2} s^{-1}.

Evaluation of pigments indicated that *G. skottsbergii* had higher concentrations of Chl *a* compared to the other specimens. These results agree with

previous reports if the literature showing that macroalgae that inhabit shaded environments have improved photosynthetic apparatus. In this sense, increased concentrations of chlorophyll are required in order to enhance the capture of solar radiation and convert the absorbed energy for growth mechanisms but not to repair damages in the photosystem (Huovinen, Gómez, 2013).

The results demonstrated that an increase in PBPs concentrations in the tetrasporophytic phase can be associated to responses to environmental stress or to the differentiation in the metabolism of these organisms in the reproductive phase. The PBPs act as storage proteins and are used in the biosynthesis of compounds during adaptive processes (Kumar et al., 2010) or serving as nitrogen reserve (Rai, 1990). According to Zubia, Freile-Pelegrín & Robledo (2014), high concentrations of nitrogen assist seaweeds to maintain their integrity against radiation stress and increase their antioxidant defenses. This antioxidant action is mainly due to its ability of PBP to neutralize reactive oxidants (Kumar et al., 2011).

The concentration of PE in relation to the other pigments was significant in the studied samples and their development phases, mainly in *G. skottsbergii*, which had values in its tetrasporophytic phase twice the found in *I. cordata* and in *M. laminarioides*. Organisms that inhabit infralittoral regions such as *G. skottsbergii* (depths >10 m) may have high concentrations of PE since PBP is used to absorb radiation in the blue and green spectrum (Hamid et al., 2015). According to Navarro, Mansilla & Plastino (2010), PE and PC have the ability to favor the acclimatization of phycobilisomas during prolonged periods of solar radiation. Higher levels of PE and PC can be observed as a process of acclimation in the species *I. cordata* that inhabit the lower infralittoral zone, however more expressive results were found for *M. laminarioides* that were exposed to long periods of solar irradiation in the upper infralittoral zone.

Results of the ratios between PBP indicate changes in the concentration of phycobilisomes (PBS) or in the algae antenna system. It can be observed that the PC/APC ratio had a small increase among the studied macroalgae, although not significantly, showing that the developmental phases did not influence this PBP ratio. According to Loder, Knoetzel, Wieneke (2001) that analyzed acclimation responses of photosynthesis in *Palmaria decipiens*, the PC/APC is associated to the number of stems of PBP while PE/PC and PE/APC are related to the sizes of the stems in PBP. Ratios regarding PBP/Chl *a* and PBP/PBP indicated variations among the

development phases of the sub-Antarctic red macroalgae with significance differences mainly in *M. laminarioides*. We believe that the results are related to environmental stress, already described in other studies, as well as to the metabolic modifications in seaweeds due their reproductive stage.

6. Conclusions

Analysis of pigments and photosynthetic parameters indicated that *I. cordata* and *M. laminarioides* which are found in the upper and middle infralittoral zone were adapted to solar radiation during tidal changes while *G. skottsbergii* found in the infralittoral zone was adapted to areas of low brightness. The results showed that differences in photosynthetic parameters and pigment concentration were closely related to development phases, algal species and to environmental factors such as habitat, cyclic sea level changes and solar radiation.

Conflict of Interest: The authors declare that they have no conflict of interest.

7. References

Bouchard JN, Roy S, Campbell DA (2006) UVB Effects on the Photosystem II-D1 Protein of Phytoplankton and Natural Phytoplankton Communities. Photochem Photobiol, 82(4):936-951.

Dobkowski KA, Flanagan KD, Nordstrom JR (2019) Factors influencing recruitment and appearance of bull kelp, Nereocystis luetkeana (phylum Ochrophyta). J Phycol, 55:236-244.

Gómez I, López-Figueroa F, Ulloa N, Morales V, Lovengreen C, Huovinen P, Hess S (2004) Patterns of photosynthesis in 18 species of intertidal macroalgae from southern Chile. Mar Ecol Prog Ser, 270:103-116.

Hamid N, Ma Q, Boulom S, Liu T, Zheng Z, Balbas J, Robertson J (2015) In: Tiwari BK, Troy DJ (Eds). Seaweed minor constituents. Seaweed Sustainability: Food and Non-Food Applications. Cambridge, Massachusetts, pp193–242.

Huovinen P, Gómez I (2013) Photosynthetic characteristics and UV stress tolerance of Antarctic seaweeds along the depth gradiente. Polar Biol, 36:1319–1332.

Jeffrey SW, Humphrey GF (1975) New spectrophotometric equations for determining chlorophylls *a*, *b*, *c1* and *c2* in higher plants, algae and natural phytoplankton. Biochem Physiol Pflanz, 167:191–194.

Kalisch B, Dörmann P, Hölzl G (2016) DGDG and Glycolipids in Plants and Algae. In: Nakamura Y, Li-Beisson Y (eds) Lipids in Plant and Algae Development. Subcellular Biochemistry, v 86. Springer, Cham.

Han SV (2006) Variations in lipid composition among diferente developmental stages of *Gracilaria verrucosa* (Rhodophyta). Bot Mar, 49:34–38.

Kumar M, Kumari P, Gupta V, Reddy CRK, Jha B (2010) Biochemical responses of red alga *Gracilaria corticata* (Gracilariales, Rhodophyta) to salinity induced oxidative stress. J Exp Mar Biol Ecol, 391:27–34.

Kumar M, Gupta V, Trivedi N, Kumari P, Bijo AJ, Reddy CRK, Jha, B (2011). Desiccation induced oxidative stress and its biochemical responses in intertidal red alga *Gracilaria corticata* (Gracilariales, Rhodophyta). Environ Exp Bot, 72:194–201.

Kursar TA, van der Meer JP, Aberte RS (1983) Light harvesting system of the red alga *Gracilaria tikvahiae*. I. Biochemical analyses of pigment mutations. Plant Physiol, 73:353–360.

Loder UH, Knoetzel J, Wieneke C (2001) Acclimation of photosynthesis and pigments to seasonally changing light conditions in the endemic Antarctic red macroalga *Palmaria decipiens.* Polar Biol, 24:598-603.

Mach PM, Winfield JL, Aguilar R A, Wright KC, Verbeck GF (2017) A portable mass spectrometer study targeting anthropogenic contaminants in Sub-Antarctic Puerto Williams, Chile. Int J Mass Spectrom, 422:148–153.

Mansilla A, Ojeda J, Rozzi R (2012) Cambio climático global en el contexto de la Ecoregión subantártica de Magallanes y la reserva de biosfera Cabo de Hornos. Ann Inst de la Pat Ser Cs Nat, 40:69–76.

Marambio J, Mendez F, Ocaranza P, Rodriguez JP, Rosenfeld S, Ojeda J, Murcia S, Terrados J, Bischof K, Mansilla A (2016) Seasonal variations of the photosynthetic activity and pigment concentrations in different reproductive phases of *Gigartina skottsbergii* (Rhodophyta, Gigartinales) in the Magellan region, sub-Antarctic Chile. J Appl Phycol, 29:721-729.

Marambio J, Rodriguez JP, Mendez F, Ocaranza P, Rosenfeld S, Ojeda J, Rautenberger R, Bischof K, Terrados J, Mansilla A (2017) Photosynthetic performance and pigment composition of *Macrocystis pyrifera* (Laminariales, Phaeophyceae) along

a gradient of depth and seasonality in the ecoregion of Magellan, Chile. J Appl Phycol, 29(5):2575-2585.

Maxwell K, Johnson N (2000) Chlorophyll Fluorescence - A Pratical Guide. J Exp Bot, 354:659-668

Meredith MP, Stammerjohn SE, Venables HJ, Ducklow HW, Martinson DG, Iannuzzi, Leng MJ, van Wessem JM, Reijmer CH, Barrand NE (2017) Changing distributions of sea ice melt and meteoric water west of the Antarctic Peninsula. Deep Sea Res Pt II: Top Stud Oceanogr, 139:0–57.

Navarro NP, Mansilla A, Plastino EM (2010) *Iridaea cordata* (Gigartinales, Rhodophyta): responses to artificial UVB radiation. J Appl Phycol, 22:385–394.

Navarro NP, Huovinen P, Gómez I (2016) Stress tolerance of Antarctic macroalgae in the early life stages. Rev Chil Hist Nat, 89:1-9.

Ocaranza-Barrera P, González-Wevar CA, Guillemin ML, Rosenfeld S, Mansilla A (2018) Molecular divergence between *Iridaea cordata* (Turner) Bory de Saint-Vincent from the Antarctic Peninsula and the Magellan Region. Journal of Applied Phycology. 1-11. http//doi.org/10.1007/s10811-018-1656-2.

Platt T, Gallegos CL, Harrison WG (1980) Photoinhibition of photosynthesis in natural assemblages of marine phytoplankton. J Mar Res, 38:687–701.

Qian F, Luo Q, Yang R, Zhu Z, Chen H, Yan X (2014) The littoral red alga *Pyropia haitanensis* uses rapid accumulation of floridoside as the desiccation acclimation strategy. J Appl Phycol, 27(1):621–632.

Ralph PJ, Gademann R (2005) Rapid light curves: a powerful tool to assess photosynthetic activity. Aquat Bot, 82(3):222–237.

Rautenberger R, Mansilla A, Gómez I, Wiencke C, Bischof K (2009) Photosynthetic responses to UV-radiation of intertidal macroalgae from the Strait of Magellan (Chile). Rev Chil Hist Nat, 82(1):43-61.

Rautenberger R, Bischof K (2016) Dynamic summer solar radiation in Antarctic coastal ecosystems and its effects on photosyn thesis of the endemic Antarctic brown macroalga *Desmarestia menziesii* (Phaeophyceae). Algological Studies, 151(1):123–150.

Roleda MY, Zacher K, Wulff A, Hanelt D, Wiencke C (2008) Susceptibility of spores of different ploidy levels from Antarctic *Gigartina skottsbergii* (Gigartinales, Rhodophyta) to ultraviolet radiation. Phycologia, 47:361–370.

Santos MAZ, Colepicolo P, Pupo D, Fujii MT, Pereira CMP, Mesko MF (2017) Antarctic red macroalgae: a source of polyunsaturated fatty acids. J Appl Phycol, 29(2):759-767.

Tasende MG (2000) Fatty acid and sterol composition of gamtophyte and sporophytes of *Chondrus crispus* (Gigartinacea Rhodophyta). Sci Mar, 64(4):421-426.

Varela DA, Santelices B, Correa JÁ, Arroyo MK (2006) Spatial and temporal variation of photosynthesis in intertidal *Mazzaella laminarioides* (Bory) Fredericq (Rhodophyta, Gigartinales). J Appl Phycol, 18:827-838.

Wang WJ, Li XL, Zhu JY, Liang ZR, Liu FL, Sun XT, Wang FJ, Gen Shen Z (2019) Antioxidant response to salinity stress in freshwater and marine Bangia (Bangiales,Rhodophyta). Aquatic Botany, 154:35-41.

Weykam G, Thomas DN, Wiencke C (1997) Growth and photosynthesis of the Antarctic red algae *Palmaria decipiens* (Palmariales) and *Iridaea cordata* (Gigartinales) during and following extended periods of darkness. Phycologia, 36:395-405.

Wiencke C, Clayton M, Gómez I, Iken K, Lu¨ der UH, Amsler CD, Karsten U, Hanelt D, Bischof K, Dunton K (2007) Life strategy, ecophysiology and ecology of seaweeds in polar Waters. Rev Environ Sci Biotechnol, 6:95-126.

Wong CY, Teoh ML, Phang SM, Lim PE, Beardall J (2015) Interactive effects of temperature and UV radiation on photosynthesis of *Chlorella* strains from polar, temperate and tropical environments: differential impacts on damage and repair. PLoS One 10(10): e0139469. https://doi.org/10.1371/journal.pone.0139469

Wu H, Jiang H, Liu C, Deng Y (2015) Growth, pigment composition, chlorophyll fluorescence and antioxidante defenses in the red alga *Gracilaria lemaneiformis* (Gracilariales, Rhodophyta) under light stress. S Afr J Bot, 100:27-32.

Rai AN (1990) Handbook of symbiotic cyanobacteria. CRC Press, Boca Raton, Florida, USA.

Yoon HS, Nelson W, Lindstrom SC, Boo SM, Pueschel C, Qiu H, Bhattacharya D (2017) Rhodophyta. In: Archibald J, Simpson A, Slamovits C (eds) Handbook of the Protists. Springer, Cham, pp89–133.

Zacher K, Roleda MY, Wulff A, Hanelt D, Wiencke1 C (2009) Responses of Antarctic *Iridaea cordata* (Rhodophyta) tetraspores exposed to ultraviolet radiationpre. Phycological Research, 57:186–193.

Zubia M, Freile-Pelegrín Y, Robledo D (2014) Photosynthesis, pigment composition and antioxidant defences in the red alga *Gracilariopsis tenuifrons* (Gracilariales, Rhodophyta) under environmental stress. J Appl Phycol 26:2001–2010.